Copyright Warning & Restrictions

The copyright law of the United States (Title 17, United States Code) governs the making of photocopies or other reproductions of copyrighted material.

Under certain conditions specified in the law, libraries and archives are authorized to furnish a photocopy or other reproduction. One of these specified conditions is that the photocopy or reproduction is not to be "used for any purpose other than private study, scholarship, or research." If a, user makes a request for, or later uses, a photocopy or reproduction for purposes in excess of "fair use" that user may be liable for copyright infringement,

This institution reserves the right to refuse to accept a copying order if, in its judgment, fulfillment of the order would involve violation of copyright law.

Please Note: The author retains the copyright while the New Jersey Institute of Technology reserves the right to distribute this thesis or dissertation

Printing note: If you do not wish to print this page, then select "Pages from: first page # to: last page #" on the print dialog screen

ABSTRACT

RATE ALTERABLE TRAUMATIC BRAIN INJURY DEVICE FOR RODENT MODELS

by
Radia Abdul Wahab

Traumatic Brain Injury (TBI) is a physical impact to the head resulting in functional deficits in memory and motor systems. TBI is a prevalent problem occurring in 1.7 million people annually in the United States (Faul et al. 2010). TBIs can differ greatly in terms of the biomechanics of the impact such as magnitude, direction and rate. Indeed, it is likely that the wide range of TBI outcomes may be due to the physical characteristics of the trauma. Studies to date on impact have used injury devices with limited alterable parameters. Therefore, the existing impact studies have considered the effect of magnitude of the primary impact and have not addressed issues such as rate of pressure increase that may be important in understanding the differences in pathology associated with these impacts.

In this study a novel modular computer controlled device capable of inducing controlled TBI is designed. To achieve maximum control and sensitivity, a closed loop voice coil control device is utilized, to more accurately and precisely generate the temporal force function delivered by the FPI device. This device enables generation of pressure profiles very similar to the ones generated from conventional FPI devices; in addition, different aspects of the pressure profiles such as the rate can be changed. This unique feature of this device is utilized to study the pathophysiological effects of increasing rates of pressure rise time on the rodent brain.

A series of behavioral studies are conducted including neurological severity tests immediately after the injury followed by rotarod, ladder rung walk, metric and spatial information, and Morris water maze tasks between 1 to 15 days post injury. Also, the perforant path-evoked granule cell field excitability is tested. Histological characterization is performed at 4h, 24 h and 15 days post injury.

The results show that a faster rate injury results in a reduced acute cell loss and improved immediate neurological outcome, but enhanced granule cell field excitability 1-week post injury. Results from immediate and chronic behavioral analysis after the injury; suggests better functional outcome in the fast injuries compared to slower injuries. However, fast injuries show a greater progressive cell loss and similar deficits in spatial information recognition as the slower rate injuries.

RATE ALTERABLE TRAUMATIC BRAIN INJURY DEVICE FOR RODENT MODELS

by
Radia Abdul Wahab

A Dissertation
Submitted to the Faculty of
New Jersey Institute of Technology
and Rutgers University
in Partial Fulfillment of the Requirements for the Degree of
Doctor of Philosophy in Biomedical Engineering

Joint Program in Biomedical Engineering

January 2014

APPROVAL PAGE

RATE ALTERABLE TRAUMATIC BRAIN INJURY DEVICE FOR RODENT MODELS

RADIA ABDUL WAHAB

Dr. Bryan J. Pfister, Dissertation Advisor — Date
Associate Professor of Biomedical Engineering, NJIT

Dr. Viji Santhakumar, Committee Member — Date
Assistant Professor of Neurology and Neurosciences, Rutgers

Dr. Bruce G. Lyeth, Committee Member — Date
Professor of Neurological surgery, UC Davis

Dr. Kevin Pang, Committee Member — Date
Professor of Neurology and Neurosciences, Rutgers

Dr. Mesut Sahin, Committee Member — Date
Associate Professor of Biomedical Engineering, NJIT

BIOGRAPHICAL SKETCH

Author: Radia Abdul Wahab

Degree: Doctor of Philosophy

Date: January 2014

Undergraduate and Graduate Education:

- Doctor of Philosophy in Biomedical Engineering,
  New Jersey Institute of Technology, Newark, NJ, 2014
- Master of Science in Biomedical Engineering,
  George Washington University, Washington, DC, 2009
- Bachelor of Science in Electrical Engineering,
  North South University, Dhaka, Bangladesh, 2008

Major: Biomedical Engineering

Presentations and Publications:

Abdul-Wahab, R., B. Sweitek, S. Mina, S. Sampath, V. Santhakumar, and B. J. Pfister. "Precisely Controllable Traumatic Brain Injury Device for Rodent Models." Proc. of Northeast Bioengineering Conference, NY, New York. 2011.

Abdul-Wahab, R., V. Santhakumar, and B. Pfister. "Novel Device to Study Pathophysiology of Brain Injury from Blast-like Waves in Rodents." Proc. of Society for Neuroscience, District of Columbia, Washington. 2011.

Abdul-Wahab, R, E. Neuberger, F. Elgammal, V. Santhakumar, and B. Pfister. "A Novel and Programmable Fluid Percussion Injury Device Reveals Distinctive Pathological Changes Following High Rate and Standard Concussive Brain Injury." Proc. of Neurotrauma, Arizona, Phoenix. 2012.

Abdul-Wahab, R, R. Ordaz, B. Pfister, and B. Lyeth. "Characterization of Novel Rate-Alterable Voice-Coil Fluid Percussion Traumatic Brain Injury Model." Proc. of Society for Neuroscience, California, San Diego. 2013.

This work has been dedicated to my husband and my two precious daughters who were born during the course of this study and my family who supported me in this work

ACKNOWLEDGMENT

Bryan J. Pfister my Dissertation Advisor and my committee members Viji Santhakumar, Bruce G. Lyeth, Mesut Sahin, and Kevin Pang.

This work is a collaborative effort from three labs and my lab partners were Sara Mina, Suji Sampath, Bogumilie Siwetek and Matt Long, in Dr. Pfister's lab; Eric Neuberger, Fatima Elgammal, Archana Protudoor, and Akshay Gupta from Dr. Viji's lab; and Rafael Ordeaz, Gene Gurkoff, Ken Van, Xinjian, and Ali Izadi from Dr. Lyeth's lab. The work was partly funded by the New Jersey Commission for Brain Injury Research (NJCBIR).

I would also like to acknowledge the support of my family members; Ariful Huq, Nuha Arif, Aliyah Arif, Dr. Abdul Wahab, Ms Hasina Parvin, Maher Khan, Mobashwir Khan, Maruf Khan, Sadia Quader and Labanya Barik.

TABLE OF CONTENTS

LIST OF FIGURES

CHAPTER 1

INTRODUCTION AND BACKGROUND

1.1 Introduction

Traumatic Brain Injury (TBI) is a physical insult that can damage the brain tissue. Neuronal dysfunction and death leads to functional deficits in motor systems and memory, leaving the individual handicapped. Each year an estimated 1.7 million Americans sustain a TBI from which an estimated 275000 people are hospitalized. (Faul et al., 2010). TBI is caused by rapid deformation of the brain in response to an insult, resulting in a cascade of primary and secondary pathological events (Adams et al., 1980; Dimitrijevic, 1989; Lowenstein et al., 1992; Hicks et al., 1993; Hovda, 1995; Santhakumar et al., 2000, 2001; Bentzer et al., 2001; Gaetz, 2004; Cohen et al., 2007, Creed et al., 2011). Because brain tissue is viscoelastic, both rate and magnitude of the insult will affect how the tissue responds mechanically and give rise to specific pathophysiology (Hardy et al., 1994; Ommaya et al., 1994; Goldsmith and Monson, 2005; LaPlaca et al., 2007; Tamura et al., 2007; El Sayed et al., 2008; Rashid et al., 2012). Because of brain's viscoelasticity, potentially one of the largest contributors to differences in TBI outcome could be the rate of the injury – in addition to magnitude. For example a blast wave would be several orders of magnitude higher in rate compared to a head impact from a fall.

The effect of rate was established in early physical models of head injury (King Lin et al., 1975; Adams et al., 1983; Margulies and Thibault, 1992; Meaney et al., 1995; King et al., 2003), studying injury related to rotational acceleration of the head. *In vitro* models have also begun to consider the rate at which the injury is delivered (Cargill and Thibault, 1996; LaPlaca et al., 1997; LaPlaca and Thibault, 1997; Morrison et al., 1998; Geddes and Cargill, 2001; Glass et al., 2002; Geddes et al., 2003, 2006; Morrison et al., 2003; Pfister et al., 2003; LaPlaca et al., 2005, 2006;

Singh et al., 2006; Magou et al., 2011). Most of these studies show a dependency of injury impairment on injury rate. To date, there have been no animal models directly examining whether the pathophysiological outcome of injuries depends on the rate of the delivered injury (measured as the 10% to 90% rise to peak pressure of the impact) other than in rotational acceleration head injury models. This is likely due to the limitations of the available injury devices to only adjust for injury magnitude. For instance, fluid-percussion injury (FPI) and weight drop vary injury either by the height adjustment of the pendulum in FPI (Dixon et al., 1987; McIntosh et al., 1989) or height of the weight in weight drop model (Feeney et al., 1981; Dail et al., 1981; Marmarou et al., 1994; Swauchi et al., 2003). Both these devices offer a change in the severity (by a change in pressure peak) of the injury but they do not have an independent control over the rate of the injury. The new VC-FPI system created here is capable of inducing TBI by various waveforms with distinct rates and pressure peaks controlled independently using a software program. The principal concept of the device was based on the standard FPI system, but uniquely, used a closed loop control to generate distinct output pressure-wave profiles with varying rates. This allowed the independent control of rates of pressure rise and pressure peak. In addition to studying the changes in histology, since this is a survival technique, we are able to study long-term changes including later stage electrophysiology and chronic behavioral changes as a result of the variable rate injury.

1.2 Background and Purpose

Various pressure waves have been used to study TBI in the laboratory. An injury due to a pressure wave is caused by a variation of pressure (rise and decay) as the disturbance that results in an insult to the brain tissues. Many TBI studies reported in literature using

commercially available fluid percussion injury (FPI) device involves a relatively slow rising pressure wave (~7-10 ms) (Dixon et al., 1987). This is the usual rate for modeling and replicating the effects of TBIs due to motor vehicle crashes or falls. This commercially available device uses a pendulum which strikes a piston at the end of a fluid filled cylinder filled with degassed water (Figure 1.1). The transient percussion of fluid (a pulse of fluid pressure) in this cylinder is transmitted to the brain through an opening in the skull of the animal (a ~3mm diameter craniotomy performed on the parietal bone, centered at -3mm Bregma, lateral 3.5mm) via a small nozzle at the opposite end of the device. However, the only controlling parameter is the height of the pendulum, which changes the peak of the pressure wave but has no independent control over the rate at which the pressure increases or the duration of the pulse.

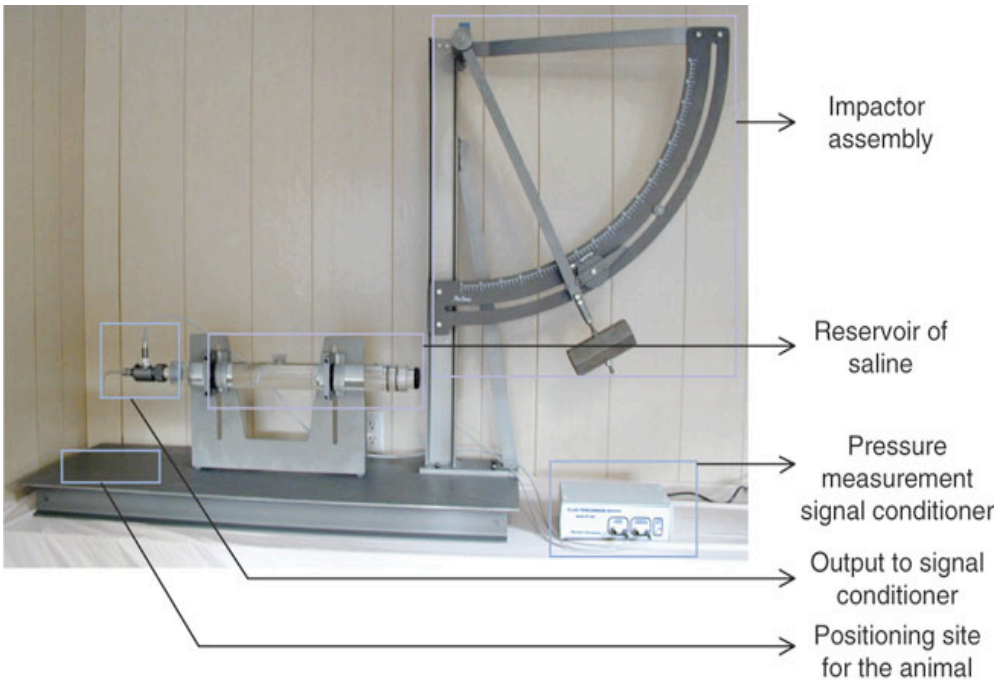

Figure 1.1 Conventional FPI Device. The injury is performed by lifting the impactor to a specific height and releasing. When released, the impactor descends and hits the reservoir and generates a pressure pulse (Rise time~7ms).

Source: Kabadi S.V., et al., "Fluid-Percussion–Induced Traumatic Brain Injury Model in Rats" Nature Protocols Volume:5, Pages:1552–1563(2010)

TBI is caused by rapid deformation of the brain in response to an insult, resulting in a cascade of primary and secondary pathological events. Because brain tissue is viscoelastic, the unique pathological response from different rate injuries would likely affect both the primary and secondary stages. Primary injury from FPI includes immediate mechanical damage to neurons, glia, and blood vessels (Thompson et al., 2005). Differences in deformation owing to the viscoelastic property of the brain; may result in differences in the extent or spread of the diffuse axonal injury (DAI) leading to distinct secondary cellular injury mechanisms such as excitotoxicity (McIntosh, 1994; Thompson et al., 2005), calcium overload (Katayama et al., 1990), and oxidative stress and inflammation (Thompson et al., 2005). The differences in secondary injury mechanisms may lead to differences in cell and axonal degeneration (Hallam et al., 2004) and synaptic dysfunction (Dietrich et al, 1999) and thereby result in distinct cognitive dysfunction.

Here a unique Voice-Coil FPI (VC-FPI) device was created to study the effects of rate on the post-traumatic pathophysiology. The principal concept of the device is based on the conventional FPI system. Lateral fluid percussion brain injury is one of the most commonly used and well-characterized experimental models of TBI, producing both focal and diffuse injury characteristics (Dixon et al., 1987; Cortez et al., 1989; Hicks et al., 1996; Graham et al., 2000; Morales et al., 2005; Thompson et al., 2005). The novel VC-FPI device is also capable of inducing a TBI with a fluid percussion. The system uses closed loop control to generate distinct output pressure-wave profiles with varying rise-times, pressure peaks and duration. Accordingly, the control enables the user to vary the rise-time and the pressure peak of the injury independently of each other. A voice coil linear actuator drives a hydraulic cylinder to produce a fluid percussion. A Proportional Integral Derivative (PID) controller closed loop control system uses encoder feedback to program

specific movements that translate into definable fluid percussion waveforms. A pressure transducer is located near the animal connection to measure the fluid percussion applied (Figure 4.1). Force generation via voice coil and computer control offer superior control over pressure wave generation, than pendulum based models. The voice-coil (i) offers maximum control and sensitivity, (ii) is cheap and portable, (iii) the parameters can be changed easily, and (iv) very fast rate injuries can be achieved.

An extreme example of a fast rate pressure waveform is the blast wave overpressure. Blast wave overpressures have a typical wave profile as can be seen in figure 1.2(a). This figure shows a blast in an open field experiment (rise time ~0.1ms). The conventional fluid percussion injury device also generates a pressure waveform, but the rise-time is much slower and hence the rate of injury is lower (Figure 1.2(b)). High rate pressure studies reported to date include studying the effects of ultrasound lithotripsy pressure waves on the brain tissues (Curra, 2009; Nakagawa et al., 2009, 2011; Tyler, 2011; Abdul-Wahab et al., 2012; Goeller et al., 2012). In some ways, these pressure waves resemble those of a blast, but have a much shorter rise-time (~30ns) as shown in figure 1.2(c) (Figure not drawn to the same scale).

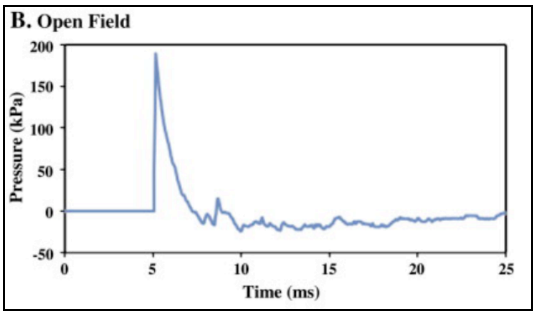

(a)

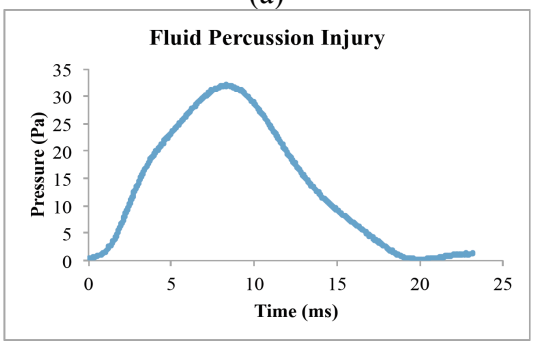

(b)

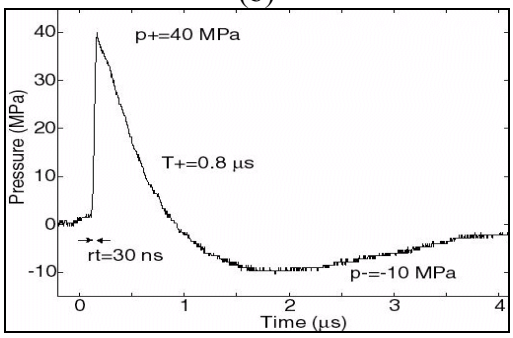

(c)

Figure 1.2 Comparison of Pressure Profiles in Literature. (a) Blast waveform: An open field shockwave generated by detonating 816.47 g (1.8 lbs) of a TNT-equivalent explosive charge in open field conditions. The static pressure was recorded 3.6 m from the source (Cernak et al., 2011). Rise time ~0.1ms. (b) Output pressure waveform from a conventional fluid percussion injury system. Rise time ~10ms. (c) Lithotripsy Waveform (Xuzhcu Lhja 2012). Rise time ~30ns. Output Pressure Waveform has a similar wave trend. However the rate is much higher (Rise time~30ns).

Source: Cernak, Ibolja, et al., "The pathobiology of blast injuries and blast-induced neurotrauma as identified using a new experimental model of injury in mice." Neurobiology of disease 41:2 (2011): 538-551. Xuzhcu Lhja Electronic Technology, http://www.lhdz.org/hdyl/add2.htm, Viewed Jan 20, 2012.

The brain is composed of discrete fluid boundaries formed by cells interfacing with one another. An ultrasound pressure wave propagating through the brain tissues, encounters different stiffness and densities and therefore different acoustic impedance

(figure 1.3). Depending on the level of impedance mismatch a number of disturbances are formed at the micro-level; which includes acoustic streaming, cavitation etc. The resulting pathophysiological effects reported from very high rate TBI studies such as lithotripsy, were primarily axonal pathology and cavitation. On the other hand pathophysiological studies conducted using conventional FPI device report cell loss as a result of the injury (Cortez et al., 1989; Smith et al., 1991; Lowenstein et al., 1992; Hicks et al., 1993, 1996; Conti et al., 1998; Floyd et al., 2003).

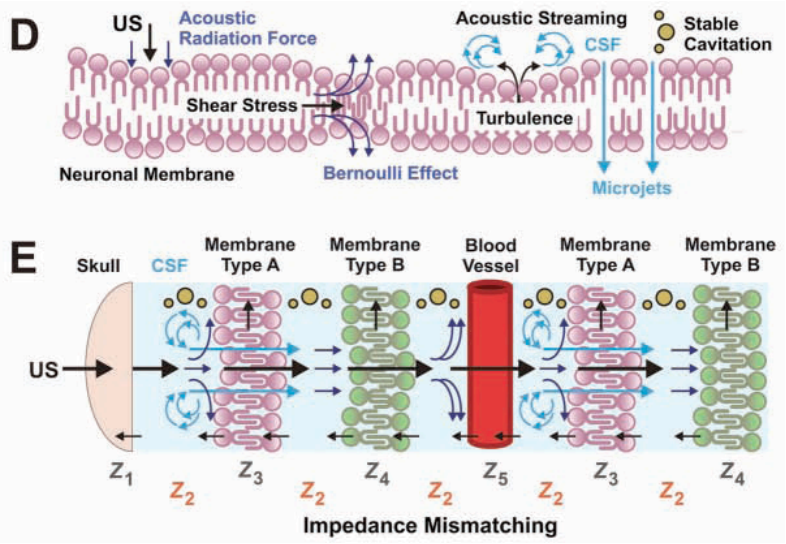

Figure 1.3 Ultrasound Axonal Pathology. Ultrasound generates very high rate overpressure, and the resulting injuries are mostly axonal pathology from shear stress, acoustic streaming, acoustic radiation force etc. Also there is cavitation due to microjets and acoustic streaming.

Source: Tyler, WJ, "Non-Invasive Neuromodulation With Ultrasound? A Continuum Mechanics Hypothesis." Neuroscientist (February 2011) 17: 25-36.

In contrast to the ultrasound lithotripsy-induced pressure waves (rise-time 30ns), blast pressure waves generated in an explosion have an approximate rise time of 0.1ms (for a mild to moderate blast injury). Therefore, since the rate of the blast pressure wave falls somewhere between a comparatively slow rate FPI device pressure wave (rise-time 5-10ms) and a much faster rate ultrasound pressure wave (rise-time 30ns); the

pathophysiological changes resulting from a blast-like pressure wave injury may have characteristics representative of both ultrasound lithotripsy pressure waves and FPI pressure waves. For instance, higher rate pressure wave injury might have less cell loss but greater axonal pathology/dysfunction than what is seen in FPI. The behavioral differences will follow from the combined effects of both types of damage. Therefore it is crucial to understand the neurological effects of varying the rate of the injury delivery.

Fluid percussion injury is one of the most extensively utilized animal models of TBI (Thompson et al., 2005; Morales et al., 2005) producing both focal and diffuse brain injury; transient suppression of reflexes immediately after injury, cellular degeneration, secondary cellular damage, axonal damage, cognitive deficit, neuromotor deficits, and alterations in electrophysiology. After FPI in rats, acute neurological reflexes are transiently suppressed (Hallam et al., 2004). Therefore the duration of suppression of the righting reflex, toe pinch response etc. have served routinely as an indicator of injury severity after FPI (Dixon et al., 1987; Schmidt et al., 1995; Carbonell et al., 1998; Hallam et al., 2004). Over days to months after a standard FPI, several groups have reported a progressive degenerative cascade persisting in selective vulnerable brain regions such as the hippocampus (Cortez et al., 1989; Smith et al., 1991; Lowenstein et al 1992; Hicks et al., 1993, 1996; Carbonell et al., 1999; Dhillon et al., 1999). Secondary progression of the injury after FPI can affect several cell types across many brain regions. However, whether the cellular and molecular responses to FPI result from initial injury, secondary process or reflect a recovery process, are yet to be determined (Thompson et al., 2005). Electrophysiological studies post FPI have shown pathological alterations including dentate hyperexcitability (Toth et al., 1997; Santhakumar et al., 2001). Behavioral difficulties with coordination, posture and steadiness of movement have been shown in several studies. Vestibulomotor tests

have been performed in order to determine the degree of fine motor coordination in FPI animals (Hamm et al., 1994, 1996, Lyeth et al., 2001). Hippocampal dependent cognitive deficits associated with spatial memory and learning has been studied with the Morris water maze tests and metric and spatial information tasks (Morris et al., 1982, Smith et al., 1991).

Objective

This study included two complementary objectives. One was to create and characterize a fluid percussion injury device capable of delivering various rates of pressure increase in animal models. The second objective was to produce a brain injury rodent model capable of investigating rate-related TBI. The effects of different rates of pressure waves to the brain on action potential generation, chronic behavioral deficits and both acute and chronic histology was studied.

Hypothesis

Moderate magnitude, high rate injury results in degeneration or alterations of the neurons and their electrophysiological properties that adversely affect the dentate network excitability, thus giving rise to distinct pathophysiological and behavioral outcomes from slow rate injury.

1.3 Specific Aims

Specific Aim 1: Device characterization: design and characterization of a computer controlled modified fluid percussion injury (FPI) device. The purpose of this aim was to compare the output wave characteristics produced by a conventional pendulum FPI device and that of a newly developed voice-coil FPI (VC-FPI) device. The characteristics

and limits of this device were studied, including the rate alterability of the device. The different wave profiles were explored: fast-rate VC-FPI (velocity 2.78m/s, acceleration 311m/s^2, rise-time ~3ms rise time), slow-rate VC-FPI (velocity 1.27m/s, acceleration 25.4m/s^2, rise-time ~4ms rise time) and standard FPI waveform from conventional FPI (~5ms rise time). The experiments in this aim did not include any animals.

Animal studies in Aim2, Aim3 and Aim4 involved the comparison of the following set of animal groups:

- Sham TBI controls: The animals went through identical anesthesia and surgery as the other groups but were not exposed to the pressure wave.
- FPI from standard FPI device: A moderate injury from a standard FPI device
- Slow-rate injury from VC-FPI device: A moderate injury at slow rate from the VC-FPI device.
- Fast-rate injury from VC-FPI device: A moderate injury at fast rate from the VC-FPI device.

Specific Aim 2: Characterization of the output pressure waveform during animal injuries. The purpose of this aim was to assess how the device performs when animals are attached to the device and injury is performed. Comparing the output pressure waveforms between 2 different aged animals (adolescent rats and adult rats). Comparing pressure profiles between a standard FPI device and two different rates from the voice coil FPI to determine the pressure peak, rise time and impulse achieved by each of these devices when adolescent animals are injured and when adult animals are injured.

Specific Aim 3: Adolescent rat TBI study including immediate behavioral response, cellular pathology and granule cell field excitability. The purpose of this aim was to study cell loss and dentate hyperexcitability as a result of an injury, at 2 different rates from VC-FPI device, in adolescent rats. Neuronal cell death is a standard measure

of damage after a TBI. However, in addition there are incidences where the cells do not die but are injured. Therefore evoked field potentials in granule cell layer, were examined to study network excitability.

Specific Aim 4: Adult rat TBI study including behavioral studies and cellular pathology: The purpose of this aim was to study both the immediate behavioral responses following the injury and chronic motor and cognitive deficits in learning for the 3 different injuries; standard FPI rate from FPI, and both fast-rate VC-FPI and slow-rate VC-FPI. This aim also studies the cell loss at acute stage and chronic stage of injuries.

CHAPTER 2

METHODS

2.1 The Voice-Coil Fluid Percussion Injury Device

A voice coil actuator driven fluid percussion system was developed to precisely control the characteristics of the pressure waveform including the pressure rise-time and peak pressure. Fluid percussions were generated by the movement of a rigidly connected hydraulic cylinder and a linear voice coil actuator (LA2-42-000A, BEI Kimco) Figure 2.1. Accordingly, the controlled motion of the voice coil and hydraulic cylinder translates into a controlled rise in fluid pressure.

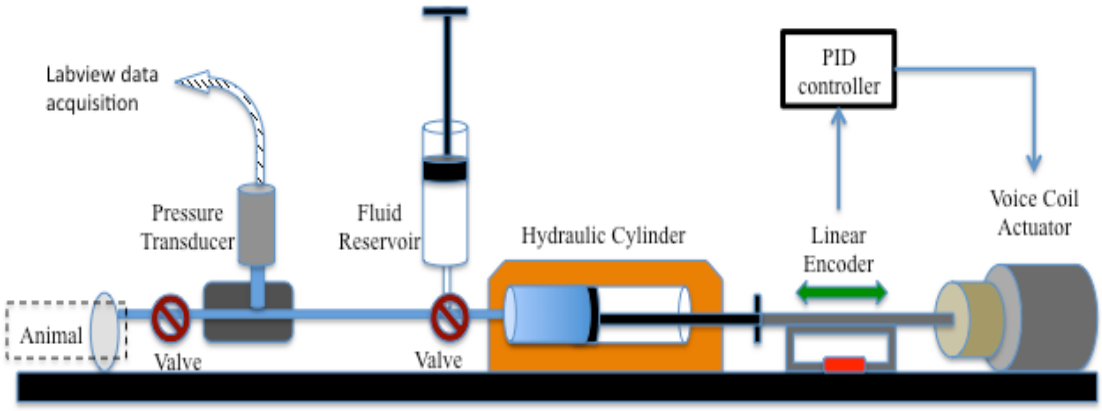

Figure 2.1 Programmable Fluid Percussion Injury System. A voice coil linear actuator drives a hydraulic cylinder to produce a fluid percussion. A PID closed loop control system uses encoder feedback to program specific movements that translate into definable fluid percussion waveforms. A pressure transducer is located near the animal connection to measure the fluid percussion applied.

The Fluid percussion injury from the VC-FPI is very similar to the commonly used pendulum fluid percussion injury system (FPI). A standard FPI system consists of a Plexiglas cylinder reservoir about 60cm long (Dimensions of the FPI cylinder are 5.08

cm inside diameter, 56.5 cm length = 364.5 cm3 total volume). At one end of the cylinder a rubber-covered Plexiglas piston is mounted on O-rings. A pendulum of adjustable height strikes the piston causing a fluid pulse to impact the brain. On the opposite end of the cylinder there is a metal housing that contains a pressure transducer. At the open end of the metal tube is a 2.6mm-ID (Inside diameter) male Luer-loc opening. During an injury the female Luer-loc, which is attached to a craniectomy in the skull of a rat (see section 2.3.3 Surgical Procedures below), can be fitted to the male Luer-loc opening (Dixon et al., 1987). In the novel VC-FPI system the fluid filled cylinder is a 10cc syringe, there is a linear voice coil actuator that is controlled by a computer program, which specifies the displacement of the piston, and its velocity and acceleration of motion. A flat-faced pressure transducer (px61v0-100gv, Omegadyne) was mounted at the output of the hydraulic cylinder to measure the applied fluid percussion. A 2.6mm-ID female luer-loc fitting connects to a male Luer-loc connector cemented to the rat skull craniotomy. A LabView program acquires the fluid percussion pressure waveform for later analysis.

The movement of the voice coil actuator is controlled by a PID controller (100S, Automation Modules) and is programmed using a terminal emulator (Teraterm) (Figure 2.1). A linear optical encoder (Zeiss, LIE 5 series, 1μm resolution) is used to close the control loop. The user specifies the displacement of the piston, and the velocity and acceleration of motion. The controller stores the position-time data from the encoder. Voice coil – hydraulic cylinder motion was programmed to make a target displacement using a triangular motion. The triangular motion represents the velocity of temporal motion that moves the system to a programmed displacement. Acceleration is also specified for the motion and is set for linear rise in velocity. The programmed velocity was chosen to achieve the desired rate of pressure rise. Displacement was specified to

develop the desired peak pressure. The optimum values for displacement and velocity for each rate (fast and slow) were determined experimentally. By changing the piston displacement, the peak pressure can be altered. By altering velocity and acceleration of the motion, the rate of pressure rise can be changed. However, on changing the velocity and acceleration, the displacement can be independently adjusted to hold the peak pressure constant.

The intent was to choose specific velocities and accelerations based on previous fast rate studies such as blast rate injuries (Celander et al., 1955; Elsayed, 1997; Cernak et al., 2001a,b; Garman et al., 2009, 2011; Long et al., 2009), and slow rate studies such as standard FPI injuries (Dixon et al., 1987; McIntosh et al., 1989). However given the speed limitations of this voice coil system, we were limited to a fluid percussion rise time of 3ms, much faster than currently used in commercial FPI systems. Any rise-time lower than that resulted in inconsistent waveforms. These resulted in waveforms with inconsistent rise-times, peak pressures, or durations. Therefore 3ms rise-time was the fastest rise-time that could be achieved with this system. Using this rate the operating velocity of the device was calculated. The slope of the output displacement-time curve was calculated for determining the velocity of motion. This maximum velocity was used as the fast rate.

In the case of the slow-rate VC-FPI operation, standard FPI injuries were studied from conventional devices as reference. The velocity that gave an output rise-time of approximately 10ms was chosen as a slow-rate VC-FPI injury. The device was tested for consistency in operation at this slow rate.

Since the voice-coil has a rigid connection with the hydraulic cylinder, the motion of the voice-coil translates into motion of the piston of the hydraulic cylinder. By having precise control of the motion of the piston in the hydraulic cylinder, we have control over

the pressure pulse waveform. Computer control enables one to vary the rate and the severity of the injury independently of each other.

2.2 Closed System Device Characterization

2.2.1 Characterization of Pressure Waveform Generation in the VC-FPI System

The linear movement of the voice coil and that of the piston of the hydraulic cylinder generate fluid percussions. In order to map out voice coil displacements to generated pressure waveforms in a closed system, first the valve at the animal injury site (in Figure 2.1) was closed and pressure waveforms from various voice coil displacements were recorded. A slow pressure waveform was generated and compared with a standard waveform from the commonly used FPI device (VCU FPI device was used for the injury of Adolescent rats and AmScien Instruments FPI device was used for the injury of Adult rats). A range of input displacements from 0.001m to 0.023m were programmed and the associated pressure peaks were recorded.

In order to verify the smoothness and uniformity of output displacement of the piston, three input displacements were chosen around the moderate injury range (1.5-2.15atm) (McIntosh et al., 1989) and the corresponding output displacements were recorded using the linear encoder. The VC-FPI device was shown to be capable of generating pressure waveforms with different rise-times while keeping the pressure peak constant, and also pressure waveforms were generated with different pressure peaks while keeping the rise-times constant. This was carried out by altering the velocity and the displacement independent of each other. Larger displacements resulted in higher pressures and higher velocities resulted in faster rates. Similar pressure peak with different rise-times could be used to perform injuries with similar severity but different rates of injuries. Whereas,

different pressure peaks with similar rise-times could be used to perform injuries comprising of similar rates but differences in severity.

2.2.2 Waveform Analysis for Comparing VC-FPI Device in Two Different Modes of Operation; Fast-rate and Slow-rate; and Standard waveform from FPI.

The average pressure peak, rise time and impulse were calculated from pressure-time data collected from the pressure transducer. Voice coil – hydraulic cylinder position and time data was collected from the linear encoder for comparison to the pressure waveform. Pressures developed under various displacements were mapped using a closed system, valve 1 closed, Figure 2.1. Fluid percussion delivery was later characterized with a rat attached to the system.

From the pressure waveforms (Figure 4.1a, chapter 4) the time taken for the pressure to rise from 10% increase to 90% of the peak was calculated as the rise time, this is equivalent to the rate at which the injury is delivered. Also, from the pressure waveforms the peak of each wave was recorded, which was the maximum pressure point of the pressure waveform. The pressure peak for the different devices and modes of operations were compared.

The impulse of the pressure waveforms was calculated as the area under the pressure-time curve using the following formula:

$$I = \sum_{t=s}^{e} P(t) \qquad (2.1)$$

Where "I" is the Impulse (units Pa.s), "P(t)" is the output pressure waveform, "t=s" is the start of the positive pressure region, "t=e" is the end of the positive pressure region. The

impulse of the injury was therefore calculated by the area under the pressure vs time curve. For the entire duration of the pressure wave, every 1ms of the waveform, the pressure peak was noted and thereby the area under the curve was cut into 1ms duration intervals. Then the area in each of these intervals were calculated by trapezium rule, followed by summation of all the intervals under the pressure curve, to give us the total area under the curve.

Studying the pressure waveforms in a closed system, we then compared the pressure waveforms in animal injuries, for both adolescent and adult rats (see further discussion in the following section).

Lateral Fluid Percussion Injury

2.3 Device Characterization During Animal Injuries

The animals were injured following the protocol described in the next two sections (2.4 and 2.5) the device was used to perform traumatic brain injuries to adolescent and adult rats. The following sections describe the methodology for testing the performance of the device when animals were injured.

2.3.1 Comparison of Pressure Waveform

Fluid percussion waveforms were characterized using VC-FPI device with adult and adolescent rats. Optimum voice coil – hydraulic cylinder motion settings determined with a closed system will be different with a compliant load on the system (i.e. rat head). Measured fluid percussions were used to adjust the voice coil motion settings to achieve the desired pressure rise and peaks. Optimum motion control settings were compared to

pressure peaks, rise-times, durations and impulses of the different injuries from the FPI and VC-FPI device.

Various pressure waveforms were generated with adult and adolescent rats attached. Representative pressure waveforms were compared based on having similar pressure peaks, rise-times and durations to the mean values of the corresponding groups. These pressure waveforms consisted of a set of pressure waveforms generated with adult rats and adolescent rats injured from a commonly used FPI system. Another set of injuries was generated from fast-rate VC-FPI and slow-rate VC-FPI pressure waveforms in the presence of adolescent rats and adult rats and with the valve at the animal injury site open (Figure 2.1). Animal attached at the injury site offers less mechanical resistance at the output compared to the closed system. The various sets of pressure waveforms generated from these experiments were used to compare the pressure peaks, rise-times and impulses of the different injuries from the FPI and VC-FPI device. Also the displacement charts for these injuries were generated using the data from the linear encoder. The displacement waveforms were also compared to ensure consistent motion of the voice-coil actuator.

2.3.2 Fluid Percussion Waveform Analysis

The average pressure peak, rise time and impulse were studied. These values were determined from the pressure waveforms collected during injuries with animals. The pressure peaks, rise-times and impulses were calculated in the same way as done in the previous section when characterizing the device in the closed system.

2.3.3 Subjects and Experimental Design

Sixty-six adult male Sprague-Dawley rats (Harlan, Indianapolis, IN), 300-350g and thirty-six adolescent rats (postnatal days 24–26) male, Wistar rats (Charles River), 35-65g were used for the experiments. Animals were housed in individual cages in a temperature (22°C) and humidity controlled (50% relative) animal facility with a 12-hour light/dark cycle. Animals had free access to food and water during the course of the experiments. Animals were held in the animal facility for at least 7 days prior to surgery. The Institutional Animal Care and Use Committee at the University of Medicine and Dentistry in New Jersey (Adolescent rat experiments) and University of California at Davis (Adult rat experiments) approved all animal procedures in these experiments.

The investigator was blind to the injury for all animal experiments included in this study during the behavioral and histological testing. Three groups of animals were included in the investigation of adolescent rats and four groups for the investigation of adult rats. All injuries were of moderate severity, which was determined by the peak of the pressure wave (Adolescent rats 1.77atm and adult rats 2.15atm). In the adolescent animals the three groups comprised of the fast-rate VC-FPI and slow-rate VC-FPI and a sham TBI group. In addition to these three groups there was a fourth group of injuries that comprised of animals injured using the FPI system. However, this was only performed for device characterization and these animals were not included in the pathophysiological studies. For the adult animals the four groups included in the study: a fast-rate VC-FPI and a slow-rate VC-FPI group, a FPI injury group using the FPI system and a sham TBI group. All four groups were included in the pathophysiological studies. Table 2.1 shows the various studies that were performed. From here onwards the adolescent and adult study is discussed in separate sections.

Table 2.1 Animal Study Groups

Specific Aim#	Group Name	Injury type	Age during injury	End point	No. of animals
Specific Aim 3 (Adolecent animal study)	**Histology**	Sham TBI	3.5 wk	2-4h	n=2
		Sham TBI	3.5wk	1wk	n=2
		Slow-rate VC-FPI	3.5 wk	2-4h	n=4
		Slow-rate VC-FPI	3.5 wk	1wk	n=5
		Fast-rate VC-FPI	3.5 wk	2-4h	n=4
		Fast-rate VC-FPI	3.5 wk	1wk	n=7
	Electrophysiology	Sham TBI	3.5 wk	1wk	n=4
		Slow-rate VC-FPI	3.5 wk	1wk	n=4
		Fast-rate VC-FPI	3.5 wk	1wk	n=4
Specific Aim 4 (Adult animal study)	**Cognitive studies**	Sham TBI	3mths	16d	n=12
		Standard FPI	3mths	16d	n=9
		Slow-rate VC-FPI	3mths	16d	n=10
		Fast-rate VC-FPI	3mths	16d	n=11
	Histology	Sham TBI	3mths	24h	n=6
		Standard FPI	3mths	24h	n=6
		Slow-rate VC-FPI	3mths	24h	n=6
		Fast-rate VC-FPI	3mths	24h	n=6

2.4 Adolescent Rat Experiments

One set of adolescent animals consisting of injured and sham TBI animals, were euthanized 4 h after the injury and the brain tissue was processed for analysis of acute neuronal degeneration. One week post injury another set of adolescent animals were euthanized and brain tissue was extracted and electrophysiological recordings were carried out.

2.4.1 Surgical Procedure

Standard surgical methods for lateral fluid percussion injury were followed as described earlier (Dixon et al., 1987; Lowenstein et al., 1992; Toth et al., 1997; Santhakumar et al., 2000, 2003; Gupta et al., 2012). The rats were first anesthetized with a Ketamine/Xylene i.p. injection. The rats were then mounted on a stereotaxic device, and a scalp incision made along midline. Followed by a ~3mm diameter craniotomy performed on the parietal bone. (Centered at -3mm Bregma, lateral 3.5mm). Careful measures were taken to keep the dura intact. Which included, carefully drilling the hole to avoid any damage to the dura and removal of the bone fragments to avoid piercing the dura. A rigid plastic injury tube (Modified Luer-loc needle hub, 2.6mm inner diameter) was secured over the exposed, intact dura with cyanoacrylate adhesive. The assembly was secured to the skull with cranioplastic cement.

Once the surgery was completed, the rats were allowed to recover over-night in the vivarium under normal conditions. On the following day the rats were anesthetized using isoflurane in an airtight gas chamber for <10sec. Then the animals were taken out from the chamber and the implanted injury tube was connected to the fluid percussion cylinder and the injury was delivered.

2.4.2 Traumatic Brain Injury

Three different groups of adolescent rats were used in each experiment. The experiments included histology and electrophysiology. The 3 groups included fast-rate VC-FPI (rise time ~3ms) injury and slow-rate VC-FPI (rise-time ~10ms) injury, and sham TBI animals. The peak of the pressure waveform was within moderate injury level (1.77atm) (McIntosh et al., 1989). Sham animals were subjected to all surgical and anesthetic procedures, but without delivery of fluid pressure pulse to the brain.

The injury was performed by an input command into the PID controller determining the acceleration, velocity, displacement and direction of motion. This command in the PID controller resulted in a horizontal motion of the voice-coil and thereby the piston of the hydraulic cylinder, giving rise to the required pressure wave. This horizontal motion of the voice-coil replaces the descending of a pendulum in the standard FPI device. Other aspects of the injury were the same as the conventional fluid percussion injury and includes the transfer of a pressure pulse that results in a displacement and deformation of neural tissue. The pressure transducer next to the injury site recorded the pressure wave and the data was collected in a computer using a LabView data acquisition program as has been discussed earlier. This was done to ensure that all animals received consistent brain injuries at the targeted pressure.

2.4.3 Immediate Pathophysiology

The rats were observed for 15 minutes after the injury for possible immediate seizures, transient apnea or death (Dixon et al., 1987; Lowenstien et al., 1992; Toth et al., 1997). Seizures were identified by muscle stiffening or sudden cessation of activity followed by uncontrolled jerking or spasms. On the Racine Seizure scale anything stage 2 and above

was counted as a seizure. Seizure rates and death rates were plotted on a chart as percentage of total injuries.

2.4.4 Tissue Collection and Sectioning

Rats were euthanized at 4h for acute histological assessment. The time point was based on previous literature studies (Hallam et al., 2004; Zhao et al., 2003; Zhong et al., 2005; Feng et al., 2011; Gupta et al., 2012). Animals were deeply anesthetized with sodium pentobarbital (100mg/kg i.p.) followed by transcardial perfusion with 100ml of 0.1M sodium phosphate buffer (pH=7.4) followed by 350ml of 4% paraformaldehyde (pH=7.4). The brains were extracted and macroscopically visualized for hemorrhage. Brains were removed and post-fixed in 4% paraformaldehyde at 4°C. Using a vibratome, 40μm horizontal sections were cut. Every serial section was saved in 24-well culture plates.

2.4.5 Acute Histology: Neuronal Degeneration

Neuronal degeneration was quantified using the histofluorescent stain, Fluoro-Jade C (Schmued et al., 1997; Schmued and Hopkins, 2000, Gupta et al., 2012) 4h after TBI. Previously hematoxylin and eosin (H&E) or Nissl type stains (Schmued et al., 1997) were used to count surviving cells and were often used as an indirect measure of neurodegeneration. Fluoro-Jade is a more sensitive, definitive and selective marker of neuronal degeneration. However, the exact mechanism by which this stain detects degenerating neurons is unknown.

Standard Fluoro-Jade staining procedures were used. Briefly, sections mounted on gelatinized slides were air dried, hydrated and incubated in 0.06% potassium permanganate before being stained with 0.001% Fluoro-Jade C in 0.1% acetic acid in the

dark for 30 min. The sections were immersed in xylene and cover-slipped with DePeX mounting medium (Electron Microscopy Sciences, Fort Washington, PA).

2.4.6 Cell Counts

The number of FJ-C positive degenerating neurons in the region of interest was quantified using microscopy. Cell counts were performed using the Optical Fractionator probe of Stereo Investigator V.10.02 (MBF Bioscience) using an Olympus BX51 microscope and a 100× oil objective. In each section, the hilus was outlined by a contour traced using a 10× objective. Sampling parameters were set at 100×: counting frame, 50 × 50 μm; dissector height, 25 μm; and top guard zone, 4 μm. Approximately 30 sites per contour were sampled using randomized systematic sampling protocols. In each section, the cell count was estimated based on planimetric volume calculations using Stereo Investigator (West et al., 1991; West, 1993).

2.4.7 Electrophysiology

The electrophysiology recording was done at 1-week post injury. Procedures followed were similar to previous studies (Toth et al., 1997; Santhakumar et al., 2000, 2001; Gupta et al., 2012). First the animals were anaesthetized in 1-3% Isoflurane. They were decapitated and brains removed and cooled to 4ºC oxygenated artificial cerebrospinal fluid (aCSF). The sucrose aCSF contained (in mM) 85 NaCl, 75 Sucrose, 24 NaHCO3, 25 glucose, 4 MgCl2, 2.5 KCl, 1.25 NaH2PO4 and 0.5CaCl2. Then using a vibratome (Leica, VT200S), horizontal brain slices ~ 400μm were sliced yielding 6 slices. The slices were sagitally bisected into two hemispherical components and ipsilateral component was incubated in 32ºC in aCSF in a submerged oxygenated holding chamber and kept at room temperature and saturated at 95% O2 and 5% CO2 at pH 7.4 for 1-6 hours. Individual

slices were transferred to an interfaced recording chamber for recording. The slices were perfused with recording aCSF. Recording aCSF consisted of (in mM): 126 NaCl, 2.5 KCl, 2 CaCl2, 2 MgCl2, 1.25 NaHPO4, 26 NaHCO3, and 10 d-glucose saturated with 95% O2 and 5% CO2 and at pH 7.4. Field recordings were performed in an interfaced recording chamber (BSC2, Automatic Scientific) perfused with recording aCSF at 34ºC and oxygenated. Patch pipettes (micropipettes) were filled with recording aCSF.

The electrophysiological recordings are recorded as field potentials via electrodes placed close to the cell bodies of granule cells. In a naïve animal the field EPSPs evoked by a stimulation of the entorhinal fibers does not lead to population spike in most cases and hence minimal population spike amplitude is seen. However, if there is any compromise to the inhibitory control or if there is an increase in excitability there is an increase in population spike amplitude. Stimulation of the perforant pathway evokes action potentials generation in the granule cells, which can be measured as population spikes in field recordings. Generation of action potentials in granule cells of the dentate gyrus is under control of inhibitory interneurons (Buzsaki et al., 1983; Halasy and Somogyi, 1993; Soltesz et al., 1995).

Perforant path fibers were evoked at 4mA, 50μs, just outside the molecular layer at the junction of the dorsal blade and the crest as previously described (Toth et al., 1997) and recordings were obtained from granule cell layer of the dentate gyrus. Recordings were obtained using an AxoPatch200B amplifier and digitized at 10kHz with a DigiData 1440A (Molecular devices), and population spike amplitude were measured. The population spike was quantified by measuring the difference between the negative peak and the averaged values of the 2 positive peaks.

2.5 Adult Rat Experiments

One subset of injured and sham TBI animals were euthanized 24 h after the injury and the brain tissue was processed for analysis of acute neuronal degeneration (sham: n=6, FPI: n=6, Slow-rate VC-FPI: n=6, Fast-rate VC-FPI: n=6). Another subset of the animals performed in chronic behavioral studies and were euthanized on day 15 post injury and brain tissue was extracted and processed for measurement of chronic neuronal survival (Sham: n=12, FPI: n=9, Slow-rate VC-FPI: n=10, Fast-rate VC-FPI: n=11). The effects of different pressure rise-times were evaluated on chronic cognitive performance in a series of cognitive tests that included rotarod, ladder rung walk, metric spatial information task, and Morris water maze tasks all between days 1-15 post injury on the previously mentioned second set of animals; before they were euthanized for chronic neuronal survival study.

2.5.1 Surgical Procedure

Standard surgical methods for lateral fluid percussion injury were followed as described earlier (Dixon et al., 1987; Lowenstein et al., 1992; Toth et al., 1997; Santhakumar et al., 2000, 2003; Gupta et al., 2012). The procedure followed for anesthetizing was different between the adult and the adolescent rats. Briefly, the adult rats were anesthetized with 4% isoflurane in a 2:1 nitrous oxide/oxygen mixture and intubated. Then mechanically ventilated (Model683; Harvard Apparatus, Hollister, MA) with 2% isoflurane in a 2:1 nitrous oxide/oxygen carrier gas for the duration of the surgery.

The rats were mounted on a stereotaxic device (model 900; KOPF Instruments, Tujunga CA), a scalp incision made along midline, and a 4.8mm diameter craniotomy was performed on the parietal bone (centered at -4.5mm Bregma, lateral 3mm). A rigid

plastic injury tube (modified Luer-loc needle hub, 2.6mm inner diameter) was secured over the exposed, intact dura with cyanoacrylate adhesive. The assembly was secured to the skull with cranioplastic cement (Plastic One, Roanoke, VA). Two skull screws 2.1mm diameter and 6mm length were placed into burr holes, 1mm rostral to Bregma and 1mm caudal to Lambda. Rectal temperature was continuously monitored and maintained within normal ranges during surgical preparation by a feedback temperature controller pad (Model TC-1000; CWE Ardmore, PA).

2.5.2 Traumatic Brain Injury

Four injury groups were studied: 1) Standard rate injury from a conventional FPI device (rise time ~8ms), 2) fast-rate VC-FPI device (rise time ~3ms), 3) slow-rate VC-FPI (rise time ~10ms), and 4) sham TBI animals. The maximum pressure magnitude was kept constant for each group (2.15 atm). Sham animals were subjected to all surgical and anesthetic procedures, but without delivery of fluid pressure pulse to the brain.

Standard FPI was induced using a commercially available device (VCU Biomedical Engineering, Richmond, VA) as described earlier (Dixon et al., 1987; Lowenstein et al., 1992; Toth et al., 1997; Santhakumar et al., 2000, 2003; Gupta et al., 2012). All VC-FPI system injuries were produced using the newly designed and fabricated device. Descriptions of both devices are in the previous section (2.1).

For the standard FPI device, injury was induced by a descending pendulum striking the piston, which injected a small volume of saline epidurally into the closed cranial cavity, producing a brief displacement and deformation of neural tissue. The resulting pressure pulse was measured in atmospheres by an extracranial transducer (model SPTmV100PG5W02; Sensym ICT) placed very close to the injury site, and

recorded on a digital storage oscilloscope (model TDS 1002; Tektronix Inc., Beaverton, OR).

The injury was performed by an input command into the PID controller determining the acceleration, velocity, displacement and direction of motion. This command in the PID controller resulted in a horizontal motion of the voice-coil and thereby the piston of the hydraulic cylinder, giving rise to the required pressure wave. This horizontal motion of the voice-coil replaces the descending of a pendulum in the standard FPI device. Other aspects of the injury were the same and the pressure data was collected in a computer using a LabView data acquisition program.

Once the surgery was completed, rats were disconnected from the ventilator, the injury tube was connected to the fluid percussion cylinder, and a moderate fluid percussion pulse (~2.15 atm) was delivered. Immediately after TBI, rats were ventilated with a 2:1 nitrous oxide/oxygen mixture in the absence of isoflurane. The plastic injury tube and skull screws were removed and the scalp incision was closed with 4-0 braided silk sutures and immediate neurological severity analysis was performed (described below in section 2.5). Sham TBI rats were subjected to all anesthetic and surgical procedures but a fluid pulse to the brain was not delivered, as described earlier.

2.5.3 Immediate Pathophysiology

Immediately after TBI the rats were ventilated with air in the absence of isoflurane. As soon as spontaneous breathing was observed (~3min post injury) the animals were extubated, and an assessment of the righting reflex and toe pinch response begun. Righting reflex was performed in order to assess vestibular equilibrium neuromuscular responses. Righting reflex assessment was performed by placing the rat in a supine

position at regular intervals (~30sec intervals) to test the rat's ability to spontaneously recover to a prone position. In the toe pinch response the toe is firmly pinched between the fingers to elicit a withdrawal response by the animal. Right and left hind paw toes were gently pinched at regular intervals (~15sec intervals) to check for responsiveness in noxious stimulation. The TBI injury magnitude, righting time, toe pinch response and rectal temperature were recorded.

2.5.4 Tissue Collection and Sectioning

Rats were euthanized at 24h for acute histology assessment, and at 15d for chronic histological assessment. The time points were based on previous literature studies (Hallam et al., 2004; Zhao et al., 2003; Zhong et al., 2005; Feng et al., 2011; Gupta et al., 2012). Animals were deeply anesthetized with sodium pentobarbital (100mg/kg i.p.) followed by transcardial perfusion with 100ml of 0.1M sodium phosphate buffer (pH=7.4) followed by 350ml of 4% paraformaldehyde (pH=7.4). The brains were extracted and macroscopically visualized for hemorrhage area. Brains were removed and post-fixed for 24h in 4% paraformaldehyde at 4°C. Brains were then cryoprotected in 10% sucrose solution for 1 day followed by 2 days of 30% sucrose solution and then rapidly frozen on powdered dry ice. Using a sliding microtome (American Optical, Model 860), 45µm coronal sections were cut. Every serial section was saved in 24-well ure plates. Systematic random sampling techniques were used for selecting tissue sections for staining and stereological analysis.

2.5.5 Acute Histology: Neuronal Degeneration

Neuronal degeneration was quantified using stereological techniques at 24h for adult rats after TBI using the histofluorescent stain, FluorJade-B (FJ-B) (Schmued et al., 1997; Schmued and Hopkins, 2000, Gupta et al., 2012). Standard Fluoro-Jade staining procedures were used. Briefly, tissue sections were mounted on gelatin-coated slides in 0.1M PB and distilled H_2O at 1:1 ratio and air-dried overnight. The slide-mounted tissue sections were subsequently immersed in100% alcohol (3 min), 70% alcohol (1min), dH_2O (1 min), and 0.006% potassium permanganate (15 min). Sections were rinsed in dH_2O (1 min), incubated in 0.001% FJ-B (Histo-Chem Inc., Pine Bluff, AK) staining solution in 0.1% acetic acid for 30 min, rinsed again in H_2O (3 min), and air-dried. Finally, the sections were immersed in xylene and cover-slipped with DePeX mounting medium (Electron Microscopy Sciences, Fort Washington, PA).

2.5.6 Stereological Cell Counts for acute neuronal degeneration

The number of FJ-B positive degenerating neurons in the region of interest was quantified using stereological methods. Tissue sections were selected by taking every fifth section starting at Bregma -3.1mm and ending at Bregma -4.7mm for a total of 7 sample sections per brain for the coronal sections. The FJ-B cell counts were made on an epifluorescent microscope (Nikon E600, Nikon, Tokyo) under a mercury arc lamp with a FITC fluorescent filter cube (Nikon B-2A, Tokyo) using a motorized stage (MS-2000, Applied Scientific Instruments, Eugene OR) and computer software (Stereologer^{TM} version 1.3, Systems Planning and Analysis, Inc., Alexandria, VA).

Degenerating cell counts were made in a region of interest encompassing the stratum pyramidale of the dorsal hippocampus CA2-3. The border of the stratum

pyramidal was defined by the pyramidal layer entry into dentate gyrus at the lateral tips of the dorsal and ventral blades of the dentate granule cells on one end and at the other end by the narrowing of the stratum pyramidale at the intersection of the CA1 to CA2. Criterion for counting degenerating neurons (FJ-B positive) included green fluorescing, morphologically distinct cell bodies with at least one clearly identifiable dendrite. The region of interest was outlined using a 2X objective. Neuronal identification and cell counting was performed using a 20X objective.

Chronic Behavioral Evaluation

2.5.7 Rotarod Test:

The vestibular-motor system was assessed with rotarod device. Procedures were followed as described previously (Hamm et al., 1994; Jenkins et al., 1999; Rustay et al., 2003). Animals were trained on the rotarod in four trials over 2 days. The rotarod was operated at a constant speed throughout the training and test days (10 revolutions/minute). On the training days animals were required to walk on the rotating rod for 4 minutes and were placed back on the rod if they fell during the training.

Animals were given 3 baseline trials prior to the surgery on the day of the injury and three trials on each post-injury experimental day (1, 4, 7, 11 and 15 days post injury). Tests were terminated when an animal either fell off the rod or after 2 minutes. The duration the rat managed to stay on the rotarod was recorded. The following figure represents an animal on a rotarod during a trial.

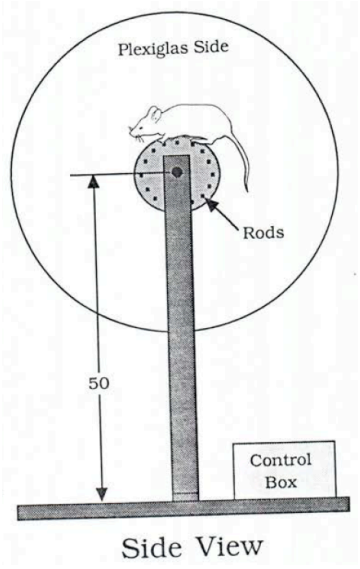

Figure 2.2 Rotarod test. Rats were placed on the rotarod, which revolved at 10 rev/min constant velocity. The duration before fall was recorded. [*Hamm et al., 1994*].

Source Hamm, Robert J., Brian R. Pike, Dianne M. ODell, Bruce G. Lyeth, and Larry W. Jenkins. "The Rotarod Test: An Evaluation of Effectiveness in Assessing Motor Deficits Following Traumatic Brain Injury." *Journal of Neurotrauma* 11.2 (1994): 187-96.

2.5.8 Ladder-rung-walk Test:

Fine motor coordination was assessed with the ladder-rung-walk test. Rats were trained to walk across a horizontal, level ladder 1.1m length X 10cm width. This ladder was bounded between 20cm high transparent Plexiglas walls on both sides. The ladder steps consisted of 0.25cm diameter rungs, with 1.25cm spaces between them. The rats were trained to escape from an aversive auditory stimulus by walking across the ladder in order to enter a goal box at the opposite end. The noise was terminated when the rat entered the goal box at the opposite end of the ladder. The test consisted of 3 such trials. The number of times each leg went down through the rungs was counted as “slips”. The total time required for the rat to traverse the ladder was also recorded. The rats were trained on the ladder for 2 days before the injury and then baseline was recorded prior to the surgery on the day of the injury. The test was performed on days 1, 4, 7, 11 and 15 post-injury. Each

trial on the baseline and test days was recorded using a video camera and later the videos were viewed for analysis.

2.5.9 The Metric and Spatial Information Task

The metric and spatial information task (Goodrich-Hunsaker et al., 2005, 2008) investigated the rat's ability to recognize spatial changes in the environment. It consisted of a habituation period where the exploration duration of the two novel objects is recorded. In this habituation period the novel objects were separated by a fixed distance. Then there was a test period where the objects were moved closer together and the increase in exploration time was recorded. An increase in exploration time during the test period indicated the rat's ability to recognize the change in the object spacing during the test period.

The task is performed on a platform made of white acrylic, 1.22m in diameter, 8cm thick, and 1.1m above the ground. On day 6 and 7 post injury the rat was allowed to explore the platform without the presence of any objects. This was done to habituate the rats to the environment (platform and surroundings). The task was performed on day 8 post-injury. The task consisted of a 15 min habituation period followed by a 5 min test period. The habituation and test period were separated by a 5 min timeout period in which the animal was returned to its home cage. The habituation and test periods were recorded using a ceiling-mounted video camera (Logitech® Webcam Pro 9000). The 15 min habituation period was subsequently broken down into three 5 min bins. During the habituation period there were two objects positioned in the center of the platform 68 cm from each other. The rat was placed on the edge of the platform, equidistant from each object and facing in the direction of both objects. The rat was allowed to explore freely for 15 min. After 15 min the rat was taken off of the platform and placed back in the

home cage for a 5 min timeout period. During this time the platform and objects were cleaned with a 70% alcohol solution and the distance between the two objects was decreased to 34 cm. To start the test period, rats were placed back onto the platform in the same location and allowed to explore freely for an additional 5 min. The amount of time spent in active exploration with the objects, defined as active object sniffing, physical contact, and rearing, was measured for each 5 min interval. Both habituation and test phases were conducted in low light levels.

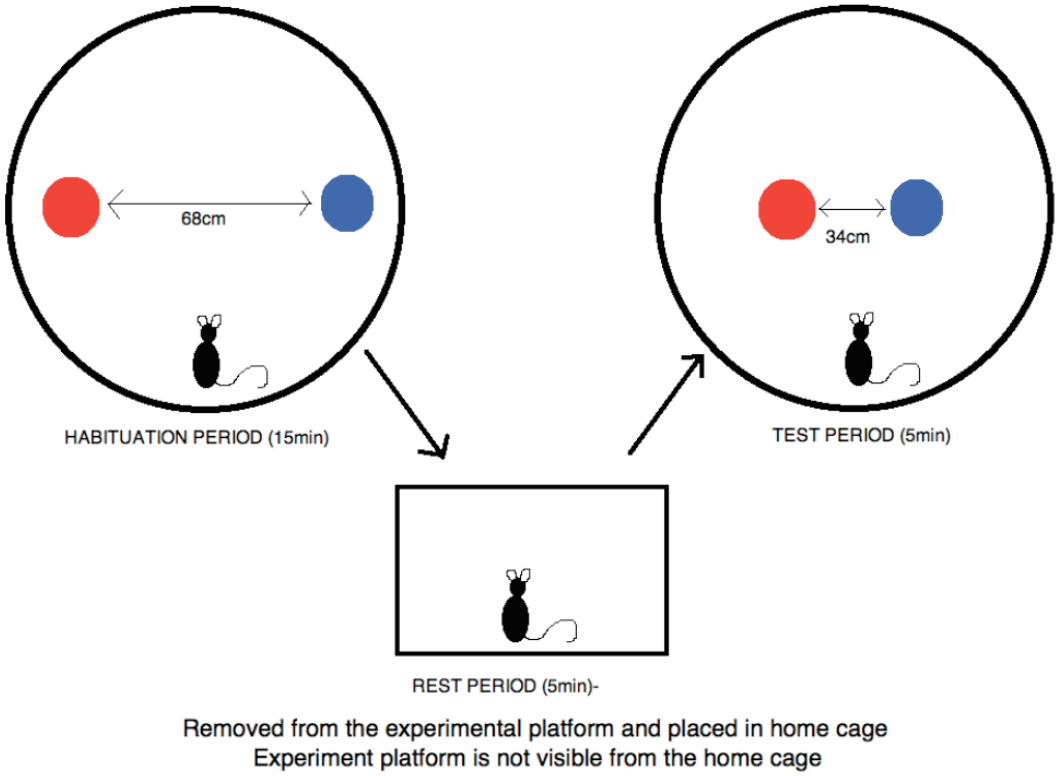

Figure 2.3 The Metric Spatial Information Task: The rat is placed on the platform with two novel objects 68cm apart and allowed to explore freely for 15 min. It was then moved to a home cage for 5 min followed by a 5 min test period in which the object were moved to 34cm apart. The total time for which the rat actively explored the objects was recorded for every 5 min.

Since the absolute exploration time can vary significantly from subject to subject due to the difference in innate curiosity of the animal, the percentage exploration time spent in each 5min intervals was plotted. The formula used is as follows:

$$E = \frac{T_{\text{int}erval}}{T_{total\,\text{exp}loration}} X100 \qquad (2.2)$$

where "$T_{interval}$" is the total time the rat spent exploring the objects in that interval, "$T_{totalexploration}$" is the total exploration time over the habituation and the test period.

2.5.10 Morris-Water-Maze task

Spatial learning/memory performance was assessed with a Morris water maze task on days 11-15 post injury (Morris, 1984). This study involved a hidden platform acquisition to assess spatial learning and memory. The Morris-water-maze is an open-field swimming task. It is an extensively characterized procedure that is especially sensitive to lesions and dysfunction in the hippocampus and has been used extensively in TBI research.

The test apparatus consists of a large white circular tank (183 cm diameter by 60 cm high) filled with water to a depth of 22 cm. Water temperature was maintained at 24-28°C. A transparent circular escape platform (12.8 cm diameter, 20 cm high) was placed in a fixed location in the tank 2 cm below the water surface. Four consistent visual cues were located on the wall of the test room outside of the maze. Each hidden platform trial started by placing the rat in the water close to, and facing the wall of the tank in one of the four start locations in front of the visual cues. Once the rats were in the water they were allowed 120s to find and mount the escape platform. After they mounted the platform they were left there for 30s in order for them to explore the cues and learn the location of the platform. If they were unable to find the platform within 120s, the rat was placed on the platform for 30s before being removed. The starting quadrant was changed randomly for each trial so that the rat was forced to learn the spatial location of the escape platform, rather than simply a swimming direction or response (ie. right vs. left). Subjects received a 4-min inter-trial interval in a warmed holding cage before being

returned to the maze for subsequent trials. Rats received 4 trials per day over 5 consecutive days. Data from all trials were recorded using a video tracking system and analyzed with a data acquisition system (Poly-Track Video Tracking System version 2.1, San Diego Instruments Inc, San Diego, CA). Time to find and mount the submerged platform and distance swam were recorded. Performance for each day was the mean latency of four trials to find the platform.

Short term and long term memory was also analyzed (Feng et al., 2011). Short term memory was assessed by evaluating performance between the first trial of one day and the fourth trial of the same day, inter-trial time of 16 min. Long term memory was evaluated from the performance between the fourth trial of one day with the first trial of the next day; 24 h inter-trial time. These short-term and long-time time differences were termed "memory retention". Thus a positive latency to platform indicated that the MWM performance improved and the memory of the location of the hidden platform was retained. Conversely, a negative value for "memory retention" indicated a worsening of performance and that memory of the location of the hidden platform was not retained.

2.5.11 Chronic Histology: Neuronal Survival

On day 15 post-injury after the completion of all the behavioral tests, brain sections were stained with cresyl violet and surviving pyramidal neurons were quantified using stereological techniques. Tissue sections (45μm) were mounted on gelatin-coated slides and dried overnight before cresyl violet staining. Sections were dehydrated at room temperature by a series of ethanol immersions: 70% (2 min x1), 95% (2 min x2) and 100% (2 min x2) followed by immersion in xylene (16 min). Sections were then rehydrated in a series of ethanol immersions: 100% (2 min x2), 95% (2 min x2) and 75%

(2 min x1), then rinsed with distilled water (30s x2). Sections were next stained with cresyl violet acetate (0.1%) for 6 min followed rinsing in distilled water (15s x2), differentiation by immersion in 95% ethanol with 0.15% acetic acid (8min), and dehydrated in a series of ethanol immersions: 95% (30s x2), 100% (30s x2) and cleared by immersion in xylene (5 minx2). Sections were cover-slipped with Permount (Fisher Scientific, Hampton, NH).

2.5.12 Deformation of Hippocampus

Images of the cresyl violet stained slices were saved and Image J was used to measure the diameter of the contralateral and ipsilateral hippocampus in coronal slices. Then the percentage change in diameter of ipsilateral hippocampus was calculated with reference to the contralateral hippocampus and thus the deformation of the hippocampus was assessed.

$$D = (C - I) * 100 / C \qquad (2.3)$$

"D" is the deformation in %, "C" is the diameter of the hippocampus on the contralateral side (uninjured side) and "I" is the diameter of the hippocampus on the ipsilateral side (injured side).

2.5.13 Stereological Cell Counts

The number of cresyl violet stained neurons in the region of interest was quantified using stereological methods. Tissue sections were selected by taking every fifth section starting at Bregma -3.1mm and ending at Bregma -4.7mm for a total of 7 sample sections per brain for the coronal sections. The cell counts were made on a microscope (Nikon E600, Nikon, Tokyo) with a motorized stage (Bioprecision2, Ludl Electronic Products, Inc.,

Hawthorne, NY) using computer software (Stereo Investigator™ 8.0, Microbrightfield, Inc., Williston, VT).

Surviving neuronal cell counts (15d) were made in a region of interest encompassing the stratum pyramidale of the dorsal hippocampus CA2-3. The border of the stratum pyramidal was defined by the pyramidal layer entry into dentate gyrus at the lateral tips of the dorsal and ventral blades of the dentate granule cells on one end and at the other end by the narrowing of the stratum pyramidale at the intersection of the CA1 to CA2. The criterion for selection and quantification of surviving neurons was a morphologically distinct cell body. The region of interest was outlined using a 10X objective. Neuronal identification and cell counting were performed with a 100X oil objective.

CHAPTER 3

STATISTICAL ANALYSIS

Data analysis was performed using SPSS software (version 17, Chicago IL). General linear model was used for analysis. Alpha level was set to 0.05 for rejecting nulls hypothesis. Data for body weights, and temperature measurements and also for pressure peaks, rise times and impulse were expressed as mean± standard error of mean (SEM) and analyzed using one-way analysis of variance (ANOVA) followed by Bonferroni where appropriate.

All other animal data, including apnea, seizure rates, righting times and toe pinch response, metric spatial information task and electrophysiology data were expressed as mean±SEM. Significance was tested by student's t-test and chi-square test for comparing two sets of data where appropriate. For degenerating neuronal counts (from Fluoro-Jade staining) and surviving neuron counts (from Cresyl violet staining), each were analyzed using a one-way ANOVA and a Dunnett post-hoc analysis.

Behavioral data for rotarod test, ladder rung walk test, and Morris water maze latency was analyzed using repeated measures of ANOVA with assessment days as the repeated variable within subjects followed by Bonferroni post-hoc analysis. Additionally, the difference in latency to platform between the four trials within a day as well as the difference in latency to platform between first trial of a session and the fourth trial of the previous day's session was used as a measure of short-term and long-term memory and was analyzed with one-way ANOVA.

CHAPTER 4

RESULTS

4.1 Closed System Device Characterization

The voice coil Fluid Percussion Injury system (VC-FPI) creates a fluid percussion from the displacement of a fluid piston. Our first test was to compare the pressure waveform from the VC-FPI with the traditional FPI system. Figure 4.1(a) shows output pressure waveforms from both the devices. Even though the area under the curve is different between the two devices when tested under closed conditions (i.e. no rat attached), the overall properties and trend of the pressure waves remain the same. Both pressure waves had a pressure rise to a peak followed by decay to baseline. Next, in order to control the fluid percussion, programmed voice coil – hydraulic cylinder displacements were mapped to peak pressure and pressure rise times. Using a closed system (no animals at the animal injury site and valve at the animal injury site was kept closed, Figure 2.1), input displacements from 0.001m to 0.023m were programmed with a velocity of 2.79m/s and a maximum acceleration of 311m/s^2. The resulting peak pressures were linearly related (n=3 for each displacement; R^2=0.99 for linear trend line) to displacement, Figure 4.1(b). The small standard deviations in pressure peak indicate the repeatability of fluid percussion generation by the device.

Three input displacements were programmed such that they correspond to fluid percussions in the moderate injury range and the corresponding output displacements were recorded using the linear encoder. Mean displacement curves were plotted for programmed input displacements of 0.013m, 0.014m and 0.015m under closed system conditions (n=5 for each of the 3 input displacements) (Figure 4.1(c)). All the three

displacement curves showed smooth transition and uniform pattern. Resultant mean output peaks were 8.25±0.16mm, 9.12±0.0.16mm and 9.76±0.22mm respectively. The output displacements are lesser than the input displacements owing to frictional forces. Plots of the voice coil – hydraulic cylinder motion (Figure 4.1(c)) verify uniformity of output displacement of the piston.

Changes in voice coil velocity, keeping displacement constant, results in pressure waveforms with different rise-times with constant peak pressures. A displacement resulting in peak pressures of 2.15 atm programmed at two different velocities (n=1). Figure 4.2(a) illustrates the resulting pressure waveforms with constant peaks and different rise-times. Changes in voice coil displacement, keeping velocity constant, results in pressure waveforms with different pressure peaks with constant rise-times (n=1). Figure 4.2(b) illustrates waveforms with the same rise-time but different peak pressures. This demonstrates that the pressure peak and rise-times of the pressure waveforms can be varied independent of each other.

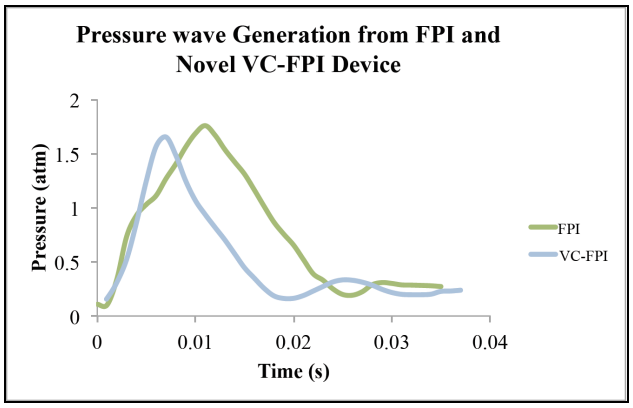

(a)

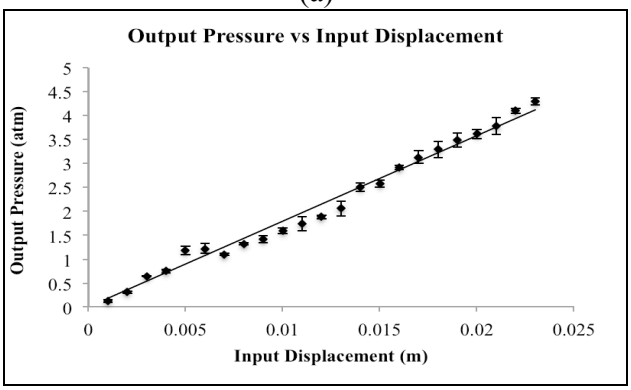

(b)

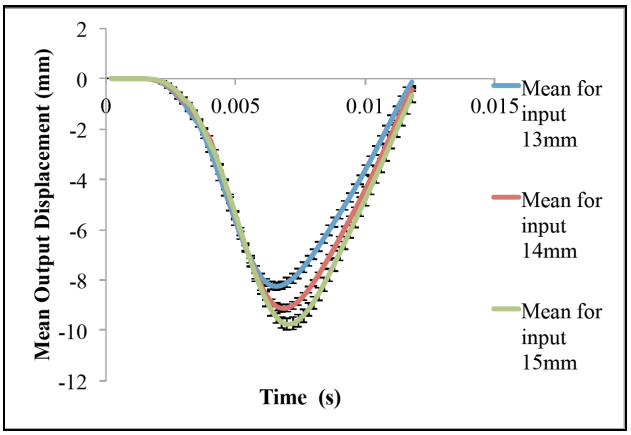

(c)

Figure 4.1 Closed System Device Characterization. (a) Output pressure waves generated by FPI and VC-FPI device. (b) Input vs Output Characteristics of the VC-FPI system. For a range of input displacements from 0.001m to 0.023m, the output pressure peaks were recorded and the results showed a linear system response. (c) Mean output displacements for 3 different input displacements around moderate injury magnitude. All three output displacements were smooth curves with no apparent ripple. Peak output displacements were 8.25±0.16mm, 9.12±0.0.16mm, 9.76±0.22mm respectively.

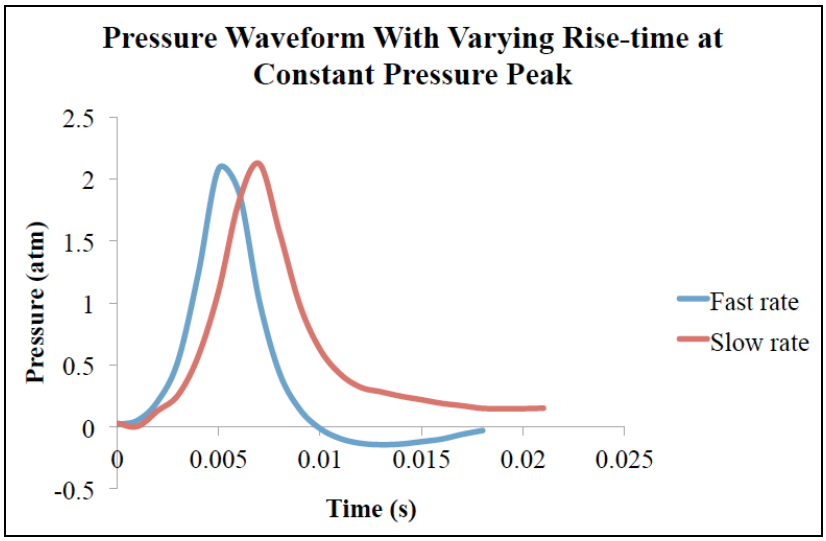

(a)

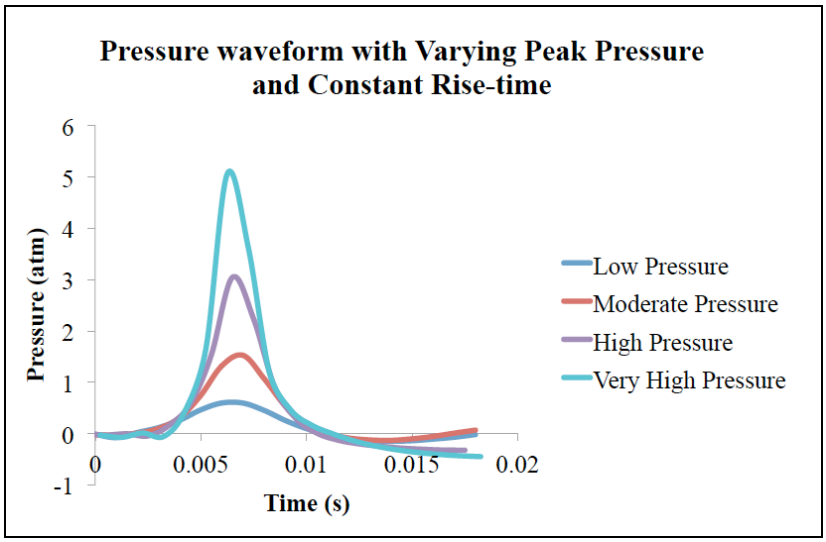

(b)

Figure 4.2 (a) Comparison of pressure waveforms of various rates but constant pressure peaks using the VC-FPI system (b) Comparison of pressure waveform with varying pressure levels but constant rate. Figure (a) and (b) shows that the VC-FPI device is capable of generating pressure waveforms at various rates keeping the peak pressure constant and also at various pressure peaks keeping the rate constant and hence is a modular device.

A unique ability of this device allows one to examine how the rise-time of the pressure of the trauma to the brain affects injury outcome. For this study our goal was to investigate the generation of pressure waves with various rise-times. We examine the

maximum velocity that could be achieved by the voice coil that would result in the fastest fluid percussion rise time. This rate can then be compared to typical and slower rates of fluid percussions. Using a mild to moderate fluid percussion magnitude of 2.15atm corresponding to a displacement of 2.5mm, we increase the velocity until maximum rise time was achieved. The maximum output velocity capable by the device was 2.78m/s, any velocity within that limit, allowed consistent motion generation. The maximum velocity generated pressure waveforms having a rise-time of 3msec (in the closed system).

In case of the slow rate operation of VC-FPI device, the velocity and acceleration (Velocity was 1.27m/s and acceleration 25.4m/s^2) that gave the slowest rise time (4msec in closed system) capable by the device, was chosen as the slow rate injury. The device was also tested for consistency in operation at this slow rate.

To compare the VC-FPI system to the standard FPI system, pressure waveforms were generated from each device. In the VC-FPI device, fast-rate (2.78m/s) and slow-rate (velocity 1.27m/s) settings were used. To compare the devices without the influence of a load (e.g. animal attached), pressure waveforms were generated without the presence of any animals and with a closed valve at the injury site (valve 1 in Figure 2.1(a)). Summary graphs were plotted for pressure peak, rise-time and impulse (Figure 4.3).

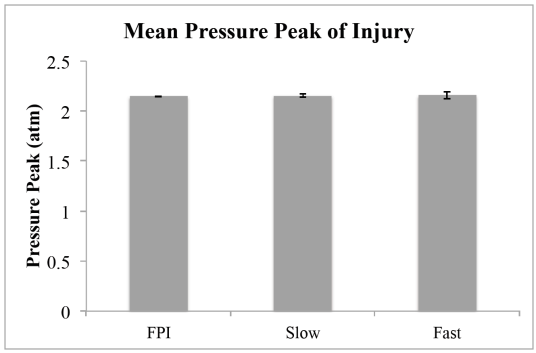

(a)

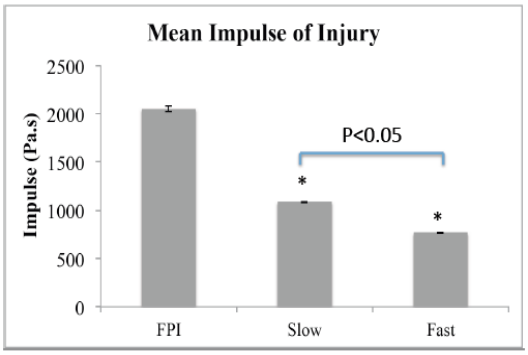

(c)

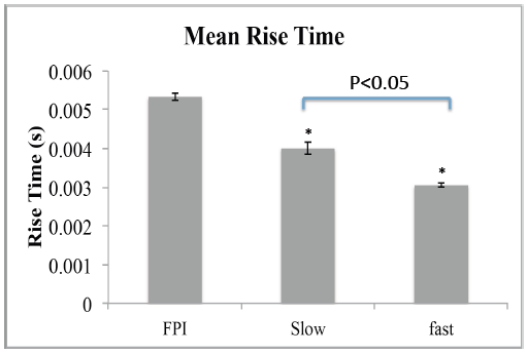

(b)

Figure 4.3 Waveform Analysis Performed During Closed System Device Characterization. Mean values were compared between commonly used FPI system and fast-rate and slow-rate from VC-FPI system. (a) Mean Pressure peaks were compared and results showed them to be similar in all three. (b) Mean rise-times were compared; rise-time for the FPI was the most, the slow-rate VC-FPI was less and the fast-rate VC-FPI was the least. (c) Mean Impulse (area under the curve) of injury was compared and also showed the same trend. Standard error bars shown in (a), (b) and (c). *Indicates significant differences by ANOVA and Bonferroni post hoc analysis between FPI and the slow and fast-rate from VC-FPI.

All values were expressed as mean±SEM (Standard Error of Mean) and analyzed using separate one-way ANOVA between groups. The pressure peaks from all the three sets were similar [2.14±0.002atm for FPI (n=10), 2.15±0.033atm for fast-rate VC-FPI (n=10) and 2.15±0.015atm for slow-rate VC-FPI (n=10), Figure 4.3 (a)]. Statistical analysis by ANOVA revealed that there was no significant difference between any of

the groups in terms of pressure peak [$F(2,27)=0.059$, $P\cong1$]. The average rise-times for fast-rate VC-FPI injury was 3.1±0.05ms, slow-rate VC-FPI injury was 4±0.15ms, and that of FPI was 5.3±0.09ms (Figure 4.3 (b)). One-way ANOVA between groups revealed that the rise times were significantly different between all the groups [$F(2,27)=121.032$, $P<0.001$]. The Impulse was then calculated from the area under the curve. The Impulse for the fast-rate VC-FPI injury was the least (762±11 Pa.s) followed by the slow-rate VC-FPI injury (1086±8 Pa.s) and the standard FPI injury was the highest (2052±33 Pa.s) (Figure 4.3 (c)) One-way ANOVA revealed that the impulse between the three groups were significantly different [$F(2,27)=1057$, $P<0.001$]. These results show that the VC-FPI is capable of generating pressure waveforms with distinct rise-times but keeping the pressure peak constant in a closed system.

4.2 Device Characterization During Animal Injuries

4.2.1 Comparison of Pressure Waveforms with Animals

The generation of fluid percussions with a rat attached was compared between devices. Fluid percussion injuries were carried out at a moderate injury peak pressure level adjusted to 1.77atm on adolescent rats and to 2.15atm on adult rats. The VC-FPI system was programmed to create a fluid percussion similar to the conventional FPI device. In addition, the VC-FPI system was programmed to create a faster fluid percussion. Figure 4.4 (a) and (b) shows representative pressure waves from adolescent and adult injuries. The slow-rate VC-FPI is closely related to the standard FPI with similar rise-time, and the fast-rate VC-FPI has a much faster rise-time than the slow-rate VC-FPI and the standard FPI pressure wave.

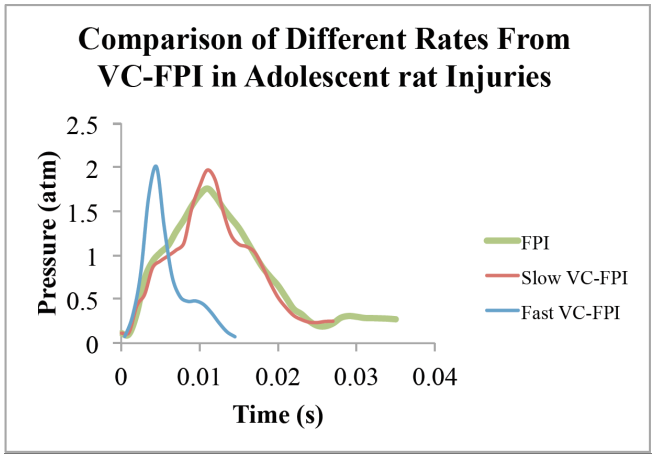

(a)

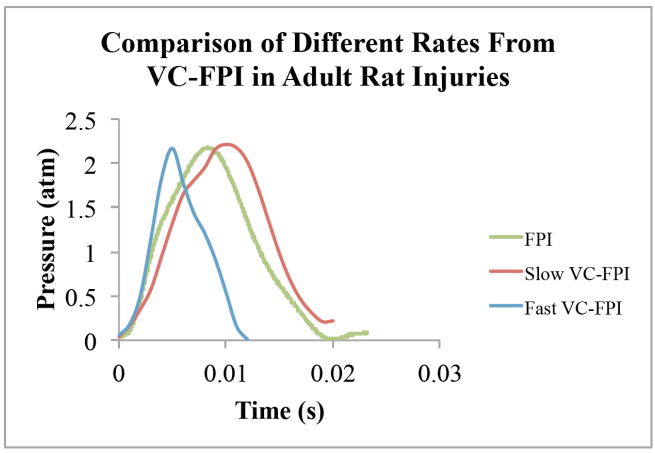

(b)

Figure 4.4 Representative Pressure Wave Profiles of the Fast-rate VC-FPI and Slow-rate VC-FPI. Using FPI and VC-FPI System with (a) adolescent rats and (b) adult rats. The graphs show fast-rate VC-FPI waveforms have shorter rise-time than slow-rate VC-FPI waveforms in both adult and adolescent animals. The graphs also show that the slow-rate VC-FPI waveform is very similar to the FPI waveform in both adolescent rats and adult rats.

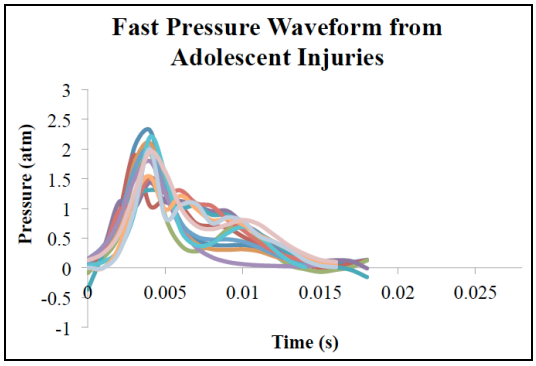

(a)

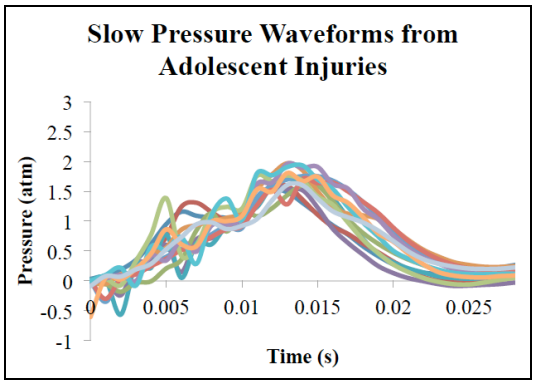

(b)

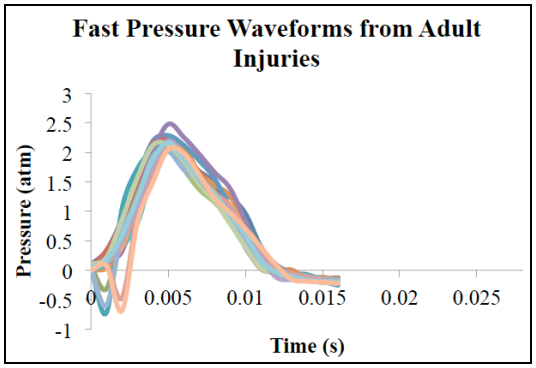

(c)

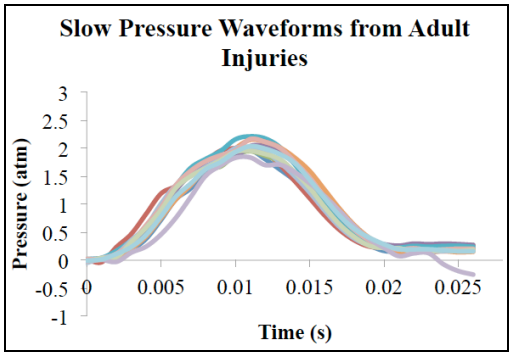

(d)

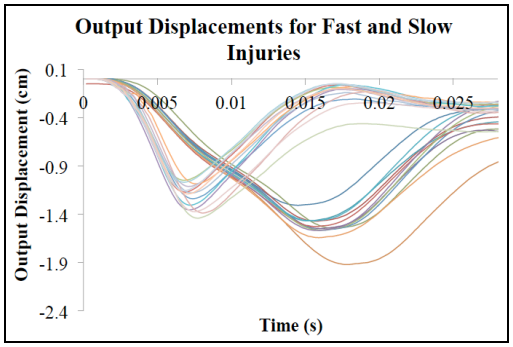

(e)

Figure 4.5 Overlapped Output Pressure and Displacement waveforms (a) fast-rate VC-FPI injuries adolescent rats and (b) slow-rate VC-FPI injuries adolescent rats. (c) fast-rate VC-FPI injuries adult rats and (d) slow-rate VC-FPI injuries adult rats. The adolescent animal injury pressure waveforms show greater number of ripples than the adult injury waveforms. (e) Overlapped output displacements for both fast-rate VC-FPI and slow-rate VC-FPI injuries for adolescent rats.

All injuries from the adolescent and adult rats in both the fast-rate and slow-rate VC-FPI injury were overlapped and plotted on charts (Figure 4.5 a-e). In the adult rats, in both fast-rate VC-FPI and slow-rate VC-FPI, the pressure waveforms were more smooth and uniform than the adolescent rats. Therefore the output displacements during the fast-rate VC-FPI and slow-rate VC-FPI injuries were also generated and overlapped on one chart. It was seen that, despite the adolescent output pressure waveforms having increased ripples than the adult rats, the displacement waveforms were smooth. This shows that the voice-coil makes a smooth and consistent motion but depending on the load, the output may be less smooth and consistent. Also, from the charts it should be noted that, the rise time was different between the fast-rate VC-FPI and slow-rate VC-FPI injuries, but the pressure peaks were kept constant.

In some of the pressure waves there is a negative pressure value just before the start of the positive pressure. However, this is not a result of any negative pressure in the system since there is no motion in that direction. The negative value may be as a result of stray voltage data from other parts of the device and not from a change in pressure.

4.2.2 Fluid Percussion Injury Waveform Analysis

A complete waveforms analysis was performed to quantify pressure peak, rise-time, and impulse, of all the injuries in the adult and adolescent rats from FPI system and VC-FPI system in both fast-rate and slow-rate modes of operation.

In order to establish the independence of the rise-time of injury from the pressure peak of the injury, the average pressure peaks were first plotted (Figure 4.6 (a)). All injuries were set up to be at a moderate injury level of 1.77atm for adolescent rats and

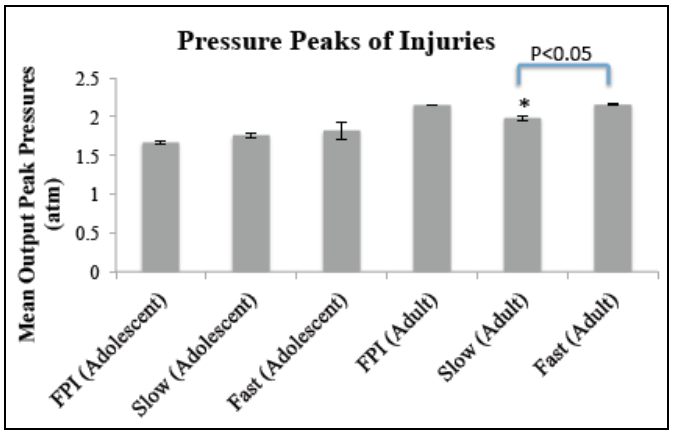

(a)

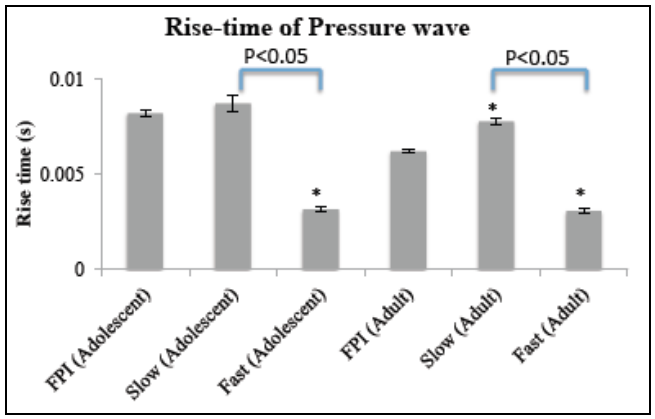

(b)

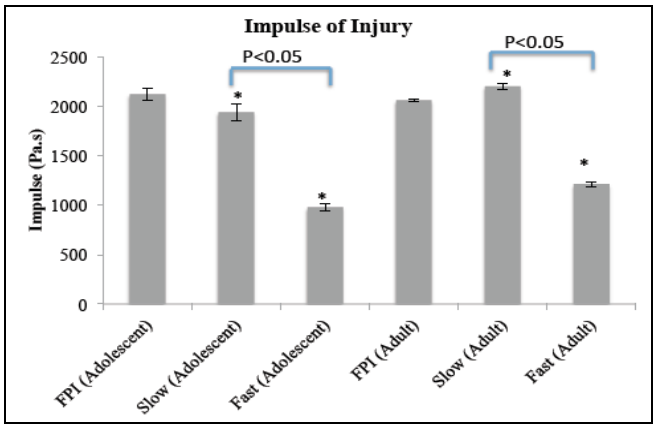

(c)

Figure 4.6 Waveform Analysis During Animal Injuries: Both adolescent and adult rats were compared. (a) Mean Pressure peaks were compared. For adolescent rats the target pressure peak for a moderate injury was 1.77 atm and that for adult rats were 2.15 atm. Mean (b) rise-times and (c) impulse response of adolescent and adult rats for FPI injuries, fast-rate and slow-rate VC-FPI injuries was compared. Standard error bars shown in (a), (b), and (c).*Indicates significance by ANOVA and Bonferroni post hoc analysis

2.15 atm for adult rats. All values were expressed as mean±SEM (Standard Error of Mean) and analyzed using separate one-way ANOVA between groups. In adolescent rat injuries, the pressure peaks from all the three sets were similar [1.67±0.03atm for FPI (n=9), 1.77±0.04 atm for slow-rate VC-FPI (n=17) and 1.82±0.11atm for fast-rate VC-FPI (n=20), Figure 4.6 (a)]. Statistical analysis by ANOVA revealed that there was no differences between any of the groups in terms of pressure peak [$F(2,43)=0.6$, $P\cong1$]. This shows that the device was capable of keeping the pressure peak constant (upon adjusting the inputs) when operating at different velocities (fast and slow-rate VC-FPI) when adolescent rats were attached at the animal injury site.

The average rise-times for FPI was 8.2±0.2ms (n=9), slow-rate VC-FPI injury was 8.7±0.4ms (n=17) and fast-rate VC-FPI injury was 3.1±0.1ms (n=20) (Figure 4.6 (b)). One-way ANOVA between groups revealed that there was a significant difference in the rise times between the groups [$F(2,43)=135.9$, $P<0.001$]. Bonferroni post-hoc analysis reveals that the difference between the rise-time of FPI and slow-rate VC-FPI was not significant, but the rise time of fast-rate VC-FPI was significantly less than the FPI and slow-rate VC-FPI. This shows that the device is capable of generating waveforms with distinct rise-times in the presence of an adolescent rat (load) at the animal injury site.

The impulse of the pressure waveform – a representation of the total energy transferred to the brain tissues instead of the rate or peak pressure alone; is the loading experienced during a TBI. The Impulse was calculated from the area under the curve. The Impulse for the standard FPI injury (n=9) was the highest (2121±61 Pa.s), followed by the slow-rate VC-FPI injury (1940±86 Pa.s) (n=17) and the fast-rate VC-FPI injury was the least (979±36 Pa.s) (n=20) (Figure 4.6(c)) One-way ANOVA revealed that there was

a significant effect of group on impulse [$F(2,43)=93.05$, $P<0.001$]. Bonferroni post hoc analysis revealed that there was a significant difference between the impulse between the standard FPI, slow-rate and fast-rate VC-FPI waveforms. Therefore the impulses of the pressure waves were significantly different between the groups when an adolescent animal was attached at the injury site, despite the fact that the pressure peaks were kept the same.

In adult rats, statistical analysis revealed that the pressure peak of FPI (2.15±0.003atm, n=23) and the fast-rate VC-FPI (2.15±0.02atm, n=21) varied within a narrow range (Figure 4.4(a)) and was not significantly different ($P>0.05$). However, the pressure peak of slow-rate VC-FPI (1.98±0.03atm, n=27) was lower than FPI and fast-rate VC-FPI [$F(2,68)=21.88$, $P<0.05$]. The average rise-times for the FPI was 6.2±0.07ms (n=13), fast-rate VC-FPI injury was 3.0±0.11ms (n=21) and that of slow-rate VC-FPI injury was 7.7±0.16ms (n=27) (Figure 4.4(b)). Results from one-way ANOVA, revealed a significant difference in rise-time by group [$F(2,58)=317.4$, $P<0.001$]. By Bonferroni post hoc analysis it was revealed that the rise-times were significantly different between all three groups at 95% confidence interval. Fast-rate VC-FPI having the shortest rise time, followed by the FPI, followed by Slow-rate VC-FPI, which had the longest rise time.

The objective was to keep the pressure peak the same between the groups and only change the rise-times between the groups in order to test the pathophysiology based on injury rates. Therefore the rise-times were significantly different. However, for the slow-rate injury group the pressure peak was lower than the other two groups. The slow-rate injury had the slowest rise-time and this group was not able to sustain a pressure

equal to the other groups. Using pressure peaks similar to other groups resulted in deaths in case of a slow-rate VC-FPI injury. Therefore a lower pressure peak was used.

The FPI injury and slow-rate VC-FPI resulted in distinct impulse response (FPI had an impulse of 2059±13 Pa.s, (n=13) and slow-rate VC-FPI had an impulse of 2198±35 Pa.s (n=27)) where the slow-rate VC-FPI injury had a higher impulse (Figure 4.4(c)). The impulse of the fast-rate VC-FPI was significantly lower (fast-rate VC-FPI had an impulse of 1211±22 Pa.s (n=21)) than both of FPI and slow-rate VC-FPI injuries. Results from one-way ANOVA, revealed a significant difference in impulses by group [$F(2,58)=331.12$, $P<0.001$]. By Bonferroni post hoc analysis it was revealed that the impulses were significantly different between all three groups at 95% confidence interval. This result shows that the impulse can be distinct even under conditions where the pressure peaks remained the same. The following table shows a summary of all the results depicted in the above figures.

Table 4.2: Summary of Results

	Peak Pressure (atm)	**Impulse (Pa.s)**	**Rise-time (ms)**
FPI (Adolescent)	1.67±0.03	2121±61	8.2±0.2
Slow-rate VC-FPI (Adolescent)	1.77±0.04	1940±86	8.7±0.4
Fast-rate VC-FPI (Adolescent)	1.82±0.11	979±36	3.1±0.1
FPI (Adult)	2.15±0.003	2059±13	6.2±0.1
Slow-rate VC-FPI (Adult)	1.98±0.03	2198±35	7.7±0.2
Fast-rate VC-FPI (Adult)	2.15±0.02	1211±22	3.0±0.1

4.3 Adolescent Rat Experiments

4.3.1 Immediate Behavioral Response

The immediate behavioral response of rats to a fluid percussion (from VC-FPI device) at the two different rates of injury (fast-rate VC-FPI is rise time 3.1±0.1ms (n=16) and slow-rate VC-FPI is rise-time 8.8±0.4ms (n=14); $F(2,36)=168.6$, $P<0.001$) but similar pressure peaks (fast-rate VC-FPI is 1.77±0.10atm (n=16) and slow-rate VC-FPI is 1.78±0.03atm (n=14); $F(2,36)=0.547$, $P\sim1$) was examined. The impulse of these groups were also calculated (960±38 Pa.s (n=16) for fast-rate VC-FPI injuries and 1954±77 Pa.s (n=14) for slow-rate VC-FPI injuries, $F(2,36)=114.9$, $P<0.001$). The percentage of rats that demonstrated immediate behavioral seizures and death was significantly lower in fast-rate VC-FPI injury than in the slow VC-FPI injuries (% rats with seizures, fast-rate=0%, n=16 and slow-rate=72%, n=18, $p<0.05$ by Chi-Square test. % Death, fast-rate=0%, n=16, slow-rate=22%, n=18, $p<0.05$ by Chi-squared test) (Figure 4.7 (a)). However there was no difference in the duration of apnea (Figure 4.7 (b)) between rats injured with fast-rate and slow-rate VC-FPI injuries (Apnea in sec, fast=19±2s, n=16 and slow=25±4s, n=18, $p>0.05$, t-test). Sham TBI rats suffered no seizures, death or apnea (n=7).

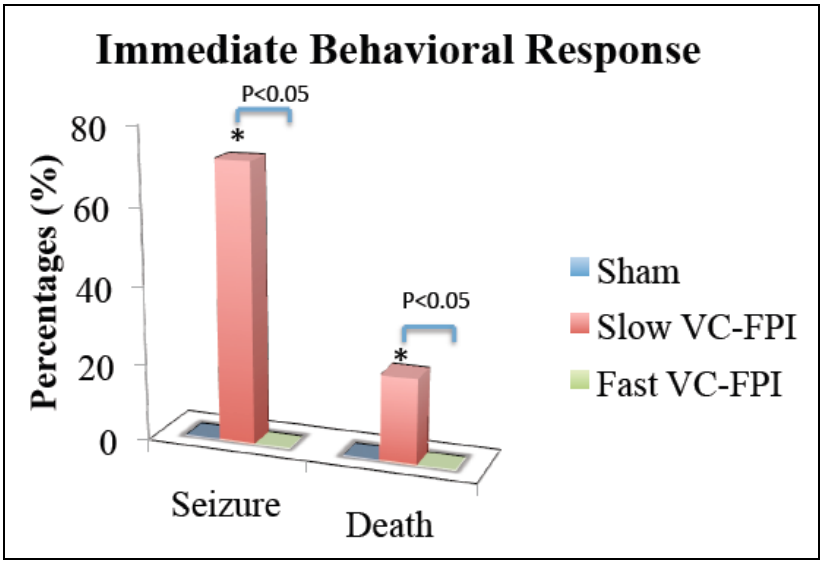

(a)

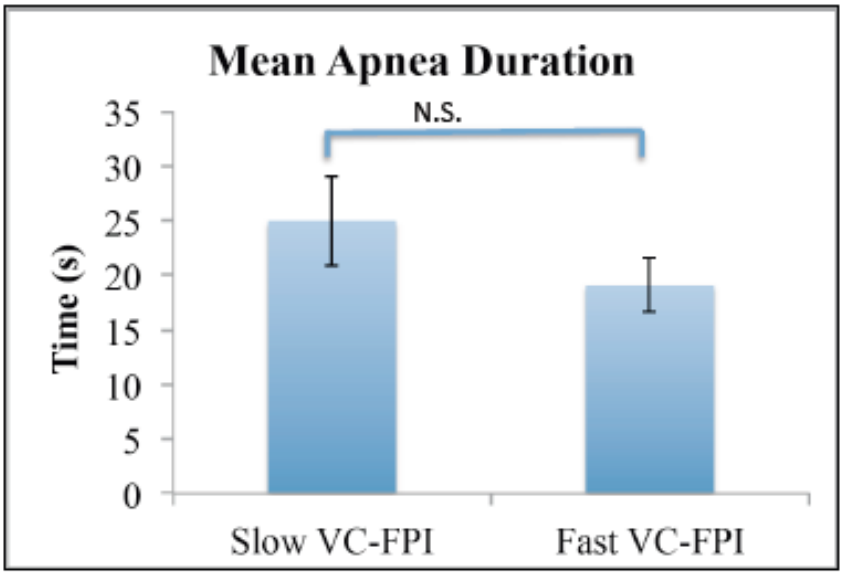

(b)

Figure 4.7 Seizure and Survival Rate and Average Apnea Duration Immediately After Injury. (a) Percentage of animals that did not seize and the percentage of animals that survived immediately after the injury was also recorded. (b) Average apnea duration for fast-rate VC-FPI injured animals (n=16) and slow-rate VC-FPI waveform injured animals (n=18) immediately after the injury, was recorded. In both cases, fast-rate VC-FPI injured animals showed improved immediate response than the slow-rate VC-FPI injured animals. *Significance tested by chi-squared test (Seizure and Death) and t-test (Apnea).

Four hours after injury a set of animals (sham: n=1, fast-rate VC-FPI: n=1, slow-rate VC-FPI: n=1) were sacrificed by transcardial perfusion of 4% Paraformaldehyde. The brains were extracted and macroscopically evaluated for differences in hemmorhage. The figure below shows the sham, slow-rate VC-FPI injury sustained and fast-rate VC-FPI injury sustained brains. This observation suggests that the slow-rate injury had greater widespread and extensive hemmorhage than the fast rate injury.

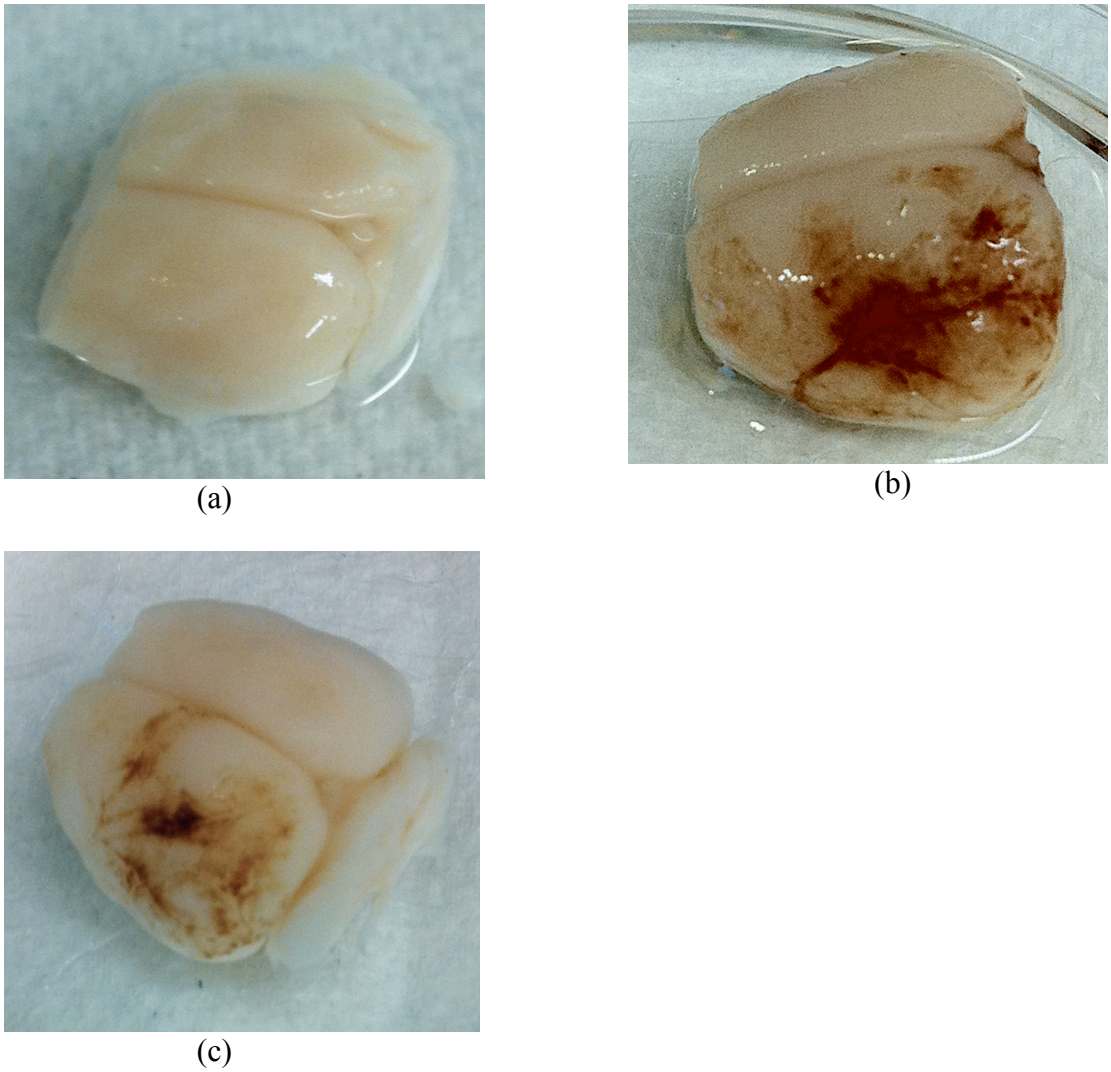

(a) (b) (c)

Figure 4.8 Representative Brain Images. This figure shows representative images that illustrate the larger hematoma following slow-rate VC-FPI injury comared to fast-rate VC-FPI injury. These images were taken from animals perfused with 4%PFA 2-4h after the injury. (a) sham TBI, (b) slow-rate VC-FPI injury sustained animal, (c) fast-rate VC-FPI injury sustained animal.

4.3.2 Acute Histology: Neuronal Degeneration

Early neuronal degeneration was examined using Fluoro-Jade (FJ-C) as a marker at 4h after TBI and quantified in the hilus of the ipsilateral dentate gyrus of sham TBI, slow-rate VC-FPI and fast-rate VC-FPI injured animals. Cells staining positive for Fluoro-Jade fluoresced brightly with prominent somata. Figure 4.9(a) shows horizontal sections of the ipsilateral hippocampus of the adolescent animals. In figure (a), shows the hilus, where

panel A shows the images from sham animals, panel B from slow-rate VC-FPI and panel C from fast-rate VC-FPI. From the figures it is apparent that the number of degenerating neurons 4h after the injury is highest after slow-rate VC-FPI, fewer in the fast-rate VC-FPI and the least in the sham TBI animals. The number of degenerating neurons in the hilus of the ipsilateral dentate gyrus was quantified (Figure 4.9 (b)). The quantification was carried out in the hilus region was different between the groups (Estimated number of degenerating hilar neurons per section, fast-FPI: 38.0±4.6, median = 38, IQR = 66.0-123.0, n = 19 sections from 3 rats; standard FPI: 165.2±27.1, median = 118.0, IQR = 84.0-200.5, n = 20 sections from 3 rats; sham: 6.7±2.8, median = 1.5, IQR = 0.0-14, n = 14 sections from 3 rats; [$F(2,4)=17.142$, $p<0.05$, ANOVA]). Bonferroni Post-hoc Analysis revealed slow-rate VC-FPI had greater number of degenerating neurons compared to fast-rate VC-FPI injured animals. All injured animals had greater numbers of degenerating neurons compared to sham animals.

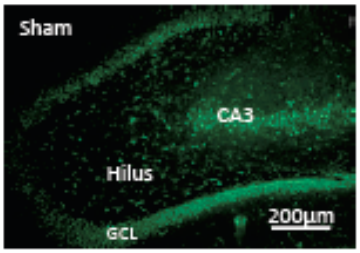

A

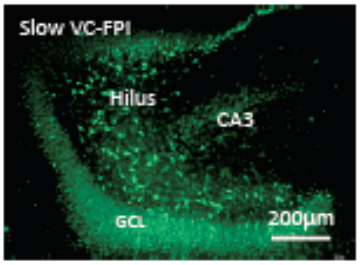

B

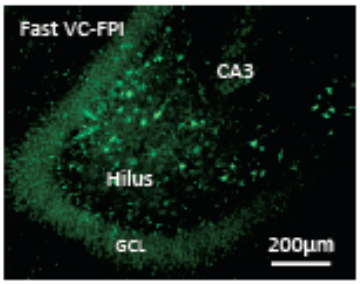

C

(a)

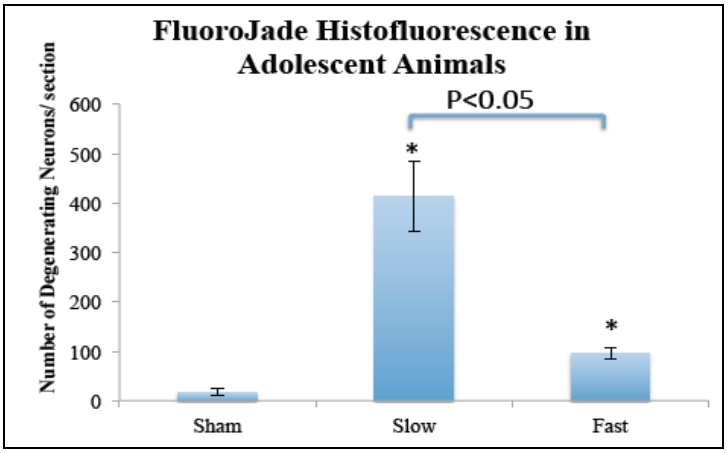

(b)

Figure 4.9 FluoroJade Histofluorescence of Degenerating Neurons 4h after Injury on Adolescent Rats. (a) Horizontal sections showing hilus of sham, slow-rate and fast-rate VC-FPI injured animals; fluorescing cells are in the process of degeneration (Panel 1). Unlike sham TBI animals, sections from rats injured by both fast-rate VC-FPI and slow-rate VC-FPI waveforms show degenerating neurons. (b) Summary plot showing degenerating neuron counts in the hilus, estimated by stereology per section. Hilar neuronal degeneration after fast-rate VC-FPI injury is significantly lower than after slow-rate VC-FPI injury. (*P<0.05 by ANOVA and Bonferroni post hoc analysis compared to sham group).

4.3.3 Electrophysiology

The granule cell population response to afferent activation was examined in order to study the effect of injury rate (fast-rate and slow-rate VC-FPI) on neurophysiology 1-week post injury. The following figures (Figure 4.10 (a) and (b)) show the outcomes of the electrophysiological recordings performed in rats injured at 2 different injury rates (fast-rate and slow-rate VC-FPI) and sham-TBI animals 1-week post injury. Figure 4.10(a) shows representative perforant path-evoked granule cell field recordings from slices from injured rats and sham TBI. The population spike amplitude is the negative spike at or near the peak. As can be seen from the figure, granule cell population response evoked by perforant path stimulation at 4mA resulted in population spike in both the fast-rate and the slow-rate VC-FPI injury, but there was no apparent population spike in the sham-TBI controls in most of the experiments. In addition, the population spike amplitude was similar in both fast-rate and slow-rate VC-FPI animals. Summary plot (Figure 4.10 (b) sham n=3, slow-rate VC-FPI n=4, fast-rate VC-FPI n=4) was generated with the mean population spike amplitudes and the resulting population spike amplitudes were not different between the fast-rate and the slow-rate VC-FPI animals. Also, both fast and slow-rate VC-FPI have an increase in average population spike amplitudes compared to the sham control.

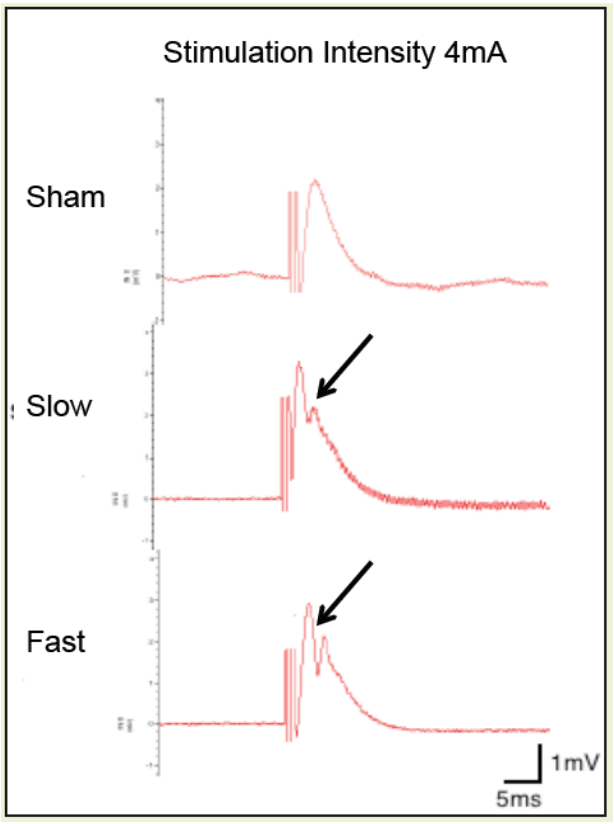

(a)

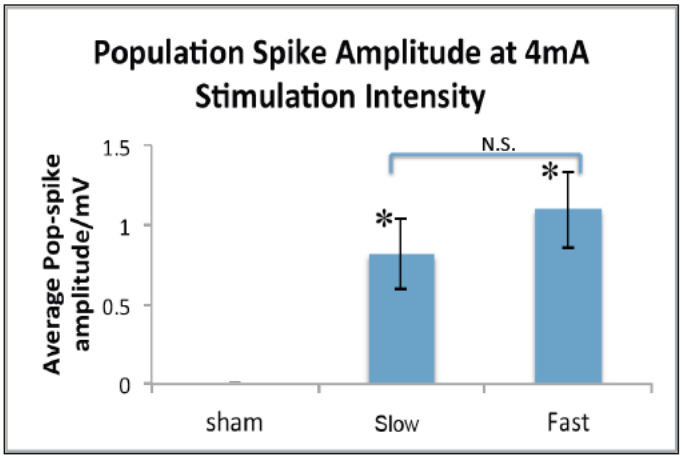

(b)

Figure 4.10 Electrophysiology Representative Curves and Summary Plot at 4mA Stimulation Intensity. Electrophysiological recordings were performed on adolescent animals. (a) Population spike amplitude for sham TBI, slow-rate and fast-rate VC-FPI at stimulation intensity of 4mA. Arrow points to a population spike which is the negative peak at or around the positive peak. The amplitude of this negative peak is the population spike amplitude. (b) Summary plot shows population spike amplitudes. Results show increase in population spike amplitude equally for slow-rate and fast-rate VC-FPI injured animals. *P<0.05 by ANOVA and Bonferroni post hoc analysis compared to sham group.

One way ANOVA between groups show a significant difference between groups in population spike amplitude [$F(2,8)=5.800, P<0.05$]. Post hoc Bonferroni test reveals that there was no significant differences between the fast-rate VC-FPI group and slow-rate VC-FPI group. An increase in dentate excitability have been suggested to predict development of long-term neurological complications (Lowenstein et al., 1992, Toth et al., 1997). In our case since both fast-rate and slow-rate VC-FPI groups show similar enhancement in dentate excitability, this shows that both the injured groups have similar impairment. Therefore, even though the fast-rate VC-FPI results in better immediate behavior and cellular injury within 4 hours after the injury than slow-rate VC-FPI, the similar enhancement in dentate excitability 1 week after injury, shows that early behavioral and cellular injury outcomes is not indicative of the severity of physiological pathology at a later time.

4.4 Adult Rat Experiments

4.4.1 Immediate Behavioral Response

The immediate behavioral response of rats to the three different rates of injury; FPI (rise-time 6.2±0.07ms, n=13), slow-rate VC-FPI (rise-time 7.6±0.2ms, n=17) and fast-rate VC-FPI (rise time 3.0±0.12ms, n=19) were examined [rise-time one way ANOVA between groups $F(2,46)=277.8, P<0.05$]. The pressure peak of FPI (2.15±0.01atm, n=13) and the fast-rate VC-FPI (2.15±0.02atm, n=19) varied within a narrow range and were not significantly different ($P>0.05$). However, the pressure peak of slow-rate VC-FPI (1.98±0.03atm, n=17) was lower than FPI and fast-rate VC-FPI; [$F(2,46)=17.3, P<0.05$]. The pressure was kept lower since any pressure higher than this resulted in immediate death in animals. The impulse calculated in these groups were 2059±13 Pa.s for FPI

injuries (n=13), 2201±43 Pa.s for slow-rate VC-FPI injuries (n=17) and 1214±25 Pa.s for fast-rate VC-FPI injuries (n=19) [$F(2,46)=317.56$, $P<0.001$]. The immediate behavioral response of rats to the two different rates of injury was examined. The duration of suppression of the righting reflex and responsiveness to toe-pinch was measured. The mean righting time and time to toe pinch response of the TBI groups was longer than sham-TBI rats as expected. It was seen in both cases that the slow-rate VC-FPI injury animals had the longest righting time, with an average righting time of 18±1.1min (n=13) and toe pinch response of 6.3±0.3min (n=12), followed by the FPI with an average righting time of 16±1.0min (n=16) and toe pinch response of 5.4±0.2min (n=16), then the fast-rate VC-FPI injured animals with an average righting time of 14±1.3min (n=14) and a toe pinch response of 5.0±0.1min (n=14), and the sham recovered fastest with a righting time of 6±0.4min (n=14) and toe pinch response of 3.8±0.2min (n=14) (Figure 4.11).

Results from one-way ANOVA, revealed significant difference in righting time by group [$F(3,53)=25.509$, $P<0.001$] and also significant difference in toe pinch response by group [$F(3,53)=24.583$, $P<0.001$]. Based on grouping using Bonferroni method and 95% confidence, the righting times and toe pinch response of the slow-rate VC-FPI injury sustained animals were significantly longer than the fast-rate VC-FPI injured animals. The slow-rate VC-FPI injured animals had similar righting times and toe pinch response times as the FPI injured group. Also, the righting time and toe response both showed that the injured groups were all significantly different from the sham group. This shows that the slow rate injury has slower immediate neurological recovery than faster rate injuries. Rectal temperature measured immediately after the injury were not significantly different between groups [$F(3,53)=2.86, P\cong0.05$].

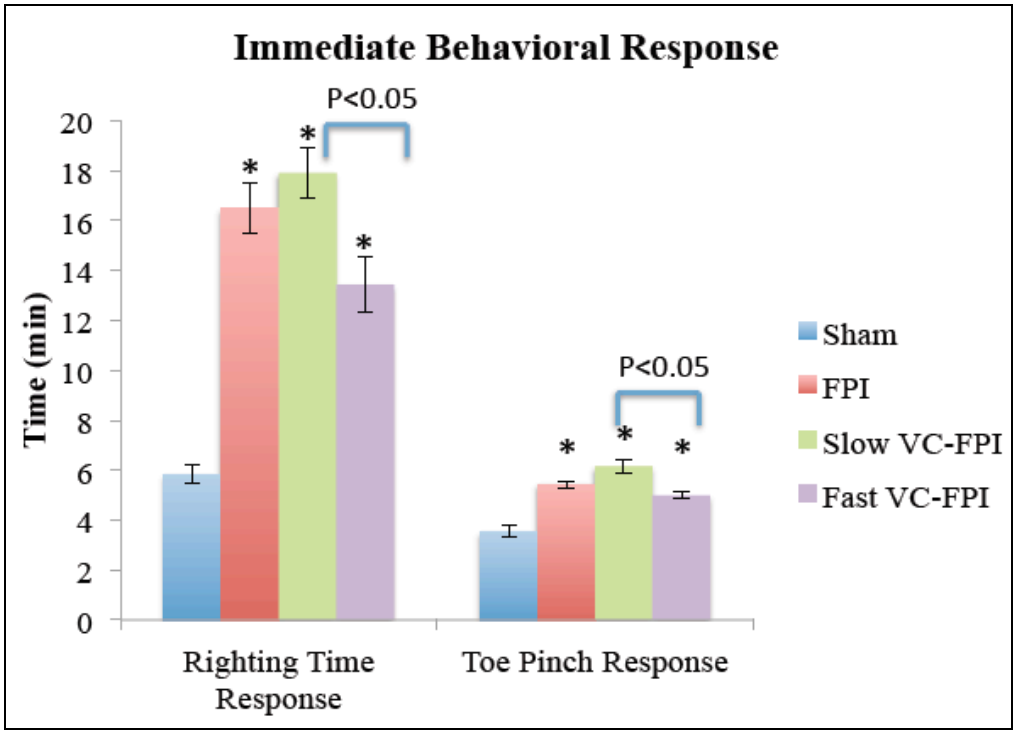

Figure 4.11 Immediate behavioral response of adult animals post injury. Righting time and toe pinch response was recorded. Righting reflex assessment was performed by placing the rat in a supine position at regular intervals (~30sec intervals) to test the rat's ability to spontaneously recover to a prone position. In the toe pinch response the toe is firmly pinched between the fingers to elicit a withdrawal response by the animal. Toe was pinched at regular intervals (~15sec intervals) to check for responsiveness in the hind limbs. *Indicates significance by ANOVA and Bonferroni post hoc analysis compared to sham TBI group.

4.4.2 Acute Histology: Neuronal Degeneration

Early neuronal degeneration was detected with Fluoro-Jade B at 24h after TBI and quantified in the stratum pyramidal CA2-3 fields of the ipsilateral hippocampus. Cells staining positive for Fluoro-Jade fluoresced brightly with prominent somata and extensive dendritic arborization. Figure 4.12(a) shows coronal sections of the CA2-3 region of the contralateral and ipsilateral hemispheres. Upon visual inspection at 20X fluorescing neurons were visible in the ipsilateral hemisphere. Also upon visual inspection there appeared to be increased number of fluorescently labeled cells in the FPI

and the slow–rate VC-FPI, compared to the fast-rate VC-FPI animal. The number of degenerating neurons in the ipsilateral hippocampus was quantified (Figure 4.12(b)). Quantification of the CA2-3 region revealed a significant difference between the injured groups (n=6 for each group) [$F(2,15)=26.7$, $P<0.001$]. Bonferroni post-hoc test revealed that compared to the slow-rate VC-FPI group there were significantly fewer degenerating neurons in the fast-rate VC-FPI group ($P<0.001$). However, there was no significant difference between the number of degenerating neurons in the FPI and the slow-rate VC-FPI groups ($P=1$) 24h after the TBI. Sham animals were essentially devoid of fluorescing cells in both hemispheres (n=6). Thus, the sham group was not included in the ANOVA. This overall result shows that slower rate injury results in greater number of degenerating neurons in the acute stage.

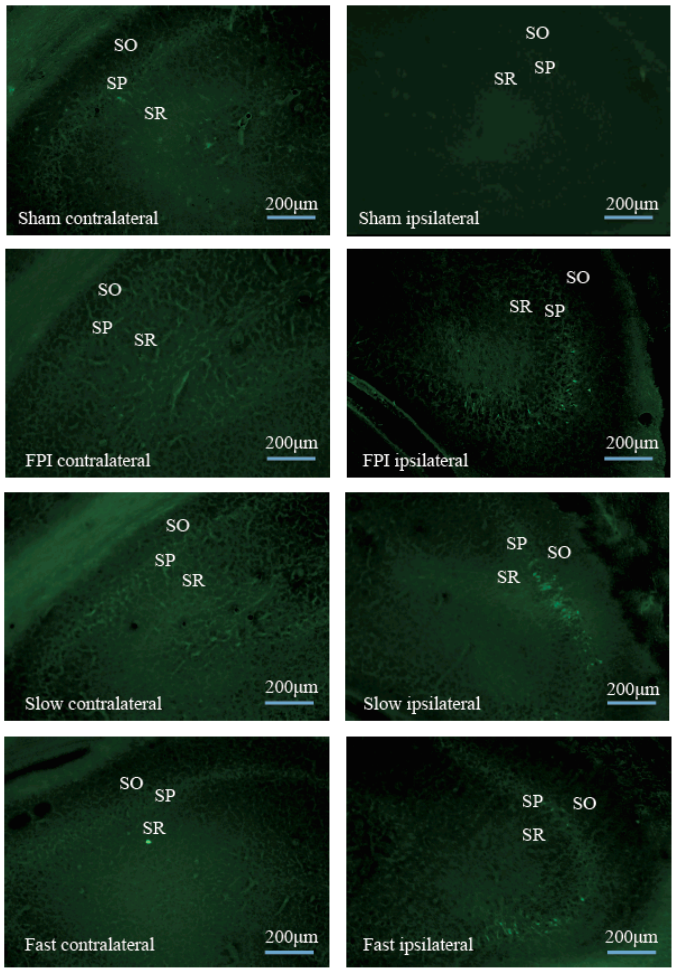

(a)

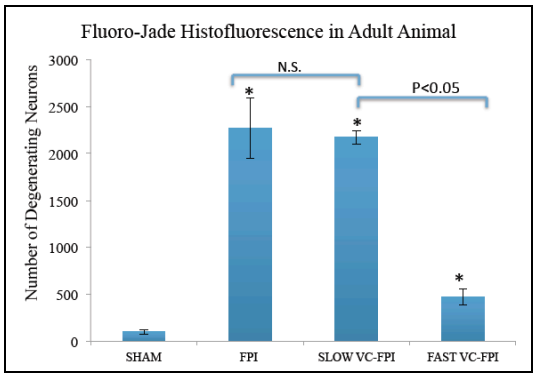

(b)

Figure 4.12 (a) and (b) shows Fluor-Jade Histofluorescence of Degenerating Neurons 24h after Injury on Adult Rats. (a) Coronal sections showing CA2-3 region of sham, FPI, slow-rate and fast-rate VC-FPI injured animals; fluorescing cells degenerating. (b) Summary plot showing degenerating neuron counts in the CA2-3 region, estimated by stereology. Neuronal degeneration after fast-rate VC-FPI injury is significantly lower than after FPI and slow-rate VC-FPI injury. (SEM scale bars shown, *Indicates significance by ANOVA and Bonferroni post hoc analysis compared to sham group).

Chronic Behavior

The chronic behavioral tests were used to evaluate the effects of the various rates of injury on the vestibular, motor, sensory recovery and also their effects on the higher cognitive skills, spatial learning and memory retention after the injury. The behavior was studied from day 1 to day 15 post-injury.

4.4.3 Rotarod Test

The first behavioral test was the rotarod test. This test assessed ambulatory function and general vestibulo-motor function. Animals were trained to walk on a rotating wheel of a rotarod for 4 min on 2 consecutive days before the injury and then tested 1, 4, 7, 11 and 15 days post-injury. Figure 4.13 shows the mean duration before fall for the four groups (sham: n=12, FPI: n=10, slow-rate VC-FPI: n=10, fast-rate VC-FPI: n=12). A repeated measure ANOVA on post-TBI day assessments revealed significant main effect of group on duration before fall [$F(3,40)=22.661$, $p<0.0001$] (i.e. there was differences between the groups when the data was collapsed across days). There was also a significant main effect of test-day [$F(4,160)=19.821$, $p<0.0001$] (i.e. there was differences between test-days if all the injury groups were combined) and a significant test-day by group interaction [$F(12,160)=3.603$, $p<0.0001$] (i.e. different groups performed differently over test-days). This shows that even though all groups recovered their motor skills, different injury groups recovered at different rates. Bonferroni post hoc tests revealed that the fast-rate VC-FPI injury group was able to balance themselves on the rotarod for significantly longer duration than the slow-rate VC-FPI injury group ($P<0.001$). This shows that the fast-rate VC-FPI injury animals recovered their ambulatory functions and general

vestibule-motor skills faster than the slow-rate VC-FPI group. There was no significant differences between the duration of balance for the slow-rate VC-FPI group and the FPI group (P=0.059) showing no differences in ambulatory function and general vestibulo-motor recovery. The Bonferroni post hoc analysis also indicated that the sham group was able to balance on the rotarod for longer duration than all the injured groups.

A set of the slow-rate VC-FPI animals (n=3 of 13 total slow-rate VC-FPI) were unable to perform in the Morris water maze study (presented below) because of inability to swim, and was therefore not analyzed on this outcome measure. However, they were included as a separate additional subgroup in the rotarod test. The duration before fall of this group increased similar to the other slow-rate VC-FPI injured group until day 7 post injury, but on the subsequent days their conditions deteriorated. This shows that there may be progressive injury in these animals that resulted in worsening of the ambulatory function and vestibulo-motor recovery.

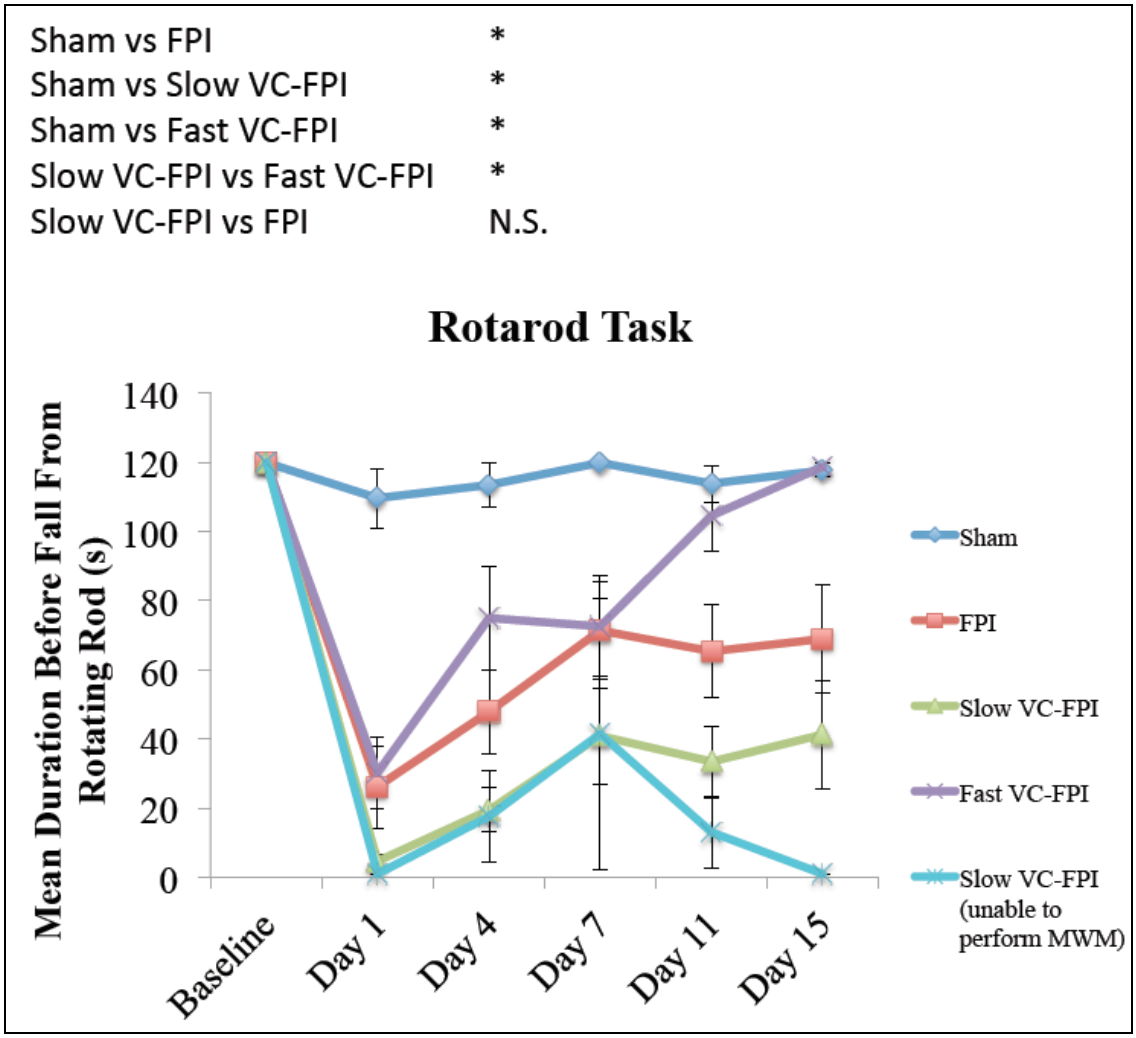

Figure 4.13 Rotarord Test Results. The time before fall for injured groups and sham control for adult rats were recorded and the mean durations for each group was plotted for the pre-injury for baseline and post-injury days 1, 4, 7, 11 and 15. One set of animals from the slow-rate VC-FPI injury was not able to swim in the Morris Water Maze (study described later). The performance of this group improved in performance until day 7 post injury similar to the other slow-rate VC-FPI injury group, but perfornance deteriorated over days 11 to 15 post-injury. (Values are mean ±SEM. * Indicates significance by ANOVA and Bonferroni post hoc analysis.)

4.4.4 Ladder Rung Walk Test

The ladder rung walk test evaluated fine motor coordination and ambulatory motor skills. The number of slips and the duration required to traverse the entire ladder length was recorded (figure 4.14).

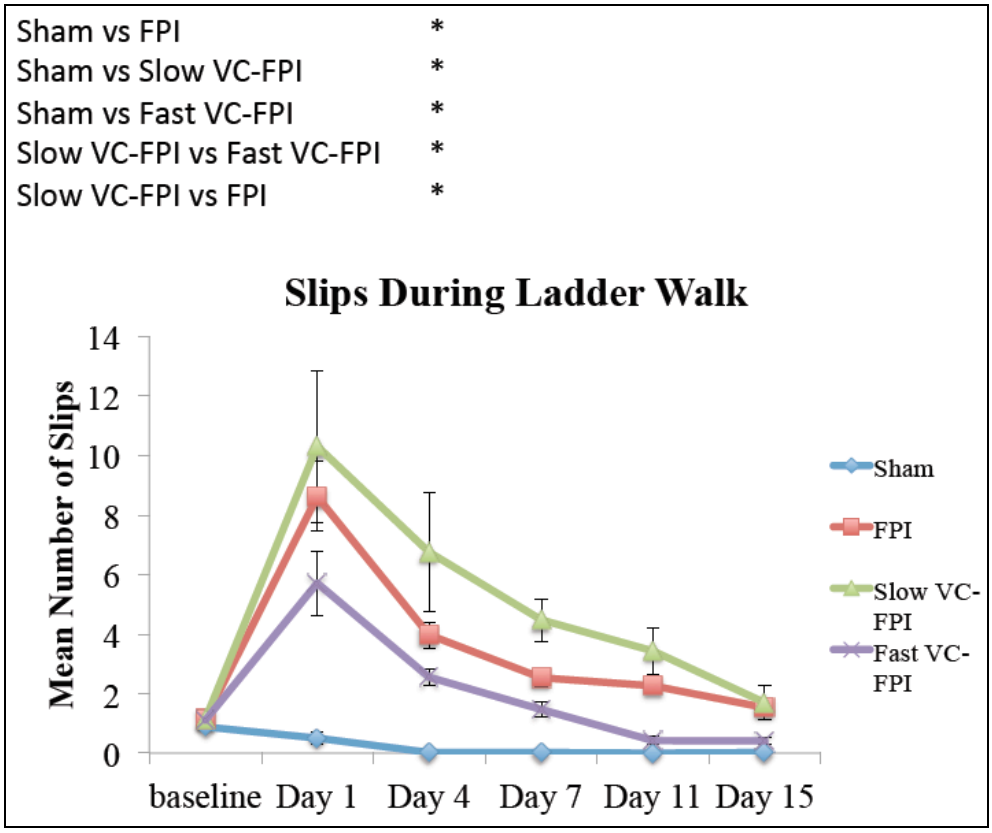

Figure 4.14 Slips During Ladder Rung Walk Test. Baseline was performed before the surgery and injury. Number of slips during the walk was recorded and the mean numbers were plotted on this chart. (Values are mean ±SEM. * Indicates significance by ANOVA and Bonferroni Post hoc analysis.)

A repeated measure ANOVA revealed a significant main effect of group (sham n=12, FPI n=9, slow-rate VC-FPI n=10, fast-rate VC-FPI n=11) on number of slips during ladder traverse period [$F(3,38)=42.629$, $p<0.0001$] (i.e. there was differences between the groups if all the test days are combined). There was also a significant main effect of test-day [$F(4,152)=73.287$, $p<0.0001$] (i.e. there was differences between test-

days if all the injury groups were combined) and a significant test-day by group interaction [$F(12,152)=8.69$, $p<0.0001$] (i.e. different groups did differently at each test-day). This shows that all groups recovered their fine motor coordination and ambulatory motor skills. However, they did so at different rates. Bonferrroni post hoc analysis revealed that the fast-rate VC-FPI group had significantly less number of slips compared to the slow-rate VC-FPI group ($P<0.001$). Also, the FPI group had significantly less number of slips compared to the slow-rate VC-FPI group ($P=0.03$) and significantly greater number of slips compared to the fast-rate VC-FPI group ($P=0.013$). Bonferroni post hoc tests indicated that the number of slips by the sham group was significantly less than all the injured groups. The baseline data was excluded from the analysis of significance. Overall, this shows that fast-rate VC-FPI injured animals have better recovery than slow-rate VC-FPI injured animals. This may be partly because the fast rate injured animals suffered from lesser initial injury (number of slips on day 1 post injury for the fast injured animals was significantly less than the slow-rate injured animals). However, this could also show that the fast-rate injured animals have faster recovery.

Ladder walk rung test time to traverses the apparatus was evaluated using a repeated measure ANOVA (Figure 4.15) and revealed a significant main effect of injury group (sham n=12, FPI n=9, slow-rate VC-FPI n=10, fast-rate VC-FPI n=11) [$F(3,38)=45.726$, $p<0.001$]. There was also a significant main effect of test-day [$F(4,152)=76.452$, $p<0.001$] and a significant group by test-day interaction [$F(12,152)=9.754$, $p<0.001$]. This shows that all groups recovered their speed in motor movement. However, they did so at different rates. Bonferroni post-hoc analysis revealed that on the test days post injury, no significant difference between the

FPI and the fast-rate VC-FPI (P=1) groups. However, the Slow-rate VC-FPI group had significantly greater time lapse compared to all the other groups (Slow vs Sham, FPI, Fast: P<0.001). The FPI (P<0.001) and fast-rate VC-FPI (P<0.001) group had significantly greater time lapse than the sham group and that the mean time lapse for the sham group was least. There was no significant difference between groups during baseline testing.

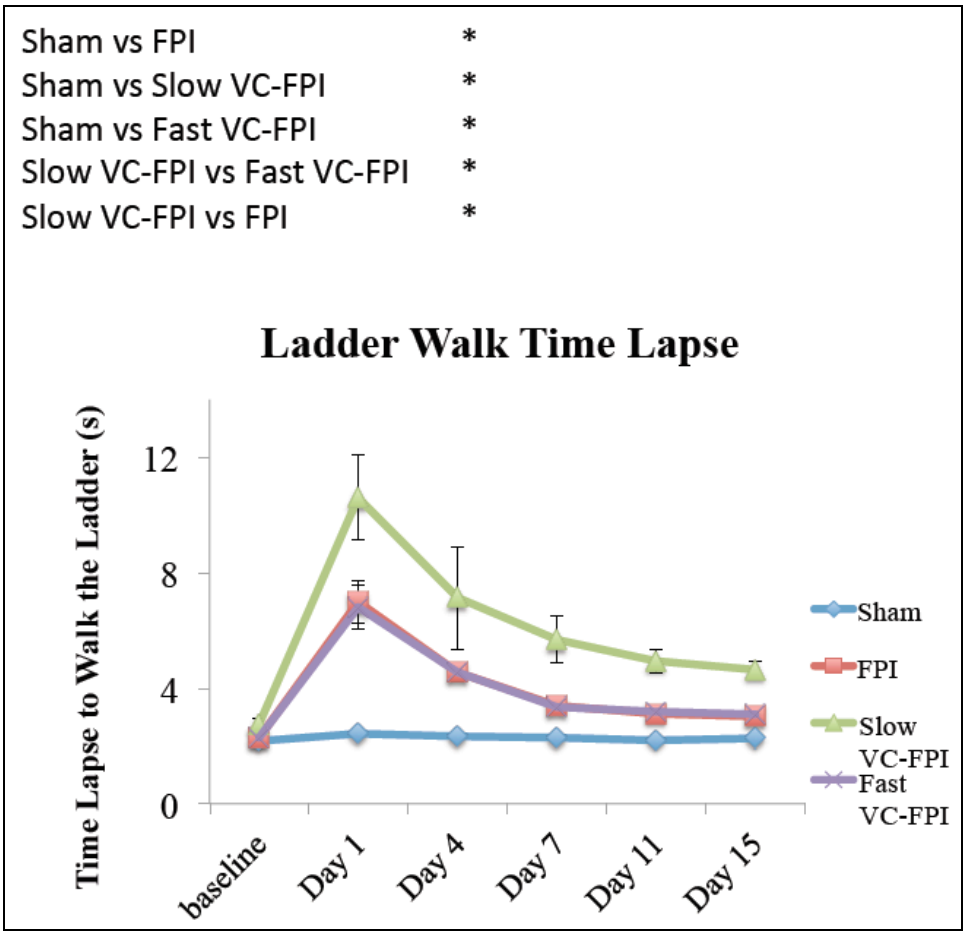

Figure 4.15 Time Lapse During Ladder Rung Walk Test. Baseline was performed before the surgery and injury. Total time taken for the animal to traverse the ladder during the ladder walk was recorded and the mean durations were plotted on this chart. (Values are mean ±SEM. *indicates significance by ANOVA and Bonferroni post hoc analysis.)

4.4.5 Metric Spatial Information Task

The metric spatial information task was used to evaluate spatial memory and perception. First it was assessed whether the rats habituate to the novel environment. Habituation is the decrease in response over time to the stimulus conditions as shown by the sham group, Figure 4.16 ($n=11$, $P<0.05$, t-test). From the percentage exploration times (Figure 4.16) it is evident the FPI group habituates ($n=9$, $P<0.05$, t-test), however the fast-rate VC-FPI injury group shows trends of habituation ($n=10$, $P\cong0.1$, t-test) and the slow-rate VC-FPI injury group does not habituate ($n=10$, $P>0.05$,t-test). This shows that other than slow-rate VC-FPI group, all the other groups habituate.

A change in percentage exploration time between the 3rd interval and the test period is indicative of whether the animal recognizes the change in the environment or not. Figure 4.16(b) shows the percentage exploration time between the third 5min interval and the test interval. The data showed that fast-rate VC-FPI and slow-rate VC-FPI injured animals were unable to recognize the decrease in distance between the objects on the platform during the test session. In addition although FPI and sham TBI rats habituated similarly to the objects; FPI was unable to detect the change in the environment but the sham control animals were able to detect the change (Figure 4.16(b)). This shows that all the injured groups were incapable of recognizing the change in the environment during the test interval.

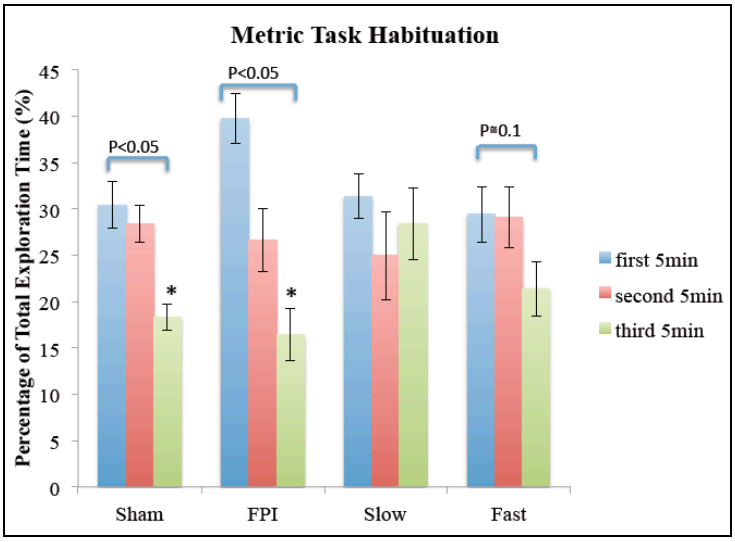

(a)

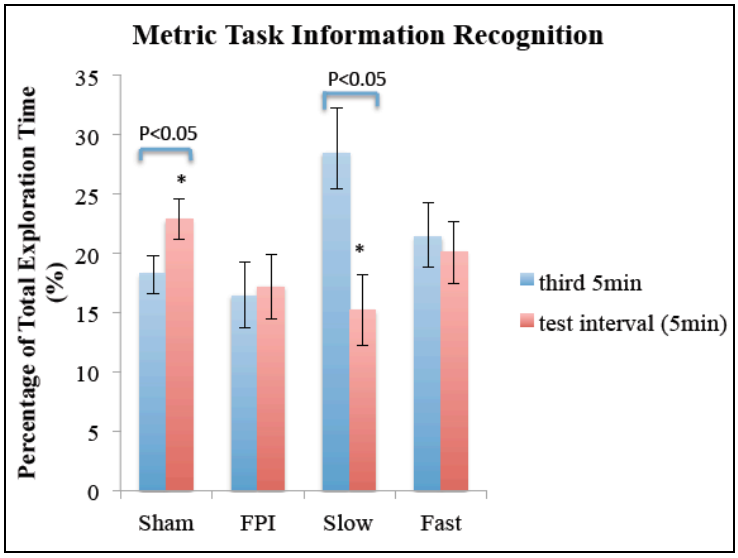

(b)

Figure 4.16 Percentage Exploration Time During Metric and Spatial Information Task. (a) Rats are placed on a circular platform with two novel object (a vaseline jar and a can of soda, both were fragrance free on the outside) separated by 68cm and let to habituate for 15 minutes (divided into three 5 min intervals). The percentage exploration time spent in each interval was presented on the chart. A decrease in exploration time during the habituation shows a that the animals are habituated. (b) Then they were given a 5 minute rest period during which they were placed in their homecage. During the break the objects were moved closer, the later distance between the two objects being 34 cm. Then there was a 5min test period. An increase in exploration time after the rest period indicates that the animals were able to recognize the "change in the environement". (Values are mean ±SEM. *indicates signifcance through t-test, P<0.05).

4.4.6 Morris Water Maze

The Morris Water Maze test was performed in order to test spatial learning and memory including: spatial memory acquisition and retention, long-term memory, and short-term memory.

4.4.6.1 Spatial Memory Retention

A repeated measure analysis of variance (ANOVA) revealed a significant main effect of group (sham n=12, FPI n=9, slow-rate VC-FPI n=10, fast-rate VC-FPI n=11) on latency to find platform (Figure 4.17) [$F(3,38)=13.072$, $p<0.0001$]. There was also a significant main effect of test-day [$F(4,152)=39.837$, $p<0.0001$] and a significant test-day by group interaction [$F(12,152)=2.845$, $p<0.0001$]. This shows that all groups learned the spatial location of the hidden platform. However, the different injury groups learned at different rates.

Sham vs FPI	*
Sham vs Slow VC-FPI	*
Sham vs Fast VC-FPI	N.S.
Slow VC-FPI vs Fast VC-FPI	*
Slow VC-FPI vs FPI	N.S.

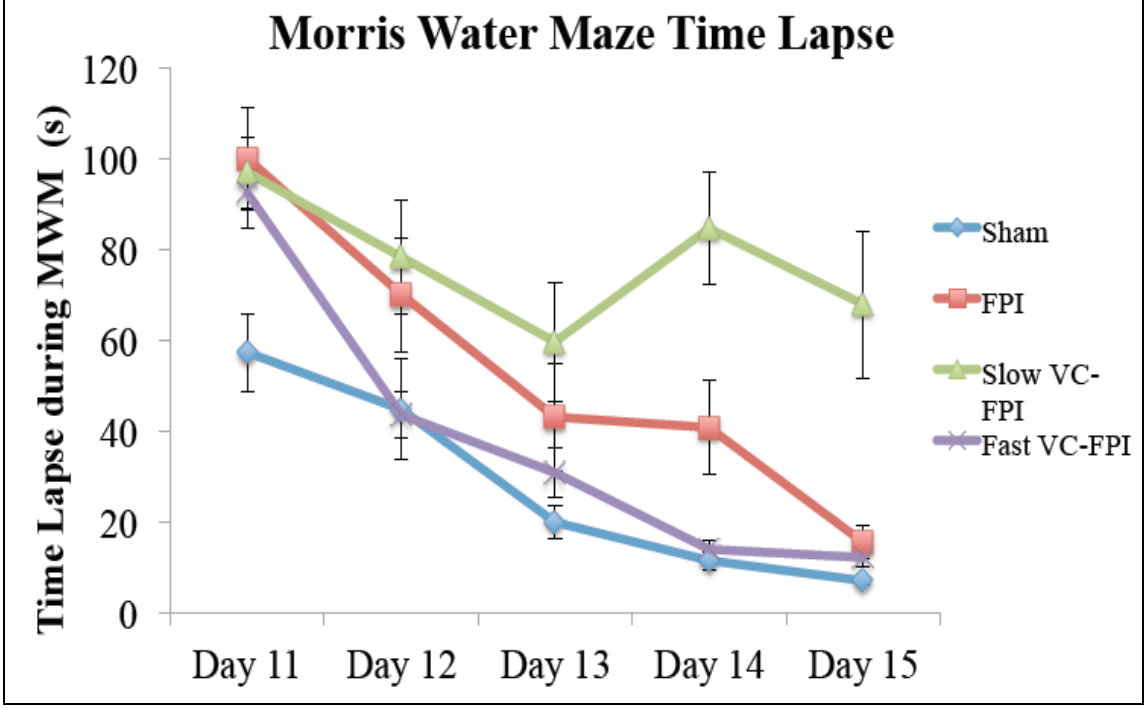

Figure 4.17 Morris Water Maze (MWM) Mean Time Lapse Before Finding the Hidden Platform. Day 11 to 15 post-injury, the animals were tested on the MWM. Four trials were performed on each day with 4 min of inter-trial rest period. For each trial the rat was started at a different quadrant with consistent visual ques in each quadrant, and the time required for the rat to find the hidden platform was recorded. The hidden platform was always kept in the same position. The median time required for each day was summarized on this chart. Learning the position of the platform indicates improved spatial learning ability. (Values are mean ±SEM. * indicates significance by ANOVA and Bonferroni post hoc analysis).

Bonferroni post-hoc test indicated that the fast-rate VC-FPI group took significantly less time than the slow-rate VC-FPI injury group ($P<0.001$) to learn the location of the platform. Bonferroni test also revealed that there was no significant difference between the slow-rate VC-FPI and the FPI group to learn the location of the

platform (P=0.096). It also revealed that there was a significant difference between the performance of the sham and that of the slow-rate VC-FPI (P<0.001) and the FPI (P=0.02) group. However, there was no significant difference between the sham and the fast-rate VC-FPI group (P=1). Overall, this shows that fast rate VC-FPI injured animal had better memory retention than slow-rate VC-FPI and standard FPI injured animals.

A repeated measure analysis of variance (ANOVA) revealed a significant main effect of group (sham n=12, FPI n=9, slow-rate VC-FPI n=10, fast-rate VC-FPI n=11) on distance swam to find platform (Figure 4.18) [$F(3,38)=11.157$, $p<0.0001$]. There was also a significant main effect of test-day [$F(4,152)=26.928$, $p<0.0001$] and a significant test-day by group interaction [$F(12,152)=2.888$, $p<0.0001$]. Bonferroni post-hoc test indicated that the fast-rate VC-FPI group swum significantly less distance than the slow-rate VC-FPI injury group (P=0.002) to find the location of the platform. Bonferroni test also revealed that there was no significant difference between the slow-rate VC-FPI and the FPI (P=0.018) group to learn the location of the platform. It also revealed that there was a significant difference between the performance of the sham and that of the slow-rate VC-FPI (P<0.001). However, there was no significant difference between the sham TBI group and the fast-rate VC-FPI (P=0.7) and FPI (P=0.2) group. Overall, this shows that fast rate VC-FPI injured animal had better memory retention than slow-rate VC-FPI and standard FPI injured animals. This also shows that, since the time lapse and the swim distance followed the same trend, the rats swam looking for the hidden platform for the entire duration that it was in the water before finding the hidden platform.

Sham vs FPI	P=0.09
Sham vs Slow VC-FPI	*
Sham vs Fast VC-FPI	N.S.
Slow VC-FPI vs Fast VC-FPI	*
Slow VC-FPI vs FPI	N.S.

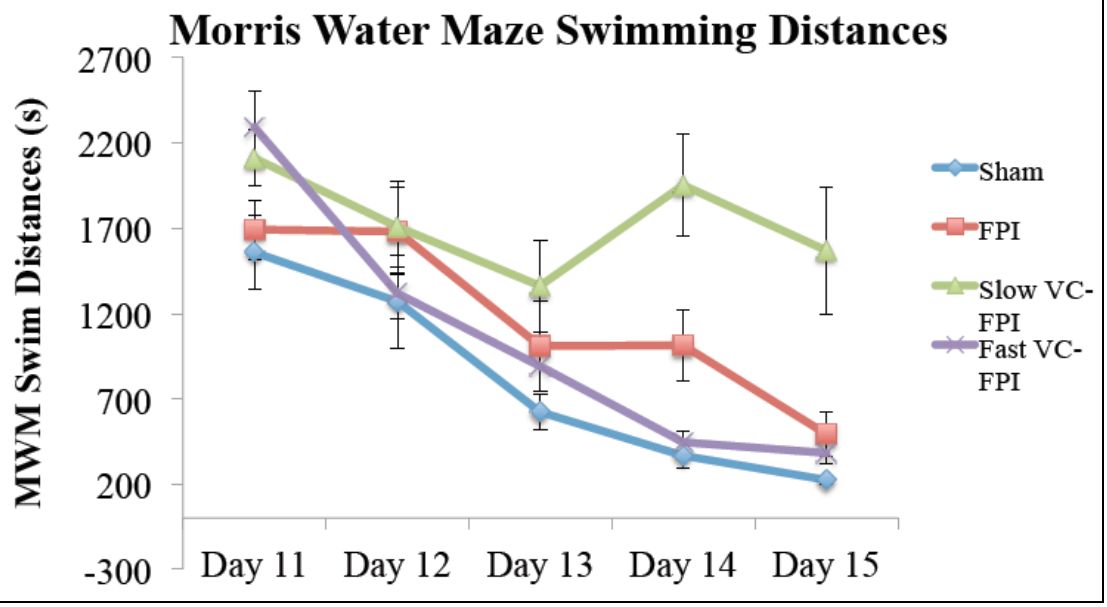

Figure 4.18 Morris Water Maze (MWM) Median Distance Traveled Before Finding the Hidden Platform. Day 11 to 15 post-injury, the animals were tested on the MWM. Four trials were performed on each day with 4 min of inter-trial rest period. For each trial the rat was started at a different quadrant with consistent visual ques in each quadrant, and the distance swum by the rat to find the hidden platform was recorded. The median distance required for each day was summarized on this chart. Learning the position of the platform indicates improved spatial learning ability. (Values are mean ±SEM. *indicates significance by ANOVA and Bonferroni post hoc analysis).

4.4.6.2 Morris Water Maze Swim Speed

On day 11-15 post-injury, measures of swim speed during Morris Water Maze test were used to differentiate motor deficits from cognitive deficits evaluation**.** Swim speeds were significantly different between groups (sham n=12, FPI n=9, slow-rate VC-FPI n=10, fast-rate VC-FPI n=11) (Figure 4.19).

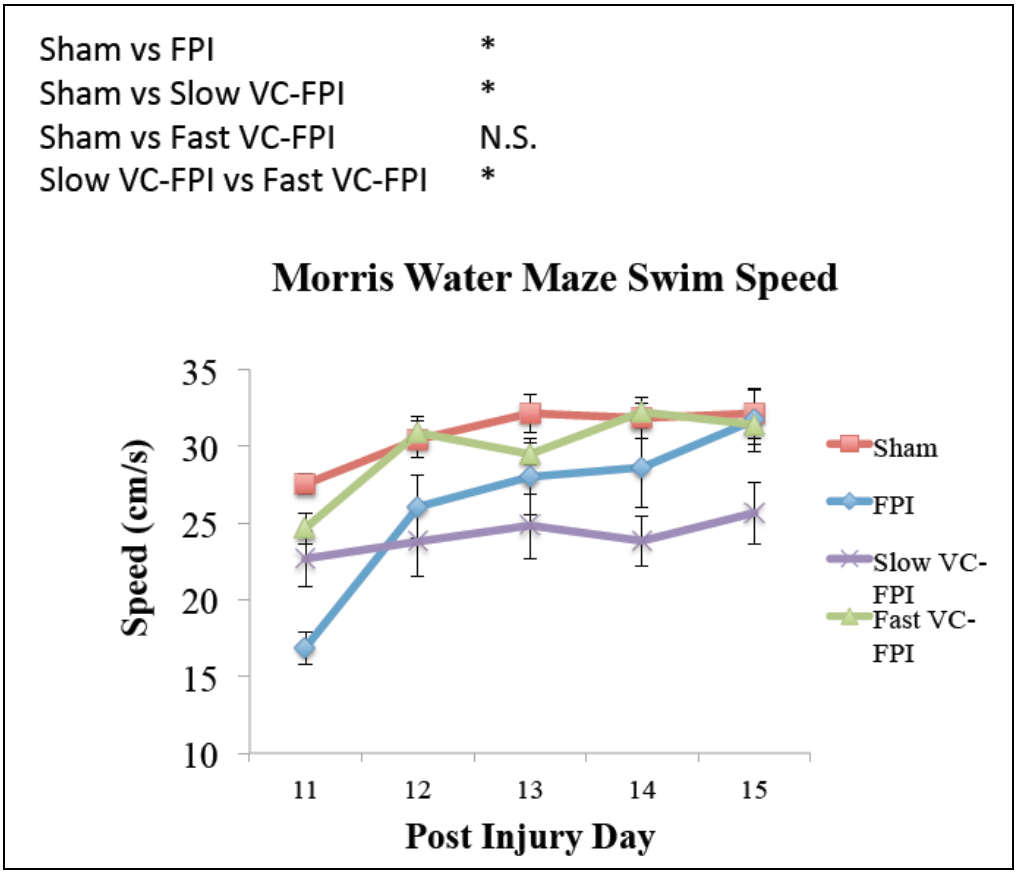

Figure 4.19 Morris Water Maze (MWM) Median Swim Speeds While Finding the Hidden Platform. Day 11 to 15 post-injury, the animals were tested on the MWM. Four trials were performed on each day with 4 min of inter-trial rest period. For each trial the rat was started at a different quadrant with consistent visual ques in each quadrant, and the swim speed during each trial was calculated by the distance and time measurements during each trial and was summarized on this chart. Higher swim speed indicated better sensory and motor performance. (Values are mean ±SEM. *indicates significance by ANOVA and Bonferroni post hoc analysis).

Repeated measures of ANOVA revealed a significant main effect of group on swim speed [$F(3,38)=9.714$, $p<0.0001$], also a significant main effect of test-day [$F(4,152)=19.886$, $p<0.0001$] and a significant test-day by group interaction [$F(12,152)=2.561$, $p<0.0001$]. Bonferroni post hoc analysis indicated that the fast-rate VC-FPI injury group had significantly greater swim speed than the slow-rate VC-FPI injury group. It also revealed that there was no significant difference between the swim

speed of sham and the fast-rate VC-FPI injury (P=1) group, but there was a significant difference between the sham group and the FPI (P=0.006) and slow-rate VC-FPI (P<0.001) groups. This shows that the slow-rate VC-FPI was at a disadvantage and might have fallen behind due to its reduced motor recovery and not the reduction of spatial recognition. However, the fact that the differences between the time-lapse for finding the hidden platform between the fast-rate and slow-rate VC-FPI being so large, shows that there was a reduction in spatial memory retention.

4.4.6.3 Short-term and Long-term Memory Assessment

In addition to measuring the mean latency to platform, the long-term and short-term memory was assessed individually (sham n=12, FPI n=9, slow-rate VC-FPI n=10, fast-rate VC-FPI n=11) (Figure 4.20). We defined short-term memory as a reduced latency to find the hidden platform between the first and the fourth trial of each day (16min inter-trial time). Long-term memory was defined as a reduced latency to platform between trial 4 of one day and trial 1 of the subsequent day (24-hour inter-trial interval). These reduced latencies were termed “memory retention”. The “memory retention” for the long-term memory and short-term memory are shown in Figure 4.18. ANOVA revealed no significant effect of group on memory retention (p>0.05). However, all the groups had positive short-term and negative long-term “memory retention” values, which shows that the animals remembered better memory retention for short-term experience than the long-term experience. However, the difference between the groups and that between the short-term and long-term within each group were not significantly different. The short-term memory in all the groups are very similar, therefore the memory impairment is probably not an issue of short term memory.

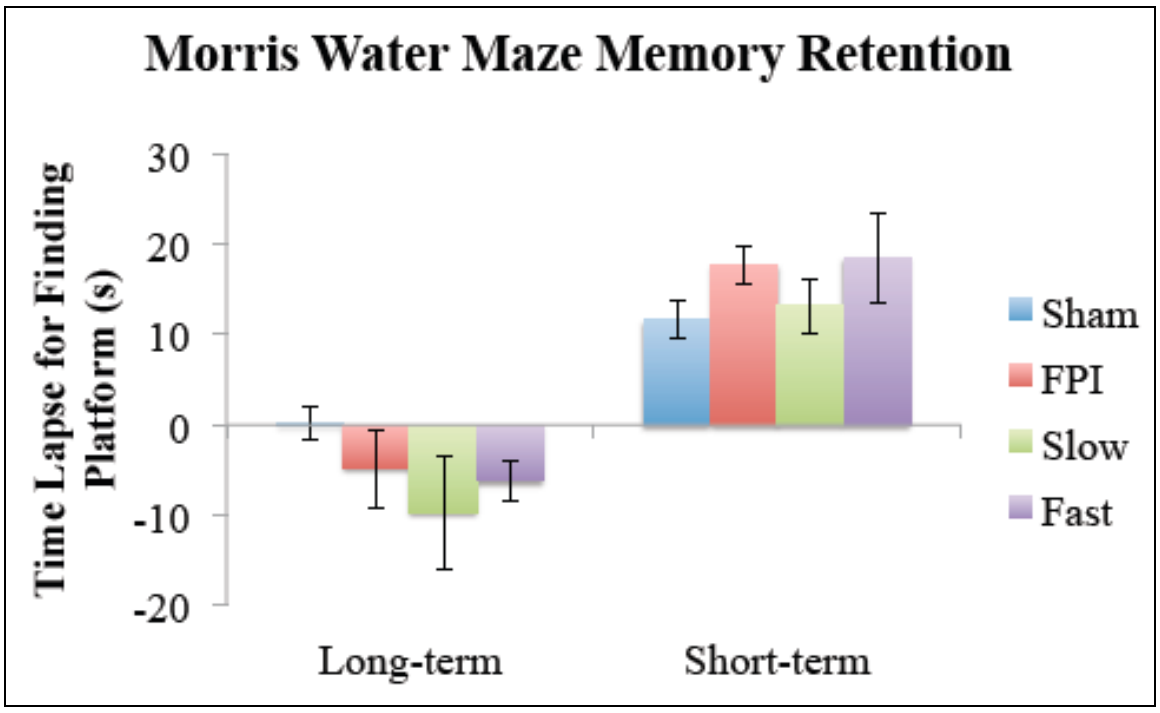

Figure 4.20 Morris Water Maze, Memory Retention for Short term and Long term. The short-term latency; between two trials of same day (4min inter-trial time); was averaged and plotted. Also the Long-term latency; between the first trial of one day and the last trial of the previous day (24h inter-trial time) was averaged and plotted. The short-term memory for all the groups was positive showing an improvement in memory retention. The long-term memory for all the groups was negative showing a decrease in memory retention.

Each trial on each of the 5 test days was plotted on a chart (Figure 4.21). Any downward trend showed the reduced latency, and was a result of memory retention from the previous trial, therefore the rats located the platform faster and the latency was lesser. Any upward trend indicated a loss of memory from the previous trial. This chart (Figure 4.21) shows that the long-term memory consists of several components including memory retention from all the previous days and not solely from the previous day.

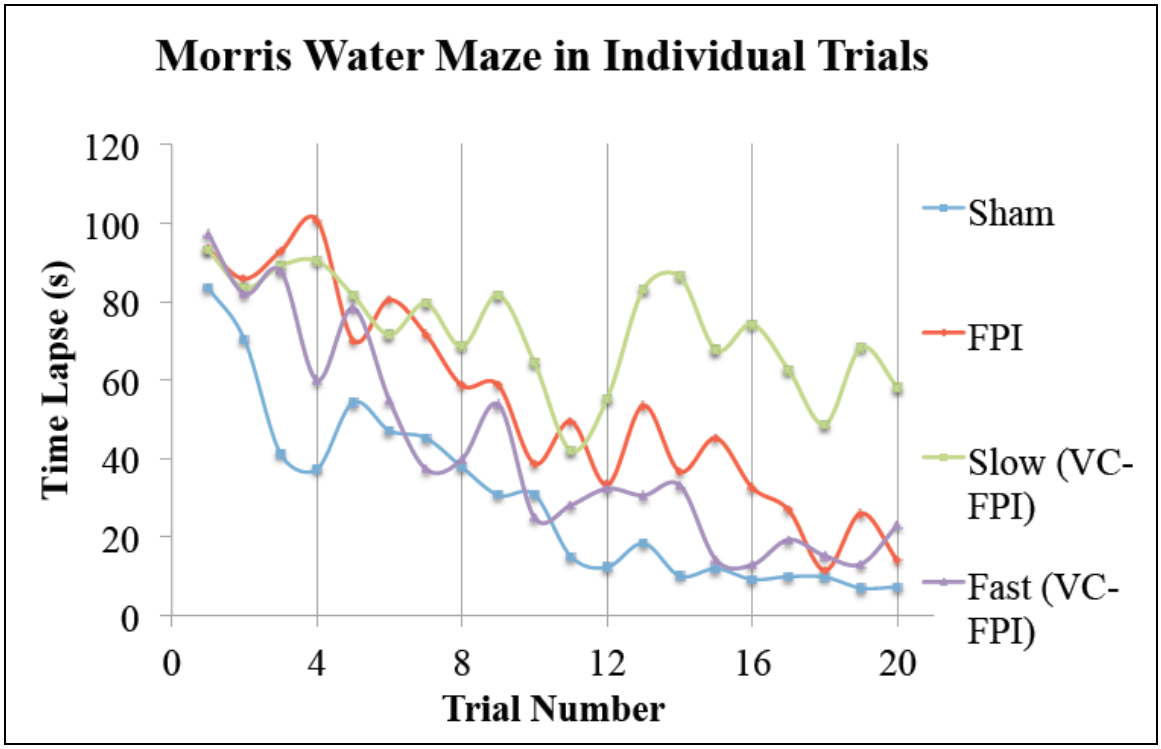

Figure 4.21 Morris Water Maze Individual Trial-by-trial Analysis for all rats, of Swim Time. Instead of summarizing the combined time lapse, this study looked at (the mean values for all animals within the injury group) each trial separately on each day. So 4 trials on 5 days provided with a total of 20 trials. A downward trend or less time lapse, shows an improvement in the learning. It can be seen that in most cases there was a downward trend within the same day (4min time separation) in all groups. An upward trend shows loss of memory. In most cases there was an upward trend between the first trial of a day and the last trial of previous day (24 h time separation).

4.4.7 Chronic Histology: Neuronal Survival

Following the MWM probe trials on day 15 post-injury, animals were euthanized and brain sections were stained with cresyl violet. Figure 4.22(a) shows contralateral side and ipsilateral sides to injury of representative animals from each group. The ipsilateral side is the side that sustained the surgery. In case of injured animals, this side was injured. It can be seen that the contralateral sides of all the animals are very similar both in injured and sham animals. In sham animals the ipsilateral side is very similar to the contralateral side. In the FPI and slow-rate VC-FPI animals, in the ipsilateral side, there is a

deformation and shrinkage of the hippocampus compared to their contralateral sides. In all the injured animals, there is also some darkening in the corpus callosum area and in the cortex around the injury site. Darkening is usually caused by cellular necrosis in a particular area.

In order to quantify the deformation of the hippocampus as result of the injury, the diameter of the hippocampus on the contralateral side and the ipsilateral sides were measured with ImageJ and percentage change in diameter was analyzed (Figure 4.23(a)). A one way analysis of variance (ANOVA) revealed a significant main effect of group [$F(3,27)=5.594, P<0.05$] showing that there was indeed a difference in the deformation of the hippocampus between the groups. There was no significant difference between the deformations of the standard FPI injured and the slow-rate VC-FPI injured group (standard FPI, n=8, slow-rate VC-FPI, n=8; $p>0.05$, t-test). However there was significant difference in the deformation between the fast-rate injured group and the slow-rate injured group (fast-rate VC-FPI n=8, slow-rate VC-FPI n=8; $p<0.05$, t-test). These results show that there is indeed a difference in the deformation due to a fast-rate VC-FPI injury compared to a slow-rate VC-FPI injury.

Pyramidal neurons in the ipsilateral CA2-3 region were quantified using stereological techniques. Analysis of cell counts identified significant decrease in mean neuronal number in CA2-3 region as can be seen in the summary plots in Figure 4.23(b) below. A one way analysis of variance (ANOVA) revealed a significant main effect of group [$F(3,28)=5.448, P<0.001$]. However, one way analysis of variance on the injured groups (without the sham TBI group) revealed no significant difference between the groups (fast-rate VC-FPI, slow-rate VC-FPI and FPI) [$F(2,21)=1.314, P=0.29$]. Dunnett

post-hoc analysis indicated all injured groups had significantly fewer surviving neurons (P=0.038, 0.052, 0.001; FPI, Slow-rate VC-FPI and fast-rate VC-FPI respectively) compared to sham group at day 15 post-injury. Therefore, these outcomes show that, fast-rate and slow-rate VC-FPI at similar peak impact pressures results in improved early neurobehavioral outcome and reduced cellular degeneration at acute stage, suggesting that fast-rate injury leads to a milder TBI than slower rate injury. However later stage cell survival quantification suggests the extent of cell loss at later stage after fast-rise injury and slow-rate injury is comparable.

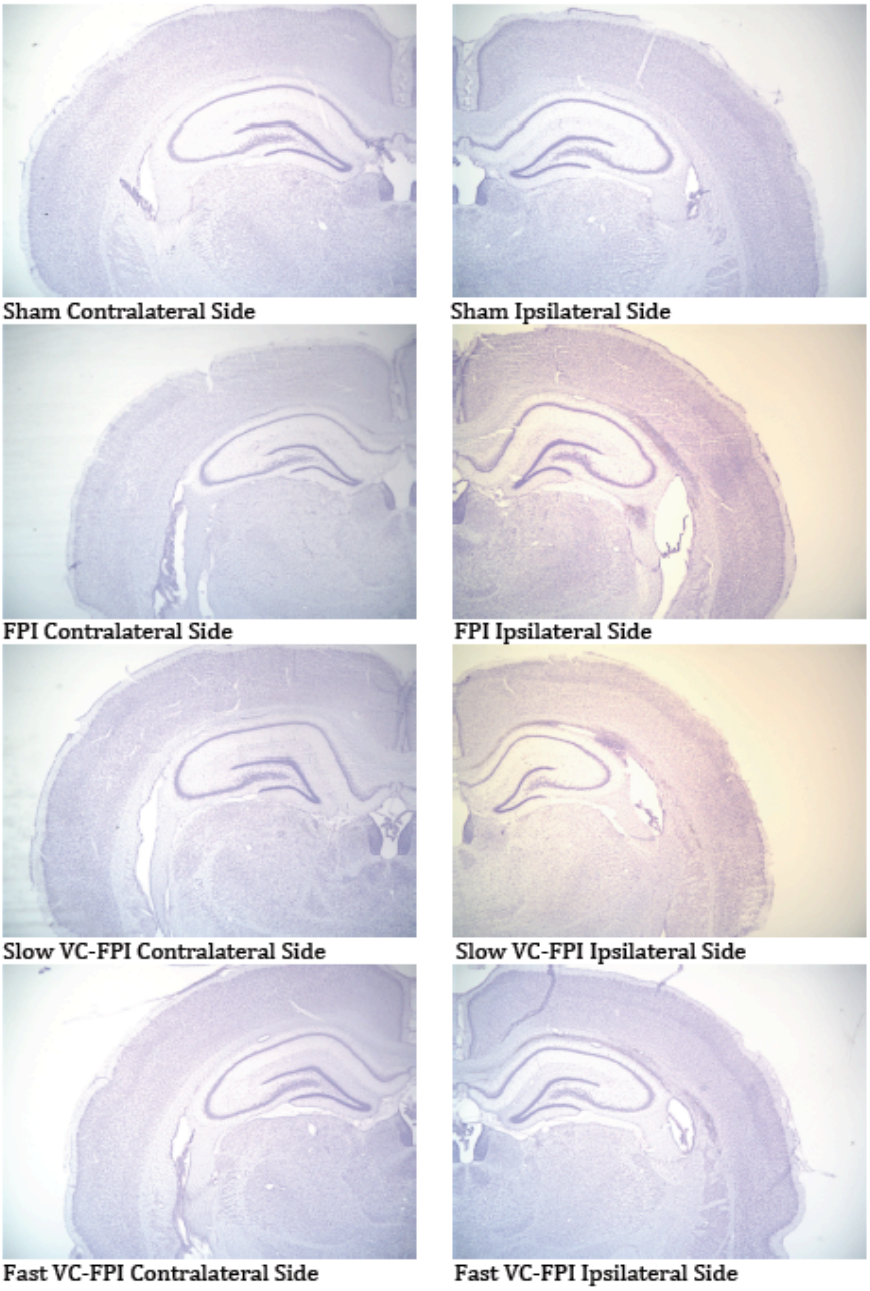

(a)

Figure 4.22 Cresyl Violet Staining of Surviving Neurons 15 days Post-injury. (a) Shows photomicrographs of representative coronal sections (-3.6mm Bregma) of the hippocampus in both ipsilateral and contralateral hemispheres. All the representative images show no apparent changes in the side contralateral to the injury. The sham group shows no apparent change in both the ipsilateral and contralateral to the injury. The injured groups show some darkening around the periphery of the hippocampus and the corpus callosum. Also in the FPI and slow-rate VC-FPI groups show a gross shrinkage or deformation in shape of the hippocampus compared to the fast-rate VC-FPI and sham animals.

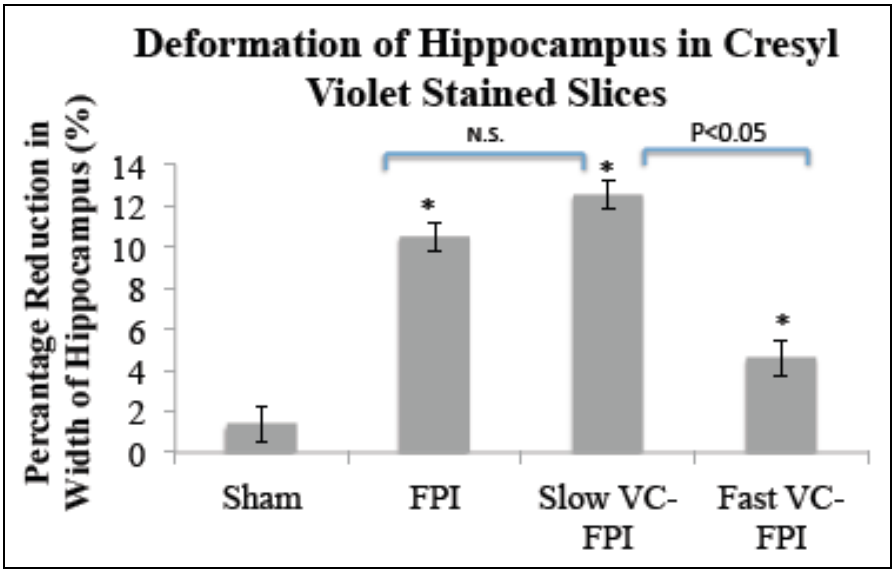

(a)

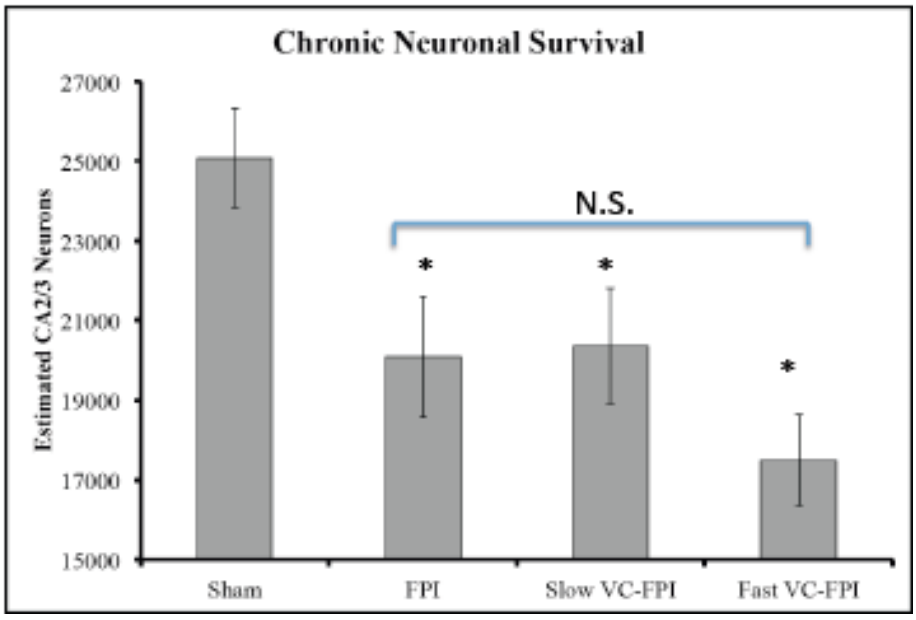

(b)

Figure 4.23 Cell Survival Quantification (a) Cresyl violet stained sections used to calculate diameter of hippocampus of contralateral and ipsilateral sides and then percentage change in diameter calculated and mean values were plotted on a chart. There was a significant difference between the change in diameter between the fast-rate and slow-rate VC-FPI (b) Summary plot showing mean stereological surviving cell counts in the CA2-3 region. There is no significant difference between the injured groups, but the sham control group had significantly higher number of surviving cells. (SEM scale bars shown, * indicates significance by ANOVA and Bonferroni post hoc analysis compared to sham.)

4.4.8 Dependency of the pathophysiology on the Impulse of the Waveform vs the Rise-time

Once the study of the pathophysiological outcome based on the injury rate was completed, the rise-time and impulse of the pressure waveform were investigated in relation to the pathophysiological outcome. In order to keep the investigation within the scope of this work, the pressure profile of a subset of animals were used, those that were slow-rate VC-FPI injured but the severity of the pathological outcome was greater than the rest of the group. These animals were not able to perform physically in most of the experiments. Hence these animals were eliminated from the overall study analysis and analyzed as a subset group (eliminated-slow-rate group). The pressure peak appeared slightly lower than the slow-rate VC-FPI injured group (Figure 4.24(a)), however the difference was not significant (t-test, P=0.2).

Then rise-times were analyzed in Figure 4.24(b). It could be seen that the rise-time of the eliminated-slow-rate group (n=3) was significantly longer than the slow-rate VC-FPI group (n=10) (t-test, P=0.002). Then to complement the findings the impulses between these two groups were studied (Figure 4.24(c)). It was observed that the Impulse was lower but not significantly different (t-test, P=0.2) between the two groups. These results show that the difference between the pathophysiology is most likely due to the differences in rise-times between the injuries.

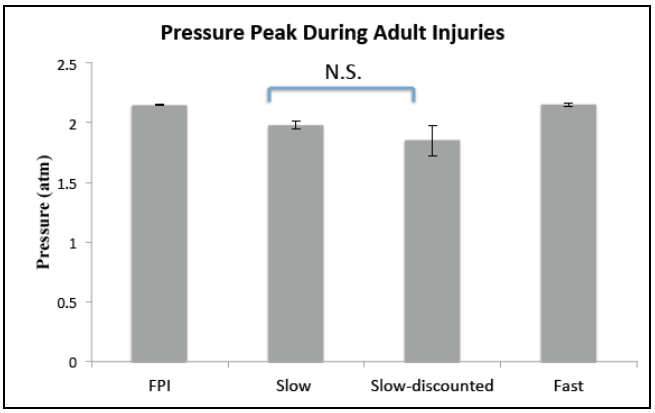

(a)

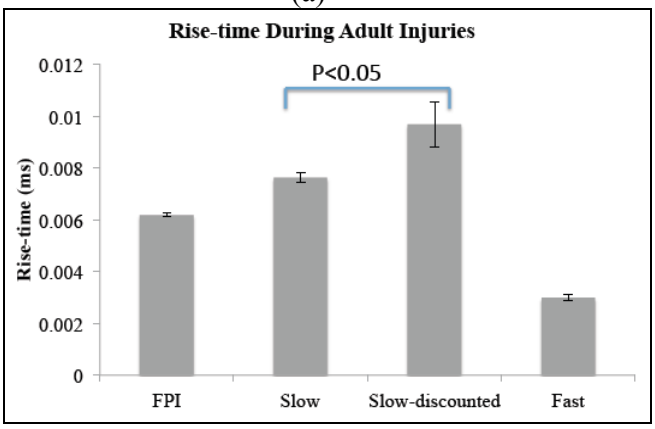

(b)

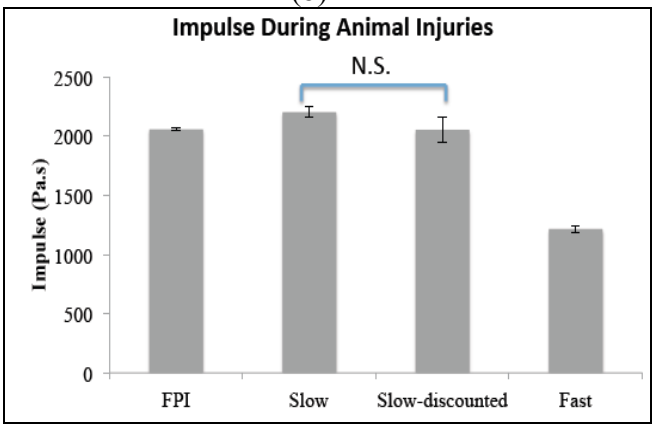

(c)

Figure 4.24 Waveform Analysis for Eliminated Slow-rate Group. In order to Study whether Rise-Time or Impulse affects the Pathophysiological Outcomes of Injuries. Pressure waveform of FPI, Slow-rate VC-FPI, Slow-eliminated group, and Fast-rate VC-FPI animals were compared. (a) Mean Pressure peaks were compared. (b) Mean rise-times were compared and (c) The impulse response was compared. The pressure peaks were similar (P=0.2, t-test), the impulse was similar (P=0.2, t-test), however it was seen that the rise-times were significantly different (P=0.002, t-test). Therefore the increased severity of this group of animals was probably due to the increase in rise-time of the injury. Standard error bars shown in (a), (b), and (c), * indicates significance by t-test.

Table 4.3 and 4.4 summarizes the pathophysiological outcomes of the animal groups in relation to the initial injury characteristics (Pressure peak, rise-time and impulse). Table 4.3 summarizes the adolescent animals and shows that in adolescent animals the change in rise time and impulse resulted in differences in immediate and early neurobehavioral and cellular degeneration, but no differences in excitability 1week post injury.

Table 4.4 summarizes the pathophysiological outcomes of the adult animals. Similar to the adolescent animals, the adult animals show milder early outcomes in fast rate and low impulse conditions, compared to the slow-rate injury and FPI injury in terms of immediate behavioral and cellular degeneration. Adult animals also showed similar cellular damage at the later stage in both fast-rate (low impulse) and slow-rate (higher impulse) injuries. Therefore even though our study investigates the relationship between rise-time and pathophysiological outcomes of injury, the resulting pathophysiology may also result from the differences in the impulse of the pressure wave.

Table 4.3: Adolescent Animal Injuries

	Pressure peak	**Rise time**	**Impulse**	**Immediate seizures**	**Immediate deaths**	**Acute cellular degeneration**	**Excitability**
Minimal	sham	sham	Sham	sham, fast	sham, fast	Sham	sham
	fast, slow	fast	Fast	Slow	Slow	Fast	fast, slow
Maximal		slow	slow			Slow	

Table 4.4 Adult Animal Injuries

	Pressure Peak	**Rise time**	**Impulse**	**Righting time**	**Toe pinch**	**Acute cellular degeneration**
Minimal	sham	sham	Sham	Sham	Sham	Sham
	slow	fast	Fast	Fast	Fast	Fast
	FPI fast	FPI	FPI	FPI	FPI	FPI slow
Maximal		slow	Slow	Slow	Slow	

	Rotarod	**Ladder slip**	**Ladder time**	**Metric task**	**MWM time lapse**	**MWM swim speed**	**Later cell survival**
Minimal	sham	sham	Sham	Sham	Sham	sham, fast	sham
	fast	fast	fast, FPI	fast, FPI, slow	Fast	FPI, slow	fast, FPI, slow
	FPI, slow	FPI	Slow		FPI, slow		
Maximal		slow					

DISCUSSION AND CONCLUSION

The Novel Voice-coil Fluid percussion injury device was successful in generating pressure waveforms at various rise-times, thus producing injuries at various rates. It was possible to vary these rise-times independent of the pressure peak of the injury. The immediate behavioral outcomes such as seizures, mortality, righting reflex, toe-pinch reflex; all showed that a faster rate injury resulted in a reduced immediate neurological severity. Chronic motor and cognitive tests revealed that fast-rate VC-FPI injured animals had faster motor recovery and better cognitive skills (learning) in the Morris water maze. However, both fast-rate and slow-rate VC-FPI injuries showed enhanced perforant path-evoked granule cell field excitability compared to sham. Also other cognitive skills (recognition) were affected equally in both fast and slow rate injuries as determined by the metric and spatial recognition task. Histo-fluorescence performed at early stage (4h and 24h post-injury) using Fluoro-Jade showed less neuronal degeneration in the faster rate compared to the slow rate and standard FPI. However, at the later stage (day 15 post-injury), neuronal survival as detected by cresyl violet stain, was similar in both rates; suggesting a possibility of higher progressive cell loss in the fast-rate VC-FPI injury.

Injuries to the brain are among the most likely traumatic insults to result in death or permanent disability and few, if any clinically effective treatments exist (Langlois et al., 2004, 2006)- facts that substantiate the need for improved laboratory models of TBI. The basic principle of the injury from the new VC-FPI device is based on the existing FPI system. However, the new VC-FPI system provides additional capabilities such as, independent control over the various parameters of the injury. The pressure comparison described in this study, shows that it is possible to vary the rise-time of the injury without

altering the pressure peak of the injury. Whereas in commonly used FPI systems the rise-time and the pressure peaks are dependent on each other since the only input variable is the height of the pendulum, which results in varying pressure peaks and each of this pressure peaks (Dixon et al., 1987).

The lateral fluid percussion injury is one of the most commonly used and well-characterized experimental models of TBI (Thompson et al., 2005; Morales et al., 2005). Some studies have shown that the extent of histological damage is associated with severity/magnitude of the injury (changing the peak of the pressure wave) (Cortez et al., 1989; Smith et al., 1991; Lowenstein et al., 1992; Hicks et al., 1993, 1996; Conti et al., 1998). Motor and sensory performance has also been studied extensively (Dixon et al., 1987; McIntosh et al., 1989; Long et al., 1996; Pierce et al., 1998; Lyeth et al., 2001; Hallam et al., 2004). Studies have also examined cognitive deficits (Lyeth et al., 1990; Smith et al., 1991; Hicks et al., 1993; Schmidt et al., 1999; Hallam et al., 2004). The FPI animal injury group in our study, sustained similar deficits and histological damage as has been shown in these aforementioned studies.

No single model has been entirely successful in producing the spectrum of changes observed in clinical TBI. However, we believe that in a model where various parameters can be changed independently, the experimental model will best resemble clinical situations. In TBI a mechanical impact induces a mechanical response at cell and tissue level that ultimately causes pathophysiological injury response (LaPlaca et al., 2007). Brain is essentially incompressible and volume does not change when it undergoes deformation (Morrison et al., 2006). Due to the non-linear viscoelastic material properties of brain tissues, the mechanical response to a low rate deformation would likely be different from the response to a high rate deformation (Koeneman, 1966; Shuck and Advani, 1972; Wang

and Wineman, 1972; Pamidi and Advani, 1978; Morrison et al., 1997). Hence, the various aspects of mechanical loading, like rate of impact and impulse among others, become crucial in determining the injury characteristics. This device is the first of its kind that enables these parameters to be independently controlled thus, providing a means to gain insight into how these parameters influence pathophysiological outcomes. From the behavioral, electrophysiological and histological changes observed, it can be deduced that these parameters differently contribute to brain pathology and functional deficits.

From a device perspective, comparison of the various rise-times from the FPI and VC-FPI device shows that the new VC-FPI is able to generate a range of different rise-times and therefore distinct rates of injury. Our results show that the voice-coil makes a smooth consistent motion, but depending on the load (closed valve, adult rat, adolescent rat) there are differences in the smoothness of the output pressure waveform. This is probably due to the fact that the pressure pulse deforms the brain tissue, and since the fluid filled cavity is continuous with the dura, the volume of the fluid in the enclosed cavity increases. This change reduces the pressure at that particular point in time (not the entire pressure waveform duration) and hence creates miniature troughs along the pressure waveform. In the fast-rate VC-FPI injury when the pressure pulse is very rapid the brain tissue does not have enough time to deform (as much), hence the output pressure waveform is smoother. In adolescent animals the brain may be more yielding ("softer") and therefore the deformation may be more prominent.

The waveform analysis also shows that in the fast-rate VC-FPI injury the rise time is independent of the load, whereas in slow-rate VC-FPI the rise time depends on the load. The adolescent brain slows the rate of rise a little more than the adult rat. This is

another effect of the deformation. On the other hand, in a standard FPI system, there is always a small variability in the output pressure peak depending on the load. This is probably also due to the deformation. The effects of deformation may not be as obvious in pressure waveforms in injuries from standard FPI system, because the volume of the fluid filled cavity is much greater, and the percentage increase in volume is smaller and hence decrease in pressure is insignificant in comparison. However, there is indeed a little drop in the peak pressure achieved when an animal is attached versus when no animals are attached, even in the standard FPI system (difference is lesser than the difference seen in the VC-FPI). But the experimenter compensates for that by adjusting the height of the pendulum before the animal injuries. In the same way, the input displacement setting is altered to achieve the higher pressure in a VC-FPI system. While we are convinced that these differences are based on the differences in the relative deformation of the load; we also suspect that part of the difference could arise from lab to lab differences in surgery, quality of the head cap connector and lab to lab FPI devices (the adult experiments were performed at a different lab from the adolescent experiments), or from the distance between the pressure sensor and the site of injury.

The device characterization studies revealed that the VC-FPI is indeed capable of generating pressure waves very similar to the standard FPI. The major aspects of the waveform such as peak pressure, rise-time and impulse can be matched between the two devices. However, the only difference seems to be the dependency of the slow-rate VC-FPI pressure waveform on the load applied. Device characterization shows that the device actually works better in the fast-rate mode and there is less dependency on the load. This is because, from viscoelasticity, the faster the deformation, the less compliant

the behavior. However, careful control of the input parameters can indeed reduce the differences in pressure peak, rise-time and impulse. Once the program has been defined, the output pressure waves are very consistent and statistics show minimal spread in the output pressure waveform parameters such as peak, rise-time and impulse. The major contribution of the VC-FPI device is the fact that the new device is the capability of generating variable rise time injuries as well as much faster injuries than a standard FPI device.

Immediate behavioral outcomes including the occurrence of behavioral seizures and mortality were significantly lower in rats subject to fast-rate VC-FPI, blast-like waveforms compared to the slow-rate VC-FPI waveform (75% immediate seizures and 20% immediate death from slow-rate VC-FPI injury versus none from fast-rate VC-FPI injury). This may be because the deformation of the brain due to the slow-rate VC-FPI injury might have been greater than that from the fast-rate VC-FPI injury; owing to the viscoelastic properties of the brain tissue. Although the duration for neurological recovery immediately after TBI, of the FPI and slow-rate VC-FPI injury animals were similar, the slow-rate VC-FPI injury animals took slightly longer to recover, which was probably because of the slightly greater impulse of the injury that they were exposed to. The toe-pinch response also followed similar patterns in terms of the time taken for neurological recovery.

Results from the acute Fluoro-histochemistry studies conducted 4h and 24h post-injury suggests that a faster rate injury results in significantly reduced acute neuronal degeneration in the Hilus (4h study) and CA2-3 hippocampus (24h study). The 4h (best transitional time point) and the 24h (maximal degeneration time point) evaluation was

chosen as two time points of importance based on previous TBI studies examining FJ staining from 30min to 7d post TBI (Zhao et al., 2003; Hallam et al., 2004; Zhong et al., 2005). This reduced immediate cellular damage at the acute stage suggests that rats exposed to faster rate injuries may have a better neurological prognosis than the slower injury sustained rats; immediately after injury.

Vestibulomotor tests determine the degree of fine motor coordination after injury. Previous studies have demonstrated that vestibulomotor deficits after FPI can persist for days to weeks after TBI (Hamm et. al., 1994, 1996). Results from the rotarod and ladder performance indicated that in general the fast-rate VC-FPI injuries resulted in faster motor and sensory recovery compared to the slow-rate VC-FPI and the standard FPI injuries. The rats injured with the slow-rate VC-FPI generally had significantly greater motor and sensory deficits compared to the fast-rate VC-FPI and the standard FPI injuries. In fact, some of the rats were unable to perform in some of the tasks and those that were able to, did poorly. The rats that were not able to perform were eliminated from the data analysis.

Several studies have consistently reported an increase in dentate network excitability 1 week post TBI using commonly used FPI system (Lowenstein et al., 1992; Toth et al., 1997; Santhakumar et al., 2000, 2001; Gupta et al., 2012). The hilar neuronal loss and increase in dentate excitability have been suggested to predict development of long-term neurological complication. Therefore we examined the granule cell population response to afferent activation in order to assess the effect of injury-rate on neurophysiological outcome 1wk post TBI. While the granule cell population response evoked by perforant path stimulation (at 4mA) rarely showed population spikes in sham-control rats, afferent

activation reliably elicited population spikes in granule cells 1wk after fast-rate and slow-rate VC-FPI injury sustained rats. Similarly summary data also demonstrated enhanced granule cell population spike amplitude after fast-rate and slow-rate VC-FPI injuries. Therefore although early behavioral assessment and neuronal degeneration 4h and 24h post-injury suggest that fast-rate VC-FPI injury leads to reduced neurological damage compared to slow-rate VC-FPI injuries; electrophysiological studies performed 1wk post-injury demonstrate similar increase in network excitability and hence similar impairment.

The metric spatial information task for spatial recognition (Goodrich-Hunsaker et al., 2005, 2008) was carried out 8d post-TBI, around the same time point (post-TBI) as the electrophysiological assessment, and similar to the increase in network excitability being similar in injured rats from all groups, the inability to recognize the spatial difference during the test session, was effected equally in all injured rats, fast-rate and slow-rate VC-FPI and standard FPI. Thus, indicating that the effect of the injury was similar in both rates, when assessing the cognitive skills related to spatial recognition.

The Morris Water Maze test was carried out between 11d to 15d post-TBI. The MWM test identifies spatial learning (time to find the goal platform and distance swum to the goal) and also some motor and sensory recovery (swim speed) (Morris, 1987). In all the tests, the fast-rate VC-FPI injury showed better performance than the slow-rate VC-FPI injury. This was partly as a result of increased cognitive skills in the fast-rate VC-FPI injured animals than the slow-rate VC-FPI injured animals, and partly due to better motor skills and hence increased swim speeds. Since, the time to find the goal platform is a combination of learning and remembering the spatial location of the goal and a function of swim speed (motor performance). Since the motor recovery (from rotarod and ladder

tests) was slower in the slow-rate VC-FPI injuries and swim speed was slower, the slow-rate VC-FPI injury sustained animals were indeed at a disadvantage. However, the large separation in performance between the time required by a fast-rate VC-FPI and that required by a slow-rate VC-FPI injured animals to find the goal is indicative that the loss of memory and learning also plays a role in their reduced performance in the Morris water maze test.

Further analysis was performed on the data from the Morris Water Maze in order to identify differences in short-term and long-term memory (Feng et al., 2011). Short-term memory impairment was very similar ($P \cong 1$) in all four sets (sham control and injured animals), but the long-term memory impairment was different. This is probably because animals show very consistent short-term memory but not so much in the long-term memory, especially in the injured animals. However, it is hard to pinpoint the deficiency in long-term memory because in case of the long-term memory, the long-term potentiation masked the long-term memory retention from each of the previous days making it difficult to calculate and is beyond the scope of this study.

After the completion of the behavioral assessment, histological assessment was carried out on day-15 post-TBI, and the surviving neurons were quantified. Results showed that despite the reduced neuronal degeneration seen at 24h post-TBI, the fast-rate VC-FPI animals showed similar cell death to the slow-rate VC-FPI injured animals, in the chronic histological assessment. This suggests a greater progressive hippocampal cell loss in the fast-rate VC-FPI injury sustained animals.

Primary and secondary injury response may vary from injury to injury. The primary injury consists of rapid deformation of the brain, leading to rupture of cell

membranes, escape of intracellular contents, and disruption of blood flow (McIntosh et al., 1994) resulting in primary necrotic death. The delayed or secondary injury is a complex series of biochemical, structural and molecular changes that in combination can lead to cellular damage by apoptosis or necrosis (Thompson et al., 2004). Because of the focal and diffuse nature of FPI, there is stretching and shearing of axons, both in the direct vicinity of the injury and in remote areas. Owing to the viscoelastic properties of the brain the primary and secondary injury response would vary. Therefore, we can speculate that the fast-rate VC-FPI injury does not necessarily reduce the effects of the injury; rather it affects the neurological system differently.

If we compare the pathophysiology between the slow-rate and the standard FPI, we see that the effects are very similar. In some areas the slow-rate VC-FPI injury does perform worse than the standard FPI, but this may be because of the slightly greater rise-time and impulse in the slow-rate VC-FPI injury group used in this study. From the pathophysiological results of the injuries we can clearly see that the fast-rate injury produces lower magnitude early neurological deficits, but the neurological deficits increase at later stages. This may be due to the lesser deformation in the fast rate injury resulting in reduced early neuronal death during the primary stage. However, axons may have been deformed, and intracellular chemicals might have been released which may have triggered delayed cell death or greater dysfunction in the secondary stage of the injury. Also due to lesser deformation in the fast-rate injury, the injury may be more focal and less diffuse than the slow-rate injury. Also, the fact that the fast-rate injury group performs better in some cognitive deficit associated with spatial memory (MWM) and

does poorly in others (Metric task) suggests that the damage due to a fast injury may be different and not necessarily a milder form of the slow-rate injury.

Previous studies in literature have shown that the pressure peak is a determining factor for pathological severity. From this study so far, it was found that the rise-time or rate is also a very crucial determining factor. However, one question stays unanswered: Does the pathophysiology that was studied here, depend on the rise-time or on the impulse? Since Impulse is the area under the pressure-time curve, it depends on both the pressure peak and the rise-time. As the pressure was kept constant (within a narrow margin) the impulse was dependent on the rise-time. Therefore in all experiments the pathophysiology that was seen under fast-rate VC-FPI, the independent variable was not only the rise-time, but also the impulse. Therefore the question was "Does the pathophysiology depend on the rate or the impulse?" From the waveform analysis of the eliminated-slow-rate group it can be seen that there is a difference in rise-time but not the impulse. This difference in rise-time and impulse from the slow-rate VC-FPI group may be due to a decrease in duration of the injury and may have been caused by injury-to-injury differences. Because of this inconsistency this subset of animals (n=3) was eliminated from the rest of the pathophysiological studies. A separate analysis of this group showed that the pressure peak and the impulse didn't vary significantly. However, there was a significant increase in the rise-time. Thus it may be the case that the severe pathological shortcomings were most likely due to the increase in rise-time. However, this is a very small group of animals (n=3), but overall the study suggests that the dependency of the pathophysiological outcome may be on the impulse as well, since the

severity of the outcome corresponds to a higher impulse in most cases. Therefore, the effect of impulse needs to be investigated further.

Investigators studying FPI injuries have primarily assessed injury outcomes to determine the severity of the injury and not assessed the actual pressure waveform (Thompson et al., 2005). To that end, the severity was determined by the return of reflexes (right-time, toe pinch response etc.) or mortality to serve as the biological indicators of severity. Therefore, when in case of adolescent animals a lower pressure peak resulted in a moderate injury than the pressure level used for adult animal injuries, the investigators considered a lower pressure peak as their target peak for moderate injury in those animals based on the biological outcome. Therefore the range of pressure peaks used for moderate injuries in literature is a fairly wide range 1.5-2.15 atm (McIntosh et al., 1989). Thus, any difference in the pressure waveform was not assessed. Same concept applied for adult animals, the investigators adjusted the pressure peaks to judge the severity of injuries, and the severity was primarily based on injury outcomes in the form of biological indicators. Investigators have justified this difference as being due to the differences in the actual configuration of the fluid percussion device variations between laboratories. However, very few investigators took interest into looking at the actual pressure waveforms. Therefore the underlying changes in rate were not quite recognized especially in FPI studies. Our study shows how determining the severity of the injury from the biological indicators may be erroneous, since in case of a faster rate injury the biological indicators immediately after the injury masks the underlying pathological severity that develops at a later stage. Therefore not only is rate (rise time of pressure wave) an important factor in the pathophysiology of an injury, investigators need to

devote their attention to the characteristics of the pressure wave of the injury and not just the biological indicators of the injury outcomes in order to determine what type of the injury the animal was subjected to, in TBI studies.

Collectively our results suggest that this new voice coil model of TBI can be used to investigate the pathophysiology associated with varying rates of TBI. The mechanical response of a non-linear visco-elastic material to a low strain rate deformation will likely be different than its response to a high strain rate (Koenemann, 1966; Shuck and Advani, 1972; Wang and Winemann, 1972; Pamidi and Advani, 1978; Morrison III et al., 1998). Systemic investigation of relevant loading parameters and the resulting responses are important for understanding injury-induced pathophysiological mechanisms and developing experimental models that are relevant to the human clinical situation. The fast-rate injury is not likely a milder form of the slow-rate injury. This is because the effect of the fast-rate injury is a lesser deformation of the brain, but similar produces an increased pressure in the brain cavity. This may result in the fast-rate injury producing different primary and secondary injuries compared to the slow-rate injury. Our findings suggest the need to investigate changes in all important injury parameters, including the rate of injury, for traumatic brain injury in laboratory models. Particularly, since reduced cellular damage and improved neurological outcome immediately after fast-rate VC-FPI injuries masks the severity of the long-term neurophysiological impairment. A deeper understanding of the pathophysiology of brain injury is necessary to more effectively care for TBI patients. This variable rate voice coil fluid percussion injury device will help in deciphering the post traumatic sequel for different rate injuries, and for development of new treatment

approaches by determining injury mechanisms across the temporal spectrum of the injury response for various rates.

References:

Abdul-Wahab, R., et al. "Mechanica Bioeffects of Pulsed High Intensity Focused Ultrasound on a Simple Neural Model." *Medical Physics* 39.7 (2012)

Adams, J. H., D. I. Graham, and T. A. Gennarelli. "Head Injury in Man and Experimental Animals." *Acta Neurochir.* 32 (1983): 15-30.

Adams, J. H., D. I. Grahams, G. Scott, L. S. Parker, and D. Doyle. "Brain Damage in Fatal Non-Missile Head Injury." *Journal of Clinical Pathology* 33 (1980): 1132-145.

Bentzer, P., G. Mattiasson, T. K. McIntosh, T. Wieloch, and P. O. Grande. "Infusion of Prostacyclin Following Experimental Brain Injury in the Rat Reduces Cortical Lesion Volume." *Journal Of Neurotrauman* 18 (2001): 275-85.

Cassen, B., L. Curtis, and K. Kistler. "Initial Studies of the Effect of Laboratory Produced Air Blast on Animals." *J. Aviat. Med.* 21 (1950): 38-47.

Cargill II, Robert S., and Lawrence E. Thibault. "Acute Alteration in [Ca2+]i in NG108-15 Cells Subjected to High Strain Rate Deformation and Chemical Hypoxia: An InVitro Model for Neural Trauma." *Journal of Neurotrauma* 13.7 (1996): 395-407.

Celander, H., and et al. "The Use of a Compressed Air Operated Shock Tube for Physiological Blast Research." *Acta Physiol. Scand* 33 (1955): 6-13.

Cernak, I., and et al. "Cognitive Deficits Following Blast Injury Induced Neurotrauma: Possible Involvement of Nitric Oxide." *Brain Injury* 15 (2001): 593-612. Print.

Cernak, I., and et al. "Ultrastructural and Functional Characteristics of Blast Injury-Induced Neurotrauma." *Journal of Trauma* 50 (2001): 695-706.

Cernak, Ibolja, et al., "The pathobiology of blast injuries and blast-induced neurotrauma as identified using a new experimental model of injury in mice." Neurobiology of disease 41:2 (2011): 538-551

Cohen, A. S., B. J. Pfister, and E. Schwarzback. "Injury-Induced Alterations in CNS Electrophysiology." *Progress in Brain Research* 161 (2007): 143-69.

Conti, A. C., R. Raghupathi, J. Q. Trojanowski, and T. K. McIntosh. "Experimental Brain

Injury Induces Regionally Distinct Apoptosis During the Acute and Delayed Post-Traumatic Period." *Journal of Neuroscience* 18 (1998): 5663-672.

Cortez, S. C., T. K. McIntosh, and L. Noble. "Experimental Fluid Percussion Injury: Vascular Disruption and Neuronal and Glial Alterations." *Brain Research* 482 (1989): 271-82.

Creed, J. A., A. M. DiLeonardi, and D. P. Fox, et al. "Concussive Brain Trauma in Mouse Results in Acute Cognitive Deficits and Sustained Impairment of Axonal Function." *Journal of Neurotrauma* 28 (2011): 547-63.

Curra, Francesco. "Comprehensive 3D Model of Shockwave Interactions in Blast-Induced Traumatic Brain Injury." *DTIC, Online Information for the Defense Community* ADA521780 (2009):

Dail, W. G., and et al. "Responses to Cortical Injury: II. Widespread Depression of the Activity of an Enzyme in Cortex Remote from a Focal Injury." *Brain Research* 211 (1981): 79-89.

Dimitrijevic, Milan R. "Restorative Neurology of Head Injury." *Journal of Neurotrauma* 6.1 (1989): 25-29.

Dixon, Edward C., Bruce G. Lyeth, John T. Povlishock, Robert L. Findling, Robert J. Hamm, Anthony Marmarou, Harold F. Young, and Ronald L. Hayes. "A Fluid Percussion Model of Experimental Brain Injury in the Rat." *Journal of Neurosurgery* 67.1 (1987): 110-19.

Elsayed, N. M. "Toxicology of Blast Overpressure." *Toxicology* 121 (1997): 1-15

El Sayed, T., A. Mota, F. Fraternali, and H. Ortiz. "Biomechanics of Traumatic Brain Injury." *Computational Methods Appl. Mechanics Eng.* 197 (2008): 4692-701.

Faul, M., Xu, L., Wald, M.M., and Coronado, V.G. (2010). Traumatic Brain Injury in the United States: Emergency Department Visits, Hospitalizations and Deaths 2002–2006. Atlanta, GA: Centers for Disease Control and Prevention, National Center for Injury Prevention and Control.

http://www.cdc.gov/traumaticbraininjury/pdf/bluebook.pdf

Feeney, D. M., and et al. "Responses to Cortical Injury. I. Methodology and Local Effects of Contusions in the Rat." *Brain Research* 211 (1981): 67-77.

Feng, Jun-Feng, and et al. "Post-injury Administration of NAAG Peptidase Inhibitor Prodrug, PGI-02776, in Experimental TBI." *Brain Research* 1395 (2011): 62-73.

Floyd, C. L., K. M. Golden, R. T. Black, R. J. Hamm, and B. G. Lyeth. "Craniectomy Position Affects Morris Water Maze Performance and Hippocampal Cell Loss After Parasagittal Fluid Percussion." *Journal of Neurotrauma* 19 (2002): 303-16.

Gaetz, Michael. "The Neurophysiology of Brain Injury." *Clinical Neurophysiology of Brain Injury* 115.1 (2004): 4-18.

Garman, R., and et al. "Blast Exposure in Rats with Body Shielding Is Characterized Primarily by Diffuse Axonal Injury." *Journal of Neurotrauma* 28 (2011): 947-59.

Garman, R., and et al. "Blast Overpressure Injury in Rats with Body Protection Produces Acute and Subacute Axonal, Dendritic and Synaptic Neuropathology." *Journal of Neurotrauma* 26 (2009): 1-53. Print.

Geddes, Donna M., and Robert S. Cargill. "An InVitro Model of Neural Trauma: Device Characterization and Calcium Response to Mechanical Stretch." *Journal of Biomechanical Engineering* 123.3 (2001): 247-55.

Geddes, Donna M., Robert S. Cargill II, and Michelle C. LaPlaca. "Mechanical Stretch to Neurons Results in a Strain Rate and Magnitude Dependent Increase in Plasma Membrane Permeability." *Journal Of Neurotrauma* 20.10 (2003): 1039-049.

Geddes-Klein, Donna M., Kimberly B. Schiffman, and David F. Meaney. "Mechanisms and Consequences of Neuronal Stretch Injury InVitro Differ with the Model of Trauma." *Journal of Neurotrauma* 23.2 (2006): 193-204.

Glass, T. F., B. Reeves, and F. R. Sharp. "Modeling Both the Mechanical and Hypoxic Features of Traumatic Brain Injury InVitro in Rats." *Neuroscience Letters* 328.2 (2002): 133-36.

Goeller, Jacques, Andrew Wardlaw, Derrick Treichler, Joseph O'Bruba, and Greg Weiss. "Investigation of Cavitation as a Possible Damage Mechanism in Blast-Induced Traumatic Brain Injury." *Journal of Neurotrauma* 29.10 (2012): 1970-981.

Goldsmith, W., and K. L. Monson. "The State of Head Injury Biomechanics: Past, Present, and Future, Part 2: Physical Experimentation." *Critical Review of Biomedical Eng.* 33 (2005): 105-207.

Gondusky J, and Reiter M. “Protecting Military Convoys in Iraq: An Examination of Battle Injuries Sustained by a Mechanized Battalion During Operation Iraqi Freedom II”. Mil Med. 170 (6): (2005): 546-549.

Goodrich-Hunsaker, N. J., M. R. Hunsaker, and R. P. Kesner. "Dissociating the Role of the Parietal Cortex and Dorsal Hippocampus for Spatial Information Processing." *Behavioral Neuroscience* 119 (2005): 1307-315.

Goodrich-Hunsaker, N. J., M. R. Hunsaker, and R. P. Kesner. "The Interactions and Dissociations of the Dorsal Hippocampus Subregions: How the Dentate Gyrus, CA3, and CA1 Process Spatial Information." *Behavioral Neuroscience* 122 (2008): 12-26.

Graham, D. I., R. Raghupathi, K. E. Saatman, D. F. Meaney, and T. K. McIntosh. "Tissue Tears in the White Matter After Lateral Fluid Percussion Brain Injury in the Rat: Relevance to Human Head Injury." *Acta Neuropathol.* 99 (2000): 117-24.

Gupta, A., F. S. Elgammal, and A. Proddutur. "Decrease in Tonic Inhibition Contributes to Increase in Dentate Semilunar Granule Cell Excitability After Brain Injury." *The Journal of Neuroscience* 32 (2012): 2523-537.

Hallam, T. M., and et al. "Comparison of Behavioral Deficits and Acute Neuronal Degeneration in Rat Lateral Fluid Percussion and Weight Drop Injury Models." *Journal of Neurotrauma* 21 (2004): 521-39.

Hamm, Robert J., Brian R. Pike, Dianne M. ODell, Bruce G. Lyeth, and Larry W. Jenkins. "The Rotarod Test: An Evaluation of Effectiveness in Assessing Motor Deficits Following Traumatic Brain Injury." *Journal of Neurotrauma* 11.2 (1994): 187-96.

Hardy, W. N., T. B. Khalil, and A. I. King. "Literature Review of Head Injury Biomechanics." *International Journal of Impact Engineering* 15 (1994): 561-86.

Hicks, R. R., and et al. "Temporal and Spatial Characterization of Neuronal Injury Following Lateral Fluid Percussion Injury in the Rat." *Acta. Neuropathol.* 91 (1996): 236-46.

Hicks, R. R., D. H. Smith, and D. H. Loweinstein. "Mild Experimental Brain Injury in the Rat Induces Cognitive Deficits Associated with Regional Neuronal Loss in the Hippocampus." *Journal of Neurotrauma* 10 (1993): 405-14.

Hovda, D. A., S. M. Lee, M. L. Smith, S. Vonstruck, M. Bergsneider, D. Kelly, E. Shalmon, N. Martin, M. Caron, J. Mazziotta, M. Phelps, and D. P. Becker. "The Neurochemical and Metabolic Cascade Following Brain Injury: Moving From Animal Models to Man." *Journal of Neurotrauma* 12.5 (1995): 903-06.

Jenkins, L. W., Y. C. Lu, W. E. Johnston, B. G. Lyeth, and D. S. Prough. "Combined Therapy Effects Outcomes Differentially after Traumatic Brain Injury and Secondary Forebrain Ischemia in Rats." *Brain Research* 817 (1999): 132-44.

Kabadi S.V., et al., "Fluid-Percussion–Induced Traumatic Brain Injury Model in Rats" Nature Protocols Volume:5, Pages:1552–1563(2010)

King, A. I., H. Yang, L. Zhang, W. Hardy, and D. C. Viano. "Is Head Injury Caused by Linear or Angular Acceleration." *IRCOBI, Conference, Lisbon* (2003):

KingLin, Y., K. B. Chandra, and D. U. VonRosenBerg. "Angular Acceleration of Viscoelastic (Kelvin) Material in a Rigid Spherical Shell- a Rotational Head Injury Model." *Journal of Biomechanics* 8.5 (1975): 285-92.

Koenemann, J. B. "Viscoelastic Properties of Brain Tissue." *MS Thesis, Case Institute of Technology, Cleveland, OH* (1966)

Langlois, J. A., W. Ruthland-Brown, and M. M. Wald. "The Epidemiology and Impact of Traumatic Brain Injury: A Brief Overview." *Journal of Head Trauma and Rehabilitation* 21 (2006): 375-78.

Langlois, J. A., W. Rutland-Brown, and K. E. Tomas. "Traumatic Brain Injury in the United States: Emergency Department Visits, Hospitilization, and Deaths." *National Center for Injury Prevention and Control, Atlanta, GA* (2004): 1-68.

LaPlaca, Michelle C., and Lawrence E. Thibault. "An InVitro Traumatic Injury Model to Examine the Response of Neurons to a Hydrodynamically-Induced Deformation." *Annals of Biomedical Engineering* 25.4 (1997): 665-77.

LaPlaca, Michelle C., C. M. Simon, Gustavo R. Prado, and D. K. Cullen. "CNS Injury Biomechanics and Experimental Models." *Progress in Brain Research* 161 (2007): 13-26.

LaPlaca, Michelle C., D. Kacy Cullen, Justin J. McLouglin, and Robert S. Cargill II. "High-rate Shear Strain of Three-dimensional Neural Cell Cultures: A New InVitro Traumatic Brain Injury Model." *Journal of Biomechanics* 38 (2005):

1093-105.

LaPlaca, Michelle C., Gustavo R. Prado, D. Kacy Cullen, and Hillary R. Irons. "High Rate Shear Insult Delivered to Cortical Neurons Produces Heterogenous Membrane Permeability Alterations." *Engineering in Medicine and Biology Society* (2006)

LaPlaca, Michelle C., Virgina MY Lee, and Laurence E. Thibault. "An InVitro Model of Traumatic Neuronal Injury: Loading Rate-Dependent Changes in Acute Cytosolic Calcium and Lactate Dehydrogenase Release." *Journal of Neurotrauma* 14.6 (1997): 355-68.

Long, J. B., and et al. "Laser-Doppler Flowmetry Measurements of Subcortical Blood Flow Changes After Fluid Percussion Injury in Rats." *Journal of Neurotrauma* 13 (1996): 149-62.

Long, J. B. "Blast Overpressure in Rats: Recreating a Battlefield Injury in the Laboratory." *Journal of Neurotrauma* 26 (2009): 827-40.

Lowenstein, D. H., M. J. Thomas, D. H. Smith, and T. K. McIntosh. "Selective Vulnerability of Dentate Hilar Neurons Following Traumatic Brain Injury: A Potential Mechanistic Link Between Head Trauma and Disorders of the Hippocampus." *The Journal of Neuroscience* 12 (1992): 4846-853.

Lyeth, B. G., and et al. "Group 1 Metabotropic Glutamate Antagonist Reduces Acute Neuronal Degeneration and Behavioral Deficits Following Traumatic Brain Injury in the Rat." *Exp. Neurology* 169 (2001): 191-99.

Lyeth, B. G., L. W. Jenkins, R. J. Hamm, C. E. Dixon, L. L. Phillips, and G. L. Clifton. "Prolonged Memory Impairment in the Absence of Hippocampal Cell Death Following Traumatic Brain Injury in the Rat." *Brain Res.* 526 (1990): 249-58.

Magou, G. C., and et al., "Engineering a High Throughput Axon Injury System." *Journal of Neurotrauma* 28.11 (2011): 2203-2218

Margulies, S. S. and L. E. Thibault. "A Proposed Tolerance Criterion for Diffuse Axonal Injury in Man." J Biomech 25.8 (1992): 917-923.

Marmarou, Anthony, Montasser A. AbdelFattah Foda, Wimer Vanden Brink, J. Campbell, H. Kita, and K. Demetriadou. "A New Model of Diffuse Brain Injury in Rats, Part 1: Pathophysiology and Biomechanics." *Journal of Neurosurgery*

80.2 (1994): 291-300.

McIntosh, T. K., and et al. "Traumatic Brain Injury in the Rat: Characterization of Lateral Fluid Percussion Model." *Neuroscience* 28 (1989): 233-44.

Meaney, D. F., et al. "Biomechanical Analysis of Experimental Diffuse Axonal Injury." J Neurotrauma 12.4 (1995): 689-694.

Morales, D. M., and et al. "Experimental Models of Traumatic Brain Injury: Do We Really Need to Build A Better Mousetrap." *Neuroscience* 136 (2005): 971-89.

Morris, R. "Developments of a Water-Maze Procedure for Studying Spatial Learning in the Rat." *Journal of Neuroscience Methods* 11 (1984): 47-60.

Morrision III, Barclay, David F. Meaney, and Tracy K. McIntosh. "Mechanical Characterization of an InViro Device Designed to Quantitatively Injure Living Brain Tissue." *Annals of Biomedical Engineering* 26 (1998): 381-90.

Morrison III, Barclay, Cater H. L, Wang C. C, Thomas F. C, Hung C. T, Ateshian G. A, and Sundstrom L. E. "A Tissue Level Tolerance Criterion for Living Brain Developed with an InVitro Model of Traumatic Mechanical Loading." *Stapp Car Crash Journal* 47 (2003): 93-105.

Morrison III, Barclay, et al. “An In-Vitro Model of Traumatic Brain Injury Utilizing Two Dimensional Stretch of Organotypic Hippocampal Slice Cultures.” *Journal of Neuroscience* 150 (2006): 192-201.

Nakagawa, Atsuhiro, Geoffrey T. Manley, Alisa D. Gean, Kiyonobu Ohtani, Rocco Armonda, Akira Tsukamoto, Hiroaki Yamamoto, Kazuyoshi Takayama, and Teiji Tominaga. "Mechanisms of Primary Blast-Induced Traumatic Brain Injury: Insights from Shockwave Research." *Journal of Neurotrauma* 28.6 (2011): 1101-119.

Nakagawa, Atsuhiro, Miki Fujimura, Hironobu Okuyama, Tokitada Hashimoto, Kazuyoshi Takayama, and Teiji Tominaga. "Shock-Wave Induced Brain Injury in Rat: Novel Traumatic Brain Injury Animal Model." *Acta Neurochirurgica Supplements* 102 (2009): 421-24.

Ommaya, A. K., Lawrence Thibault, and F. A. Bandak. "Mechanisms of Impact Head Injury." *International Journal of Impact Engineering* 15 (1994): 535-60.

Pamidi, M. R., and S. H. Advani. "Non-Linear Constitutive Relations for Human Tissue."

Journal of Biomechanical Engineering 100 (1978): 44-48.

Pfister, Bryan J., Timothy P. Weihs, Michael Batenbaugh, and Gang Bao. "An InVitro Uniaxial Model for Axonal Injury." *Annals of Biomedical Engineering* 31.5 (2003): 589-98.

Pierce, J. ES, and et al. "Enduring Cognitive, Neurobehavioral, and Histopathological, Changes Persist for up to One Year Following Severe Experimental Brain Injury in Rats." *Neuroscience* 87 (1998): 359-69.

Rashid, Badar, Michel Destrade, and Michael D. Gilchrist. "Mechanical Characterization of Brain Tissue in Compression Af Dynamic Strain Rate." *Journal of the Mechanical Behavior of Biomedical Materials* 10 (2012): 23-38.

Ritenour, A. E., et al. "Incidence of Primary Blast Injury in US Military Overseas Contingency Operations: A Retrospective Study" Annals of Surgery: (2010) 251(6): 1140-1144.

Rustay, Nathan R., Doughlas Wahlsten, and John C. Crabbe. "Influence of Task Parameters on Rotarod Performance and Sensitivity to Ethanol In Mice." *Behavioral Brain Research* 141 (2003): 237-49.

Sanders, M. J., and et al. "Cognitive Function Following Traumatic Brain Injury: Effects of Injury Severity and Recovery Period in a Parasagittal Fluid-Percussion Injury Model." *Journal of Neurotrauma* 16 (1999): 915-25.

Santhakumar, V., A. D. Ratzliff, J. Jeng, and et al. "Long-term Hyperexcitability in the Hippocampus after Experimental Head Trauma." *Annals of Neurology* 50 (2001): 708-17.

Santhakumar, V., R. Bender, M. Frostcher, and et al. "Granule Cell Hyperexcitability in the Early Post-Traumatic Rat Dentate Gyrus: The "Irritable Mossy Cell" Hypothesis." *The Journal of Physiology* 524 (2000): 117-34.

Santhkumar, V., J. Voipio, K. Kaila, and I. Soltesz. "Post Traumatic Hyperexcitability Is Not Caused by Impaired Buffering of Extracellular Potassium." *The Journal of Neuroscience* 23 (2003): 5865-876.

Sawauchi, S., and et al. "A New Rat Model of Diffuse Brain Injury Association with Acute Subdural Hematoma: Assessment of Varying Hematoma Volume, Insult Severity, and the Presence of Hypoxemia." *Journal of Neurotraua* 20 (2003):

613-22.

Schmidt, R. H., and et al. "Time Course for Recovery of Water Maze Performance and Central Cholinergic Innervation After Fluid Percussion Injury." *Journal of Neurotrauma* 16 (1999): 1139-147.

Schmued, L. C., and et al. "Fluoro-Jade: A Novel Fluorochrome for the Sensitive and Reliable Histochemical Localization of Neuronal Degeneration." *Brain Research* 751 (1997): 37-46. Print.

Schmued, L. C. "Fluoro-Jade B: A High Affinity Fluorescent Marker for the Localization of Neuronal Degeneration." *Brain Research* 874 (2000): 123-30.

Shuck, L. Z., and S. H. Advani. "Rheological Response of Human Brain Tissue in Shear." *ASME J. Basic Engineering* 12 (1972): 905-11.

Singh, A., Y. Lu, C. Chen, S. Kallakuri, and J. M. Cavanaugh. "A New Model of Traumatic Axonal Injury to Determine the Effect of Strain and Displacement Rates." *Stapp Car Crash Journal* 50 (2006): 601-23.

Smith, D. H., and et al. "Evaluation of Memory Dysfunction Following Experimental Brain Injury Using the Morris Water Maze." *Journal of Neurotrauma* 8 (1991): 259-69.

Tamura, Atsutaka, Sadayuk Hayashi, Isao Watanabe, Kazuaki Nagayami, and Takeo Matsumoto. "Mechanical Characterization of Brain Tissue in High-Rate Compression." *Journal of Biomechanical Science and Engineering (The Japan Society of Mechanical Eng.)* 2.3 (2007): 115-26.

Thompson, H. J., and et al. "Lateral Fluid Percussion Brain Injury: A 15-year Review and Evaluation." *Journal of Neurotrauma* 22 (2005): 42-75.

Thurman, David J., Clinton Alverson, Kathleen A. Dunn, Janet Guerrero, and Joseph E. Sniezek. "Traumatic Brain Injury in the United States: A Public Health Perspective." *Journal of Head Trauma Rehabilitation* 14.6 (1999): 602-15.

Toth, Z., G. S. Hollrigel, T. Grocs, and I. Soltesz. "Instantaneous Perturbation of Dentate Interneuronal Networks by a Pressure Wave Transient Delivered to the Neocortex." *The Journal of Neuroscience* 17 (1997): 8106-117.

Tyler, WJ, “Non-Invasive Neuromodulation With Ultrasound? A Continuum Mechanics Hypothesis.” Neuroscientist (February 2011) 17: 25-36.

Wang, H. C., and A. S. Wineman. "A Mathematical Model for the Determination of Viscoelastic Behavior of Brain InVivo- I Oscillatory Response." *Journal of Biomechanics* 5 (1972): 431-46.

West MJ, Slomianka L, Gundersen HJ. Unbiased stereological estimation of the total number of neurons in thesubdivisions of the rat hippocampus using the optical fractionator. *The Anatomical record*. (1991)231:482-497

West MJ. New stereological methods for counting neurons. *Neurobiology of aging*. (1993)14:275-285

Xuzhcu Lhja Electronic Technology, http://www.lhdz.org/hdyl/add2.htm, Viewed Jan 20, 2012.

Zhao, X., A. Ahram, R. F. Berman, J. P. Muizelaar, and B. G. Lyeth. "Early Loss of Astrocytes After Experimental Traumatic Brain Injury." *Glia* 44 (2003): 140-52.

Zhong, C., X. Zhao, J. Sarva, A. Kozikowski, J. H. Neale, and B. G. Lyeth. "NAAG Peptidase Inhibitor Reduces Acute Neuronal Degeneration and Astrocyte Damage Following Lateral Fluid Percussion TBI in Rats." *Journal of Neurotrauma* 22 (2005): 266-76.